IS-T-604

The Decays of ^{139}Xe and ^{139}Cs

Ph.D. Thesis Submitted to Iowa State University, August, 1973

Millard Arthur Lee

Ames Laboratory, USAEC
Iowa State University
Ames, Iowa 50010

Date Transmitted: February 1974

PREPARED FOR THE U. S. ATOMIC ENERGY COMMISSION
DIVISION OF RESEARCH UNDER CONTRACT NO. W-7405-eng-82

Available from: National Technical Information Service
Department A
Springfield, VA 22151

Price: Microfiche $1.45

The decays of ^{139}Xe and ^{139}Cs

by

Millard Arthur Lee

A Dissertation Submitted to the
Graduate Faculty in Partial Fulfillment of
The Requirements for the Degree of
DOCTOR OF PHILOSOPHY

Department: Physics
Major: Nuclear Physics

Approved:

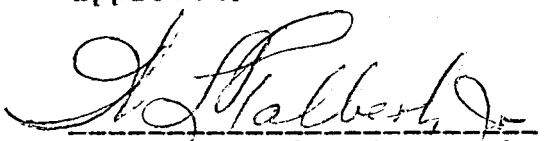

In Charge of Major Work

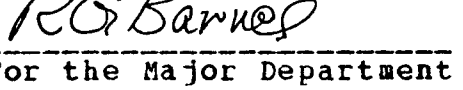

For the Major Department

For the Graduate College

Iowa State University
Ames, Iowa

1973

TABLE OF CONTENTS

The decays of ^{139}Xe and ^{139}Cs*

Millard Arthur Lee

Under the supervision of Willard L. Talbert, Jr.
From the Department of Physics
Iowa State University

Sources of ^{139}Xe and ^{139}Cs have been produced at the TRISTAN on-line isotope separator. With the aid of Ge(Li) singles and Ge(Li)-Ge(Li) coincidence measurements level schemes have been constructed for ^{139}Cs and ^{139}Ba. In the ^{139}Cs level scheme 193 of 220 observed transitions, constituting more than 98% of the gamma-ray intensity, have been placed among 50 excited levels. In the ^{139}Ba level scheme there are 62 excited levels among which are placed 161 of 177 observed gamma-ray transitions. These transitions account for more than 98% of the observed gamma-ray intensity. The Q-values for the beta decays of ^{139}Xe and ^{139}Cs were measured using a Ge(Li)-plastic scintillator coincidence arrangement. For ^{139}Xe the measured Q-value is 4.88 ± 0.06 MeV, and for ^{139}Cs the measured Q-value is 4.29 ± 0.07 MeV. Spin and parity assignments were made with the help of calculated log ft values and angular momentum transfer in stripping reactions, where available. An attempt was made to interpret some of the levels in terms of the shell model.

*USAEC Report IS-T-604. This work was performed under contract W-7405-eng-82 with the Atomic Energy Commission.

I. INTRODUCTION

The study of the nucleus dates back to the end of the last century when Becquerel discovered radioactivity while investigating a possible relationship between X-rays and optical fluorescence in some uranium compounds. Two years later Marie Curie showed that there were other elements in addition to uranium which also exhibited the property of radioactivity. These events preceded the development of the concept of the nuclear atom and, along with other work in the early part of this century, contributed toward this development. The concept of the nuclear atom was proposed by Nagaoka in 1904 (1) and later confirmed by the work of Rutherford and of Geiger and Marsden (2). Since that time many other naturally occurring radioactive nuclei have been discovered and, in addition, hundreds of different radioactive species have been prepared through various techniques.

Since those early years physicists have been striving to increase the extent of our knowledge of the nucleus by a variety of experimental procedures and by the construction of several theoretical models. The primary aim of these endeavors has been to gain an understanding of the nucleon-nucleon interaction, which would then lead to the eventual description of all nuclear properties in terms of the interactions of the nucleons.

The problem of deducing the exact nature of the nucleon-nucleon interaction is complicated by the fact that, in contrast to the atom, there is no one dominant interaction which would enable one to treat inter-nucleon interactions as perturbations. Further complicating the picture is the complex nature of the nucleon-nucleon interaction itself, which is known to be attractive for separation distances of approximately 2 fm but is strongly repulsive at separation distances of approximately 0.4 fm, and in addition has velocity-dependent, spin-dependent, and non-central terms (3).

In some respects the nucleus can be compared to a liquid drop. The nuclear density and the binding energy per nucleon do not change rapidly with the addition of more nucleons so the nucleus thus bears some similarity to a liquid drop in that it shows the effects of saturation. This is ascribed to the combined effect of the short-range repulsive nucleon-nucleon interaction and the exclusion principle which limits the number of nucleon pairs which can interact strongly (4). This similarity forms the basis of the static liquid drop model of the nucleus, which was used by N. Bohr and J. A. Wheeler to describe some aspects of the fission process (5).

A. The Neutron Rich Mass 139 Region

Nuclear fission provides one method of obtaining samples of radioactive nuclei for detailed spectroscopic studies. The fission fragments lie on the neutron rich side of the region of beta stability and consequently most of them decay by negative beta emission. The yield curves for the thermal neutron fission of ^{235}U are shown in Figure 1.

The radioactive fission product gases have been the object of several studies in recent years. The gaseous fission products, by the very nature of their gaseous state, can be separated from the other fission products with relative ease. By separating the gaseous fission fragments from the other fission fragments one then has quantities of Kr atoms with masses ranging out to A = 95 and Xe atoms out to A = 144. The independent yields of Kr and Xe isotopes resulting from the thermal neutron fission of ^{235}U have recently been measured by B. Ehrenberg and S. Amiel (6).

Once the gaseous fission fragments have been isolated there must be a separation by mass number before detailed studies of an individual isobaric chain can be carried out. The electromagnetic isotope separator has had outstanding success in this endeavor. After a single isobaric chain has been isolated by the isotope separator it is desirable to separate the activities of the individual members of the

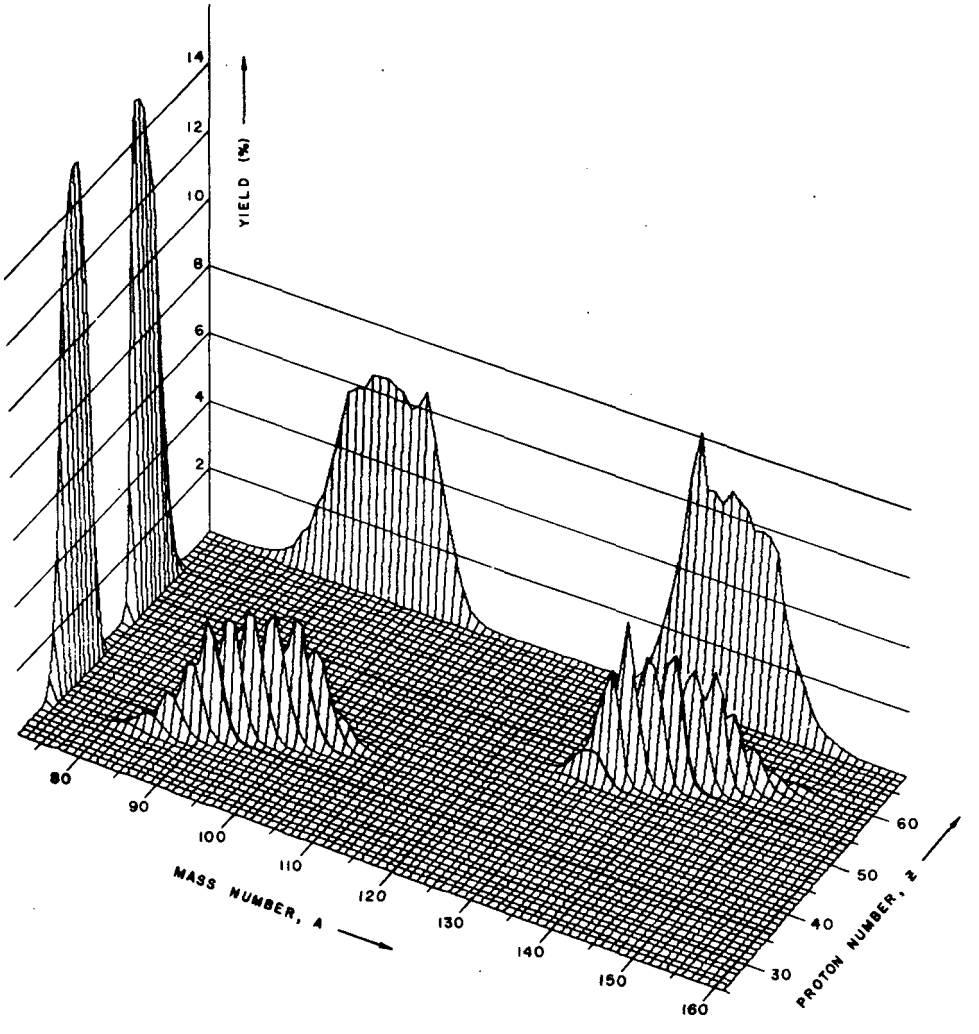

Figure 1. Fission yield of ^{235}U as a function of A and Z

chain. The moving tape collector provides a method of separating such activities by capitalizing on differences in half-lives. The TRISTAN system operating on-line with the Ames Laboratory Research Reactor located at Iowa State University has been designed to carry out these tasks and is described in the next chapter.

Among the radioactive decay chains initiated by the fission product gases, a range of nuclear types is represented. Some of these chains begin several mass units away from the region of beta stability and proceed through several daughter nuclides before ending at a stable nuclide. Such chains provide an opportunity to study the behavior of various nuclear properties as functions of Z and N. Other chains begin closer to the region of stability and consequently proceed through fewer decays before reaching the region of stability, thereby simplifying the task of separating the activities of the various members of a chain. The systematic study of all of the decays included among the chains initiated by the fission product gases will provide detailed information over a significant region of the chart of the nuclides and will make possible the observation of trends in the behavior of various nuclear properties with variations in mass number as well as atomic number and neutron number.

In the thermal neutron fission of ^{235}U the peak of the yield curve for the xenon isotopes lies at mass 139, as can

be seen in Figure 1 and in ref. 6. The decay chain commencing with ^{139}Xe and ending with stable ^{139}La is shown schematically in Figure 2. Since this chain ends with the magic N = 82 nucleus ^{139}La it presents some interesting possibilities for shell-model interpretations. The decay of ^{139}Cs to levels in the N = 83 nucleus ^{139}Ba should give information which can be interpreted in terms of single-particle excitations for the lower lying levels. The decay of ^{139}Xe to levels in ^{139}Cs should provide information which might be interpreted in terms of shell-model states available to a group of five protons outside the magic number Z = 50. The present work was undertaken in an effort to provide information which might contribute to our understanding of nuclear structure through a detailed knowledge of the energy levels of the nearly closed shell nuclei ^{139}Cs and ^{139}Ba.

In this work no attempt was made to study the decay of ^{139}Ba since it has already been studied rather extensively by several investigators. J. C. Hill and M. L. Wiedenbeck (7) and G. Berzins *et al.* (8) used Ge(Li) detectors to measure the gamma-ray energies and they have established level schemes based upon their results.

W. H. Kelly *et al.* (9) used scintillation detectors to study the beta spectra in beta-gamma coincidence experiments. They measured the Q-value for the beta decay and determined the beta branching for the beta decay to levels in ^{139}La.

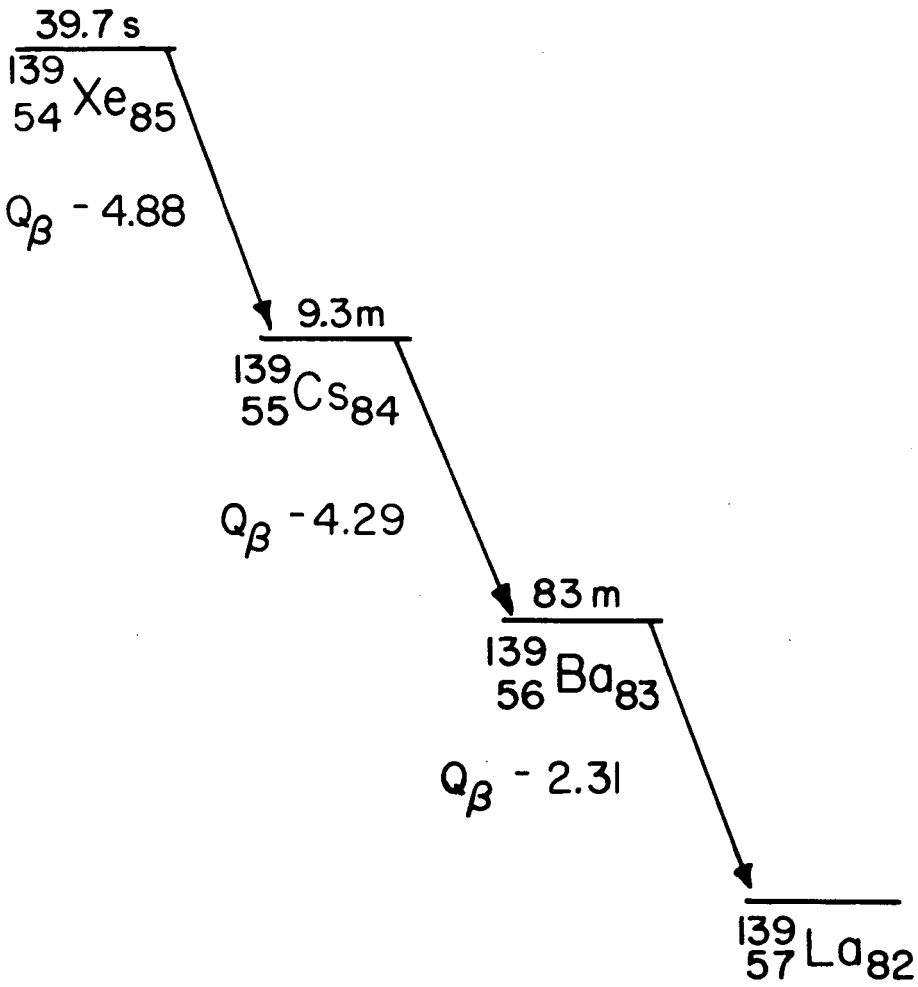

Figure 2. The A = 139 beta-decay chain studied in this work

B. Previous Work

1. The decay of ^{139}Xe

Spectroscopic studies of the decay of ^{139}Xe have been carried out by M. A. Wahlgren and W. W. Meinke (10) and by D. W. Ockenden and R. H. Tomlinson (11) using scintillation detectors. These studies were carried out in the presence of other xenon fission products and resulted in only four (ref. 11) and five (ref. 10) gamma-ray transitions being identified as following the decay of ^{139}Xe. In ref. 10 a measured value of 4.6 ± 0.2 MeV is reported for the decay energy.

The use of isotope separator on-line techniques in the study of this decay was initiated by G. Holm *et al.* who employed Ge(Li) gamma-ray detectors and an anthracene beta detector (12). They deduced a level scheme for ^{139}Cs in which fifteen gamma-ray transitions were placed among seven excited levels. Their beta-gamma coincidence experiments yielded a value of 5.0 MeV for the decay energy. They tentatively assigned an intensity of 1% to the ground-state beta branch, but the statistics of the experiment did not allow an unambiguous assignment for this branch. From their calculated log ft values they made tentative spin and parity assignments. For the ground-state spin and parity of the parent ^{139}Xe they assumed 7/2-, but also pointed out the possibility of a 3/2- assignment.

This work was followed shortly by the report of T. Alvager *et al.* who placed eleven gamma-ray transitions among five excited levels, basing their placement entirely upon energy sums and differences (13).

A study of the gamma-ray spectrum following this decay was begun by J. W. Cook and W. L. Talbert, Jr. and a partial level scheme placing 48 gamma-ray transitions among 15 excited levels was deduced (14). In the present work, 13 of these levels have been confirmed and several additional levels have been found.

E. Achterberg *et al.* have measured the internal conversion coefficients for a few of the low-energy transitions (15). They used their measured values together with data from other sources to make some tentative spin and parity assignments for the lower excited levels in ^{139}Cs. They favor an assignment of 3/2- for the ground state of the parent ^{139}Xe, basing this on the apparent small ground-state beta branch reported in ref. 12 and the measured value of 3/2- for the N = 85 nucleus ^{143}Ce (16). Their spin and parity assignments are then based upon this choice.

A summary of the previous results of decay scheme studies on ^{139}Xe is presented in Table 1. No reaction work leading to levels in ^{139}Cs has been reported, so the decay of ^{139}Xe provides the only information concerning these levels.

Table 1. Compilation of levels in ^{139}Cs found in this work and in other decay scheme studies

This work	Cook and Talbert (14)	Holm et al. (12)	Alvager et al. (13)	Achterberg et al. (15)
218.6	218.7	219.	218.8	218.71
			225.6	
289.8	290.0	290.		289.80
393.5	393.7	394.	393.6	393.65
515.1	515.3	516.	514.8	515.28
646.5				646.58
732.4	732.4	733.		732.60
891.7				
942.4	942.6	942.		
	962.4			
1006.5	1006.7	1007.	1006.4	
1020.3	1020.5			
1214.7				
	1363.2			
1395.1				
1461.3				
1508.0	1508.4			
1652.7	1653.3			
1693.8				
1738.6	1738.8			
1831.2				
2063.7				
2099.6				
2185.6	2185.4			
2304.9				
2328.8	2328.5			
2373.0				
2423.6				
2510.4				
2585.8				
2620.8				
2727.4				
2754.3				
2797.3				
2799.4				
2852.3				
2936.2				
2967.5				
2980.1				
3084.3				

Table 1. (Continued)

This work	Cook and Talbert (14)	Holm et al. (12)	Alvager et al. (13)	Achterberg et al. (15)
3130.3				
3147.1				
3156.1				
3372.7				
3375.3				
3504.7				
3815.1				
3908.2				
4299.0				

2.- Reaction studies for ^{139}Ba

The structure of ^{139}Ba has been studied rather extensively through reaction experiments, particularly with the ^{138}Ba(d,p)^{139}Ba reaction. This reaction has been used by several experimenters to obtain approximate level energies and also to determine the spins and parities of a few of these levels. R. H. Fulmer et al. used this stripping reaction on the N = 82 isotones ^{138}Ba and ^{140}Ce and reported single-particle energies for the $82 < N \leq 126$ shell (17). Their values are: $f_{7/2}$, 0; $p_{3/2}$, 0.83 MeV; $f_{5/2}$, 1.88 MeV; $h_{9/2}$, 1.9 MeV; and $p_{1/2}$, 2.25 MeV.

F. W. Bingham and M. B. Sampson used 11-MeV deuterons and analyzed the outgoing protons with a magnetic spectrometer. They reported values for the spins and parities of five of the seven levels established (18).

J. Rapaport and W. W. Buechner used 7.5-MeV deuterons and from a stripping analysis of their data they concluded that the observed $\ell_n = 3$ states are levels belonging to the $2f_{7/2}$ single particle strength (19).

C. A. Weidner et al. used 12-MeV deuterons and from their observed ℓ-values they deduced spins for the ground state and thirteen excited levels (20).

J. Rapaport and A. K. Kerman used deuterons with energies ranging from 5.0 to 7.5 MeV in order to study the reac-

tion mechanism under conditions where both the incoming and outgoing channels would be under the Coulomb barrier. They determined level energies up to 4.0 MeV excitation using an enriched target and 7.5-MeV deuterons (21).

The most recently reported study of this type was carried out by D. von Ehrenstein *et al.* using 12-MeV deuterons and a broad range magnetic spectrograph. They observed angular momentum transfers ℓ_n = 0, 1, 2, 3, and 5 which indicate population of the $2f_{7/2}$, $3p_{3/2}$, $3p_{1/2}$, $1h_{9/2}$, and $2f_{5/2}$ configurations above the closed neutron shell at N = 82. Energies were deduced for 49 levels, and spins were reported for the ground state and seven of the lower excited states (22).

In a later study, D. von Ehrenstein and M. C. Tsangarides, in collaboration with a group from the Los Alamos Scientific Laboratory, carried out a high resolution study with 12-MeV deuterons from the LASL tandem accelerator and deduced spin and parity assignments for four of the higher lying levels (23).

P. von Brentano *et al.* (24) and L. Veeser and W. Haeberli (25) have used elastic scattering of protons from ^{138}Ba to examine isobaric analogue states as compound nucleus resonances in ^{139}La, thereby inferring spins for the ground state and for four of the lowest excited states of ^{139}Ba.

J. A. Moraques et al. studied the qamma-ray spectrum followinq thermal neutron capture by ^{138}Ba with small Ge(Li) detectors in sinqles and with a Ge-NaI detector combination in coincidence. They deduced a level scheme for ^{139}Ba in which 20 qamma-ray transitions were placed among nine excited levels (26).

3. The decay of ^{139}Cs

V. A. Aksenov et al. separated Kr and Xe from other fission products by filters and used scintillation detectors to examine the qamma-ray spectra. They measured the energies of 12 qamma-ray transitions which they assigned to the decay of ^{139}Cs (27).

A later study of the decay of ^{139}Cs, also carried out in the U.S.S.R. usinq scintillation detectors, was reported by E. A. Zherebin et al. (28). They measured energies and relative intensities for 13 qamma-ray transitions and deduced a level scheme placinq these transitions amonq seven excited levels. They carried out beta-qamma coincidence experiments and beta sinqles experiments from which they obtained a value of 4.14 ± 0.10 MeV for the decay enerqy. A 4π beta scintillation counter was used to obtain an absolute calibration of their qamma-ray spectrometer and they obtained a value of 8.0 ± 1.5 for the number of 1283-keV qamma rays per 100 decays. They established a value of 90% for the ground-state beta branchinq. All three of these values are in good

agreement with the results of the present work.

The results of these studies are summarized in Table 2.

G. Rudstam *et al.* have used beta-gamma coincidence techniques to measure the Q-value for the ^{139}Cs decay, and have reported a value of 4.44 ± 0.06 MeV (29). They used NaI(Tl) detectors on the gamma-ray side of their system and consequently their gamma-ray energy resolution is of the order of 50 keV. The gamma-ray peaks on which their gates were set were all above 2.0 MeV, a region where the decay scheme had not been established until the present work. However, it is reasonable to assume, as they did, that the gating peaks represented both direct ground-state transitions and cascade transition summing.

Table 2. Compilation of levels in ^{139}Ba found in this work and in reaction studies

This work	Moraques et al. (26)		Rapaport and Kerman (21)		von Ehrenstein et al. (22)	
0.0	0.0	7/2-	0	7/2-	0	7/2-
627.2	627.3	3/2-	627	3/2-	630	3/2-
1081.9	1081.9	1/2-	1083	1/2-	1084	1/2-
1283.2			1283		1284	9/2-
	1292.6	1/2,3/2				
1308.1						
1420.7	1420.1	5/2-	1420	5/2-	1422	5/2-
1539.0			1539		1543	9/2-
1620.7			1619		1625	9/2-
1680.7			1680		1682	7/2-
1698.7			1698		1700	5/2-
1748.6			1745		1750	
1817.7						
1850.7						
1877.4						
1887.6			1893		1898	
1933.5			1930		1934	
1949.3	1952.3		1943		1952	
1998.5						
2020.8						
2037.8						
2079.3						
2089.9						
2100.1						
2110.9			2106		2112	
	2129.3	1/2,3/2	2126		2132	3/2-
2156.9	2156.0	1/2,3/2	2153		2162	
2174.0						
	2186.4	1/2,3/2	2182		2187	
2218.9						
2229.9						
2249.7						
2305.0			2300		2308	
2349.9			2361			
2375.9			2378		2368	
2380.7					2381	
			2433		2439	1/2-
2461.6						
	2481.4	1/2,3/2	2478		2484	3/2-

Table 2. (Continued)

This work	Moraques et al. (26)	Rapaport and Kerman (21)	von Ehrenstein et al. (22)
2524.5		2527	
2529.9			
2531.8		2543	2534
			2553
		2566	2574
2605.8			
2649.3			
		2667	2675
		2739	2751
		2797	2806
2847.6			2857
			2909
			2939
2997.3		2993	3007
		3023	3035
		3100	3110
3151.9		3163	
3171.6		3177	3175
			3192
		3210	3221
		3231	
		3249	
3270.2		3270	3264
			3285
			3293
3364.2			3352
3401.3			3392
3418.8			3480
			3495
			3516
			3542
			3579
3622.1			3614
3645.7			
			3675
3674.6			
3724.2			
3769.2			
3820.0			

Table 2. (Continued)

This work	Moraques et al. (26)	Rapaport and Kerman (21)	von Ehrenstein et al. (22)
3839.8			
3853.9			
3912.3			
3950.8			

II. EXPERIMENTAL PROCEDURES

The decays of ^{139}Xe and ^{139}Cs have been studied using the TRISTAN electromagnetic isotope separator operated on-line with the Ames Laboratory Research Reactor. The gamma rays following the beta decays of these two nuclides were studied in singles and in coincidence using large volume Ge(Li) detectors. Beta-gamma coincidence experiments were carried out for both decays using a plastic scintillator beta detector and a Ge(Li) gamma detector.

A. Sample Preparation and Configuration

The ^{139}Cs sources were obtained as daughter products of the ^{139}Xe decay. The ^{139}Xe atoms were obtained as fission products of ^{235}U. The uranium was in the form of uranyl stearate which was placed in an external neutron beam of the Ames Laboratory Research Reactor where the neutron flux is approximately 3 x 10^9 n/cm^2-sec. The stearate is spread on several trays mounted within an aluminum container, an assembly which will be referred to as the fission product generator (FPG). The gaseous fission products are pumped from the FPG through a 1.5-m fission product transfer line into the ion source by the separator vacuum system. A sweep gas line leading from a gas bottle through a controllable leak valve to the FPG is provided for the purposes of maintaining a stable operating pressure in the ion source and

of aiding the flow of the fission product gas atoms from the FPG to the ion source. The sweep gas is composed primarily of He (98%) with small amounts of Kr (1%) and Xe (1%) added which serve as mass markers when tuning the separator. An automatic pressure controller at the separator console, operating from the differential pump gauge, is used to regulate the ion source pressure.

B. The TRISTAN System

The essential features of the TRISTAN system are illustrated in Figure 3. Several of these features and details of its operation have been described by various members of the TRISTAN group (30 - 38). The gaseous fission product generator previously discussed is surrounded on three sides by paraffin shielding and is contained within the heavy concrete shielding, with the fission product transport line and the sweep gas line passing through a port in the wall adjacent to the ion source cage. The ions leaving the ion source are accelerated through a potential difference of 40 - 50 kV and electrostatic focusing is employed before the ions reach the magnet. Isotope separation is accomplished with a 160-cm mean radius, 90° sector magnet. The mass-separated beams then pass through a dispersion chamber before entering the collector box, in which the focal plane of the magnet is located. At the focal plane, a slit is located which consists of two aluminum plates with their vertical edges sepa-

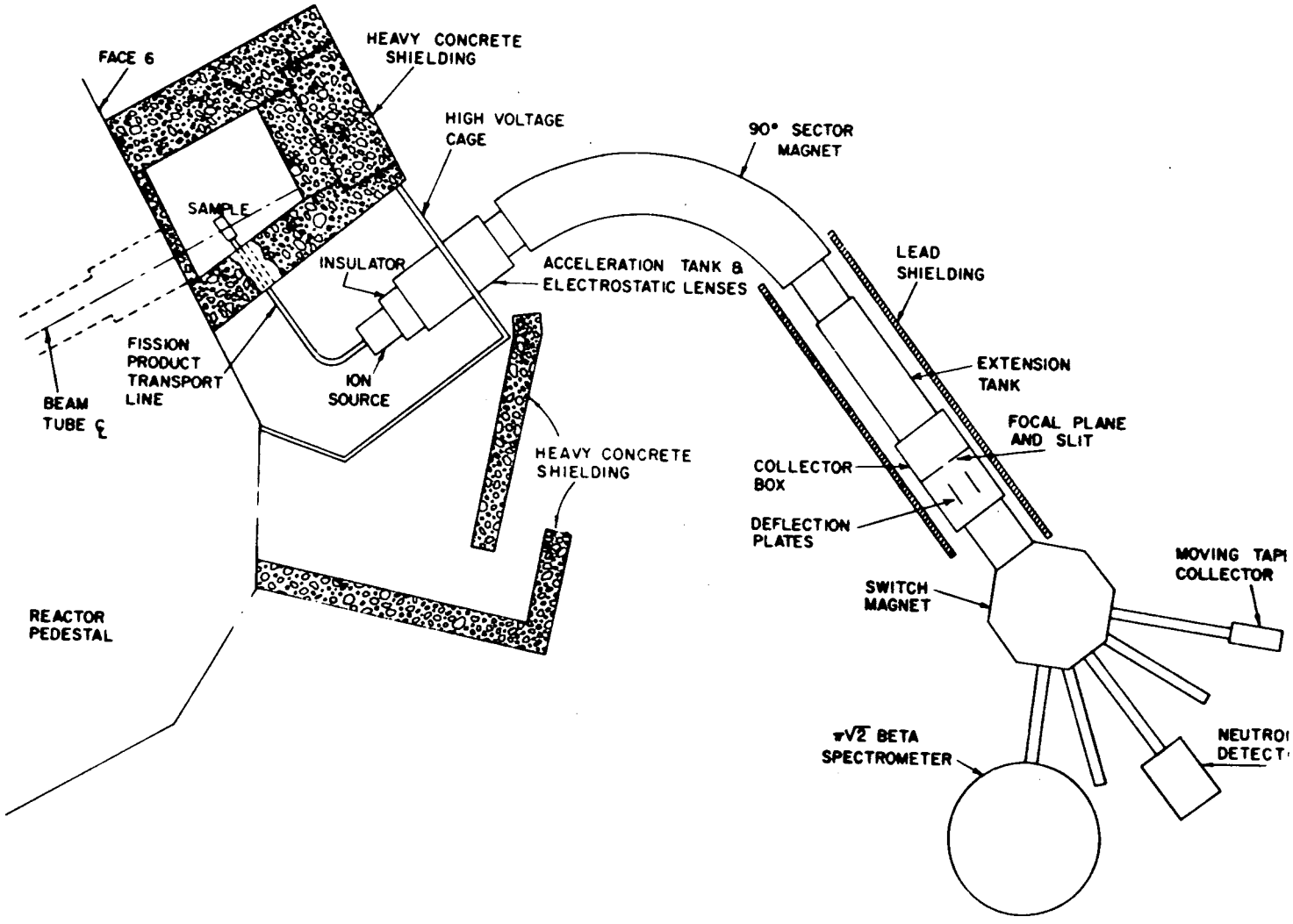

Figure 3. The TRISTAN on-line separator system

rated by a distance of approximately 3 mm. The width of a well-focused beam is of the order of 1 mm, whereas the separation between beams of adjacent mass numbers in the region of mass 139 is approximately 1.2 cm so the slit allows only the ions of the desired mass number to pass through the collector box. Cross contamination between adjacent mass numbers has been found to be negligible. Upon leaving the collector box the selected ions enter a switch magnet which allows the beam to be directed to any of five different ports. At one of the 45° ports is located the moving tape collector (MTC) where the present work was carried out. The MTC and the daughter analysis system have been described by Norman, et al. in ref. 38.

Several features of the MTC are shown in Figure 4. The beam is deposited on an aluminum coated mylar tape. The tape may be driven in a continuous mode at speeds up to 5 cm/sec or may be operated in a stepped mode where the time intervals for beam deposit, analyzer operation and tape movement are all controlled by the daughter analysis system. The parent activity is detected at Port 1 with the tape either moving in the continuous mode or as programmed by the daughter analysis system. Ge(Li) detectors may be placed on either side of the MTC at Port 1 to detect the activity at the point of beam deposit. In addition the figure shows the plastic scintillator beta detector and photomultiplier together with

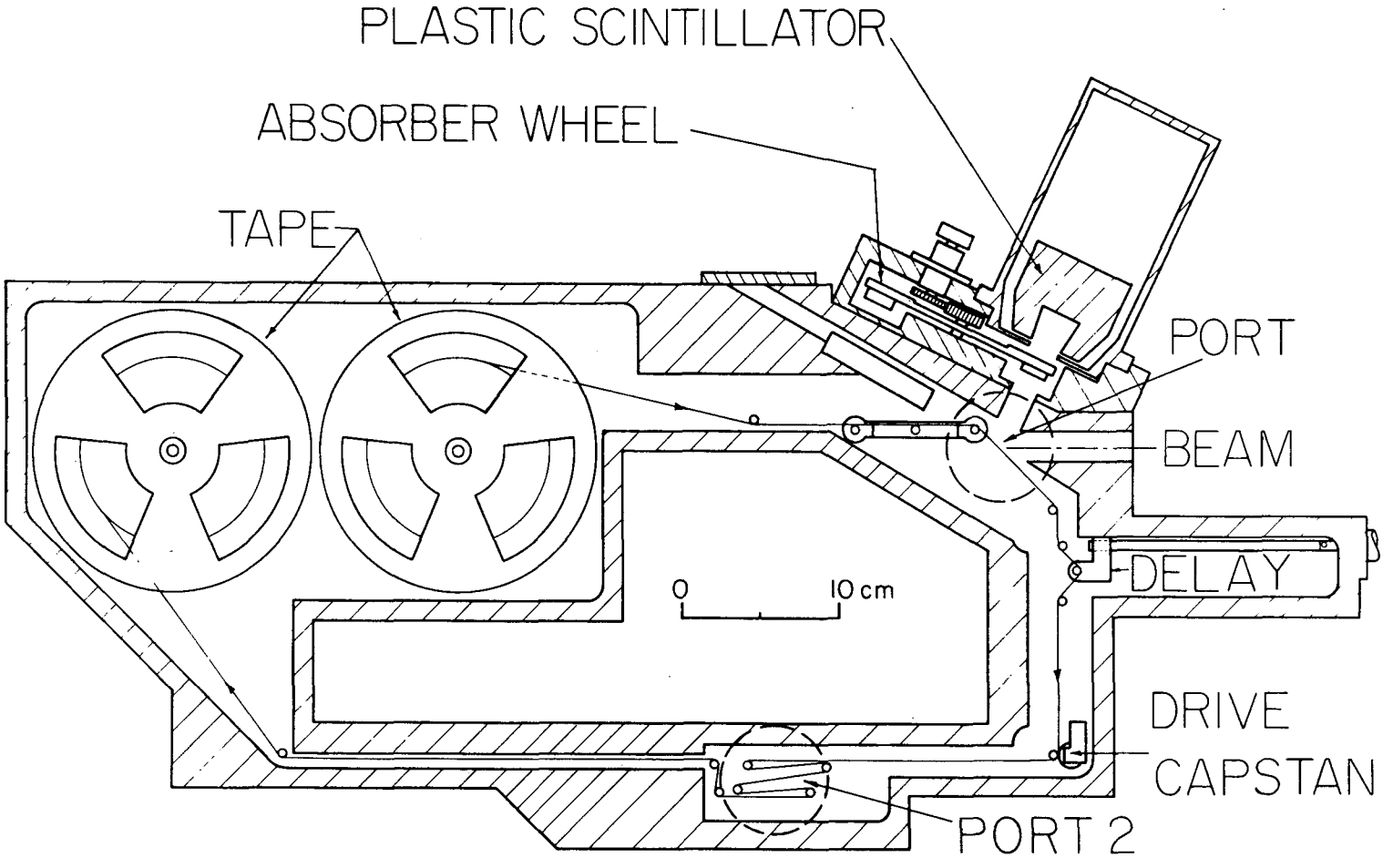

Figure 4. The moving tape collector at TRISTAN

the absorber wheel assembly mounted on top of the MTC to allow detection of beta activity at the point of deposit.

When carrying out gamma-gamma coincidence experiments the two Ge(Li) detectors are positioned 180° to each other, with one detector located on each side of the MTC. For the beta-gamma coincidence experiments the plastic scintillator detector is used together with a Ge(Li) detector on either side of the MTC.

For detection of the daughter activity the detectors are placed at Port 2. The beta detector and absorber assembly is mounted on the underside of the MTC and the gamma detectors are located on either side at the Port 2 location.

The daughter analysis system has four adjustable time intervals which together determine the length of the time intervals for collection of the beam, delay for the decay of the parent activity, operation of the pulse height analyzer, and tape transport. The time intervals chosen for the first three of these steps were determined by the computer program ISOBAR which is described in ref. 38. The time used for the transport of the activity to Port 2 is dictated by the tape speed and the distance from the point of deposit to Port 2. This distance is dependent on the setting of the variable delay loop in the MTC and on the desired location of the activity at Port 2. For detecting beta activity at Port 2 the deposit is moved to the center of the lowest loop of the tape

across Port 2 in order to get the activity as close as possible to the beta detector and to avoid having the beta particles pass through the other loops of the tape. This results in the gamma activity entering the gamma detector from a position slightly off axis but has not presented any problems. For detection of gamma rays only at Port 2 the deposit is moved to the center of Port 2 where the activity is then located on the axis of the detectors.

The daughter analysis system has a high duty factor mode which allows a new sample to be collected and to decay while the previously collected sample is being counted at Port 2. Depending on the lifetimes of the activities in a given decay chain this feature may allow the analyzer to be gated on for nearly 100% of the time. During the decay time the separator beam is deflected electrostatically by a pair of deflection plates located in the collector box. These plates are located behind the focal plane slit so there is no danger of a nearby mass being deflected into the switch magnet.

The amount of activity produced at mass 139 is sufficient to swamp the counting system so it was necessary to reduce the beam intensity reaching the MTC. This was accomplished by dropping a screen located at the focal plane of the separator such that it cut off approximately one-half of the beam.

C. Acquisition of Data

Large volume coaxial type Ge(Li) detectors were used in accumulating all the gamma-ray spectra in this study. Table 3 lists some of the characteristics of the various detectors used.

Table 3. Characteristics of gamma detectors

Detector	Active volume (cm^3)	Rel efficiency (percent)	FWHM (keV)	Peak/Compton
A	58.2	9	2.24	28
B	58.2	11	2.09	34
C	39.8	7	2.53	20
D	48.4	8	2.38	24

Each relative efficiency value in the table is the ratio of the area under a 1.33-MeV photopeak obtained with the detector to the area under the corresponding peak obtained with a 7.6-cm x 7.6-cm Na(Tl) at a source-to-detector distance of 25 cm.

Detectors C and D were used only in accumulating gamma-gamma coincidence spectra from the decay of ^{139}Xe. The gamma singles spectra and the gamma side of the beta-gamma

coincidence experiments for both decays as well as the gamma-gamma coincidence spectra from the ^{139}Cs decay were obtained with detectors A and B. All four of these detectors are of the true coaxial type.

1. Gamma-ray singles

A block diagram of the equipment used in collection of singles data is shown in Figure 5. The gamma detector was mounted at the appropriate port of the MTC and the preamplifier was mounted permanently on the detector head. The preamplifier signal was fed through approximately 5 m of coaxial cable to the spectroscopy amplifier which was located in a bin in a rack adjacent to the ADC.

The first data on the Xe decay were taken with the MTC operating in the continuous mode and with a lead collimator in front of the detector. Later experiments performed by R. J. Olson revealed that the use of this collimator resulted in energy dependent errors in the gamma-ray intensities so additional data on the Xe decay without the collimator were taken in order to obtain the correct intensities.

Attempts to determine the ground-state beta branching for the ^{139}Xe decay by an indirect calculation did not yield consistent results, so an equilibrium run was taken. In this run the beam was allowed to collect on the tape in the MTC for a period of one hour with the tape stationary. The analyzer was then turned on and the equilibrium singles

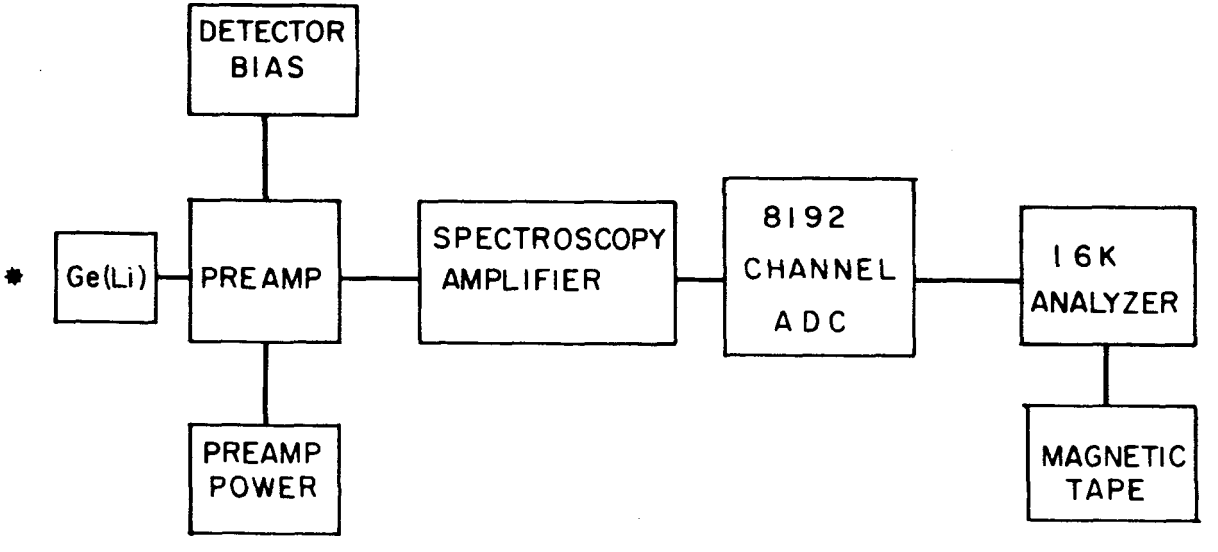

Figure 5. Block diagram of singles electronics system

spectrum accumulated for a period of one hour while the beam was still being collected on the tape. The beam current was held constant during the entire experiment.

In collecting singles data on the Cs decay the daughter analysis system was used with the detector placed at Port 2 of the MTC. The beam collection time of 247 sec, decay time of 340 sec and counting time of 576 sec used in this experiment were determined by the computer program ISOBAR using the half-lives reported by Carlson, et al. (39). The integrated activity ratios as calculated by ISOBAR for the times selected were 0.18 % Xe, 87.7 % Cs and 12.1 % Ba.

For each singles run three sets of data were taken in addition to a background spectrum. The first of these was taken with calibration sources alone in order to determine the system nonlinearities. This was followed by a run taken with the calibration sources and the unknown together. The data from this run were used to determine the energies of the stronger peaks of the unknown spectrum and these energies were then used as calibration points for the third data set, which was taken with the unknown alone.

The analyzer memory used in these experiments has a capacity of 10^5 - 1 counts per channel. In order to avoid the problem of keeping a record of overflows of the memory in certain channels the 8192-channel spectrum was written onto magnetic tape whenever the contents of the peak channel ap-

proached a few thousand counts of overflow. The analyzer memory was then reset to zero and another accumulation begun. The resulting spectra were then added together in the computer before being written on the disk pack at the computer center. In this fashion spectra containing more than 3×10^6 counts in the peak channel were obtained.

2. Gamma-gamma coincidences

For the gamma-gamma coincidence experiments the equipment was set up as shown in the block diagram of Figure 6. For the data taken on the Xe decay the detectors used were detectors C and D described in Table 3. Detectors A and B were used in the Cs experiment.

The following equipment was used in both gamma-gamma coincidence experiments:

Preamps: Ortec Model 120

Timing Filter Amplifiers: Ortec Model 454

Constant Fraction Discriminators: Ortec Model 453

Time-to-Amplitude Converter: Ortec Model 437

Single Channel Analyzer: Canberra Model 1430

Linear Amplifiers: Tennelec Model TC203BLR

Delays: Mechtronics Model 506

ADC's: TMC Model 217A

To record the coincidence events a buffer tape system was used. This system employs a 4096-channel memory in which the addresses of the two coincident gamma-ray energies are

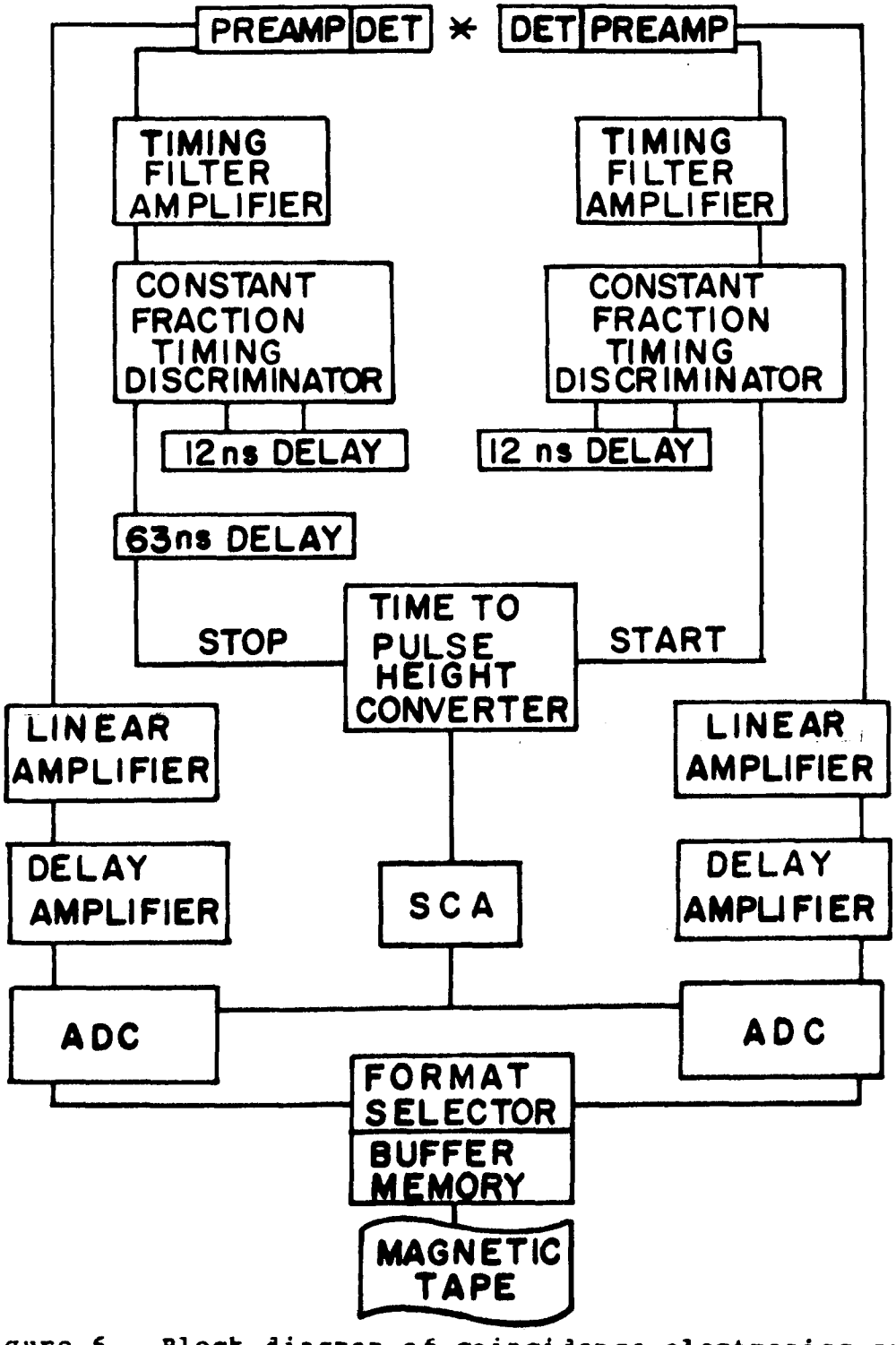

Figure 6. Block diagram of coincidence electronics system

stored in pairs. When the memory is filled the contents are written onto a magnetic tape and the memory is reset to zero before counting the next group of coincidences. The memory dumping and resetting process takes approximately one second, during which the counting system is disabled. A typical tape will hold approximately 1700 such records, and since each record contains 2048 coincidences a filled tape contains approximately 3.5×10^6 coincidence events.

In order to sort out the coincidence events the tapes are played back through the buffer system and the selected events are stored in the memory of the 16384-channel analyzer. The buffer system provides for the digital selection of up to 16 energy regions from one side of the coincidence counting system, and as a tape is played back, the address of every gamma ray detected by the other detector, which was in coincidence with a gamma ray having an energy within this region, is routed to the appropriate location in the analyzer memory. With the digital selection one can choose to look at four 4096-channel spectra, eight 2048-channel spectra or up to sixteen 1024-channel spectra. Due to the complexity of the gamma-ray spectra from both the Xe and the Cs decays it was necessary to use 4096-channel spectra almost exclusively in searching for gamma-gamma coincidences.

The timing resolution obtained in the gamma-gamma coincidence experiments had a FWHM of 23 nsec. The coincidence acceptance gate was 45 nsec.

3. Beta-gamma coincidences

The equipment used in the beta-gamma coincidence experiments was also arranged as shown in Figure 6. The essential difference between this arrangement and that used for the gamma-gamma experiments was the replacement of one of the Ge(Li) detectors and associated preamp with the plastic scintillator, photomultiplier and preamp. The plastic scintillator has been described by Wohn et al. (40).

The scintillator is made of Pilot B plastic in the form of a right circular cylinder with a diameter of 6.5 cm and a thickness of 3.5 cm. The detector has a well in the front face, having the shape of a truncated cone with an entrance diameter of 1.9 cm and a depth of 2.3 cm. The detector, photomultiplier and absorber wheel assembly are fixed to the MTC such that the source lies at the vertex of the cone, which is located at a distance of 5.7 cm from the face of the detector. For the Xe experiment the detector and absorber assembly was mounted on top of the MTC as shown in Figure 4. For the Cs experiment the entire assembly was mounted on the underside of the MTC at the Port 2 location. In both cases the two detectors were at 90° to one another. The absorber wheel contains cylinders of Be and Al of various thicknesses

and has, in addition, an open position. The calibration techniques used for the beta detector and the calibration data for the Cs experiment along with some representative beta spectra have been presented in ref. 40. The sources of ^{85}Kr, ^{88}Rb and ^{137}Xe were obtained with the TRISTAN system. Sources of ^{32}P and ^{38}Cl were prepared from reactor irradiated samples by atmospheric evaporation onto aluminized mylar film similar to the tape used in the MTC. The source material for the ^{137}Cs and ^{144}Ce sources was obtained commercially and the sources were then prepared in the same manner as the other off-line calibration sources.

The MTC has a provision for carrying out calibration of the plastic scintillator while it is mounted in its position of the MTC. A source holder capable of holding three different calibration sources can be inserted into the MTC and moved to the source position, resulting in the same geometry as is used when operating on-line with the separator. There is a rocker arm assembly in the MTC which allows the tape to be moved out of the source position when off-line calibration is being performed at Port 1. At Port 2 the source holder position is slightly below the position of the on-line source so that at this port the solid angle subtended by the well of the detector is slightly larger than is the case with the on-line source. During the beta-gamma coincidence experiments the gamma-ray detector was shielded from the beta rays by the

wall of the MTC and a 6.3-mm thick plexiglass plate covering its face. However the beta detector was open to the gamma rays so a significant fraction of the coincidence events counted were initiated by gamma rays incident on the beta-detector. The correction for these events was accomplished by placing an absorber in front of the beta detector just thick enough to screen out the beta rays and accumulating a coincidence spectrum for the gamma contribution alone. In order to determine the fraction of the total events due to Compton scattered electrons in the detector, the time required to fill the buffer memory five times was measured both with and without the absorber. The ratio of the time required with the absorber to the time required without the absorber was then taken to be equal to the ratio of total events counted (beta-gamma plus gamma-gamma) to the number of beta-gamma events. Then in accumulating data this ratio was used as the ratio of the number of buffer records obtained without the absorber to the number obtained with the absorber in place. For the Xe decay the absorber used was 1.59-cm thick Be, and for the Cs decay a 1.27-cm Be absorber was used. The correction for these events is then actually made during the playback procedure. As the tapes were played back through the buffer system the analyzer was switched to the subtract mode when the records taken with the absorber were being processed. In this manner, the gamma-gamma contribu-

tion was removed from the data.

Gates were set on several prominent gamma-ray peaks and the beta spectrum in coincidence with each of these gamma rays was then accumulated in the analyzer memory. These spectra also contained coincidence events which were gated by gamma rays in the background under the gating peak. To correct for these background-gated coincidence events, another gate of the same width was set on a nearby region of the gamma spectrum and this spectrum was then subtracted from the spectrum gated by the photopeak gate. The resultant spectrum then contained only the desired beta-gamma coincidence events.

D. Data Analysis

1. Gamma-ray spectra

In order to determine gamma energies and intensities from the singles data, four separate spectra were analyzed for each decay. The initial spectrum was taken with the calibration sources alone, and the known energies along with the peak centroids as determined by the fitting programs were used to determine the nonlinearities in the system. The next spectrum was taken with both the unknown activity and the calibration sources. The energies and centroids of the calibration source peaks and the nonlinearity data were then used to determine the energies of the stronger peaks in the

unknown spectrum. These stronger peaks were then used as calibration points in the analysis of the spectrum of the unknown alone. The fourth spectrum analyzed was a background spectrum. The sources used for the gamma-ray energy calibration included ^{56}Co, ^{57}Co, ^{60}Co, ^{133}Ba, and ^{152}Eu. The energies used were those given in the tabulation by Gunnink, et al. (41).

Several computer programs were employed in the reduction and analysis of the singles data. The output of the 16384-channel analyzer was in the form of several 8192-channel spectra recorded on computer compatible magnetic tape. The tape was carried to the Iowa State University Computation Center where all of the computing necessary in the analysis of the data was carried out on an IBM 360/65 computer system. A program called TRANSFER was used to read the spectra from the magnetic tape, add together the individual spectra and record the final sum on a disk pack.

Plots of the spectra were obtained through several utility plot routines prepared by members of the TRISTAN group. These plotting routines employ SIMPLOTTER, a high level plotting system developed by D. G. Scranton and E. G. Manchester of the Ames Laboratory USAEC and the Iowa State University Computation Center (42). The plotting is done on a Cal-Comp 11-inch drum-type incremental plotter.

Locating the peaks and the initial fitting was carried out with the use of a program called PEAKFIND, which works in a manner similar to that of a program reported by M. A. Mariscotti (43). The detailed operation of the program has been described by R. J. Olson in ref. 37. The program locates gamma-ray peaks by looking at the second differences in the number of counts versus channel number, and when the second difference is sufficiently negative for a few channels it concludes that a peak is present in that portion of the spectrum. The program can fit up to nine closely spaced peaks. The program carries out a fitting procedure, using an iterative method, for all peaks whose relative intensity exceeds a level which may be specified by the user. The output can consist of plots of all fits attempted, punched cards which may serve as input data for another fitting program, and a printed output giving values of all parameters which were varied during the fitting procedure.

In the fitting process a gamma-ray peak is divided into three regions. The low-energy side of the peak is described by an exponential decay, a backscatter tail and a skewness term. The middle region contains a pure Gaussian plus a backscatter tail, and the upper region contains a pure Gaussian and a skewness term. The backscatter term was placed in the fitting function to facilitate the fitting of spectra obtained with Si(Li) detectors and is not used in fitting

Ge(Li) spectra. With the large volume coaxial Ge(Li) detectors the skewness terms were used only for the low energy side of a few of the stronger peaks in the spectrum. With these exceptions the fitting function consisted of an exponential decay for the low-energy region and a pure Gaussian for the middle and upper regions of each peak. The fitting programs are written in a fashion which allows any of several parameters to be varied during the fitting. These include the peak centroid, the full-width-at-half-maximum (FWHM), the peak height, the crossover parameter (the distance, in channels, between the centroid and the point of demarcation between the Gaussian and exponential decay regions), and the skewness and backscatter terms. The crossover parameter and FWHM were found to vary linearly with gamma-ray energy.

After locating the peaks PEAKFIND was used primarily to determine the linearization parameters for the FWHM and crossover point as functions of gamma-ray energy. When these parameters had been determined, the FWHM and crossover parameter were held to straight line values in the subsequent fitting for a given spectrum. The punched card output contains the information necessary as input to another fitting program called SKEWGAUS.

SKEWGAUS uses the same fitting function as PEAKFIND and consequently the linearization parameters determined with PEAKFIND can be used for fixing FWHM and the crossover point

as functions of gamma-ray energy for the SKEWGAUS fitting. The program is then used to determine the centroid, area and height for each peak in the spectrum together with the errors in these quantities. The detailed operation of this program, including a description of the fitting function, is described in ref. 37.

The plots for each peak or group of closely spaced peaks obtained with PEAKFIND were examined and appropriate adjustments made to the card input regarding the number of peaks and the background behavior around each peak. SKEWGAUS has options allowing the background to be fit either as a quadratic or a linear function and the background is plotted along with the raw data and the fitting function. The graphs were examined closely to determine how well the function fit the raw data, and the fit was repeated until satisfactory agreement was obtained. An example of a fit obtained with SKEWGAUS is shown in Figure 7, and the fit for a multiplet is shown in Figure 8.

The program furnishes punched card output listing the centroid, height, area and uncertainties in centroid and height for each peak. This card output is then used in the DRUDGE program for final determination of gamma-ray energies and relative intensities.

DRUDGE was prepared by R. J. Olson and is based upon an earlier version written by K. B. Nielsen. The program is de-

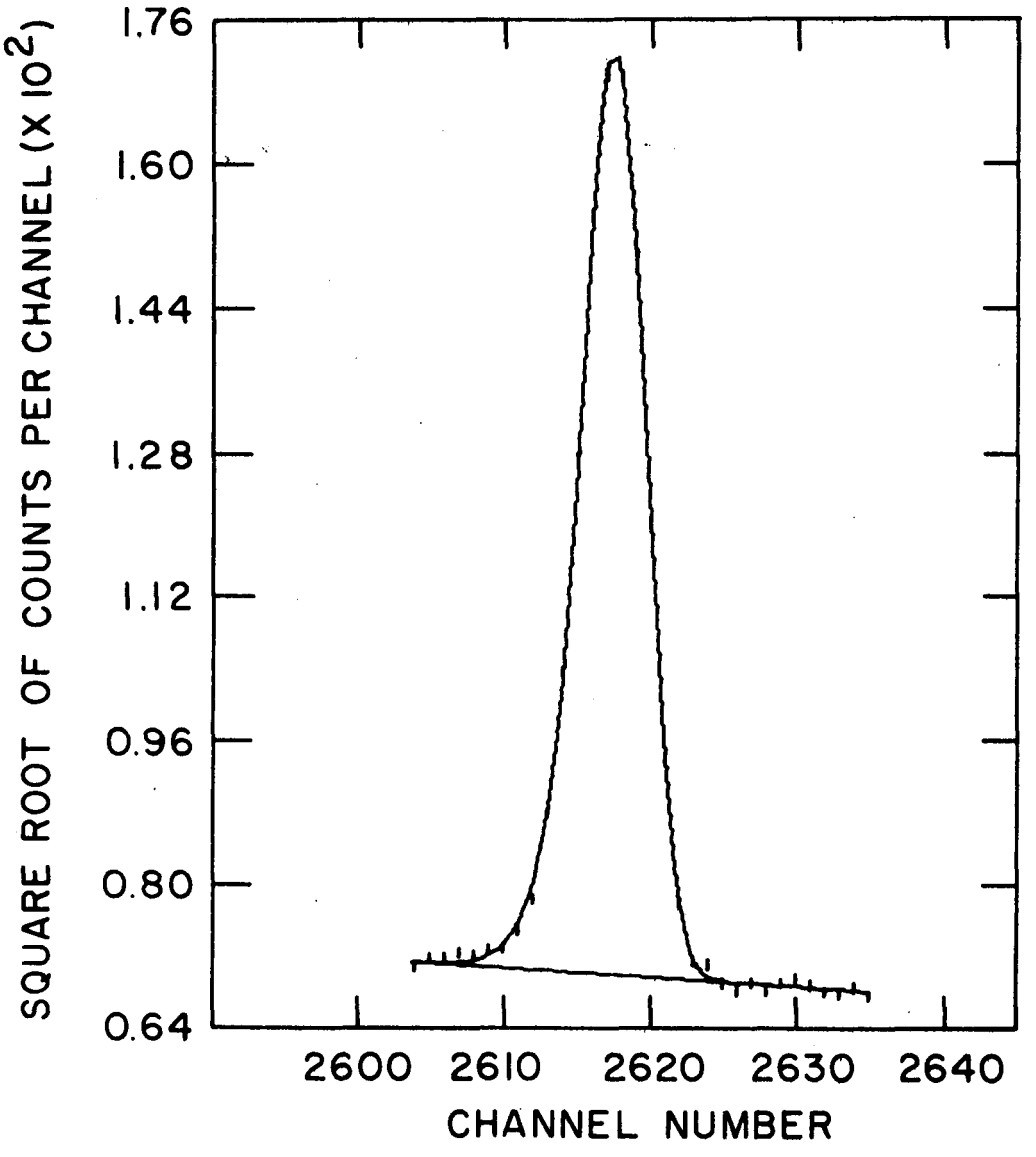

Figure 7. Typical SKEWGAUS fit for a single photopeak

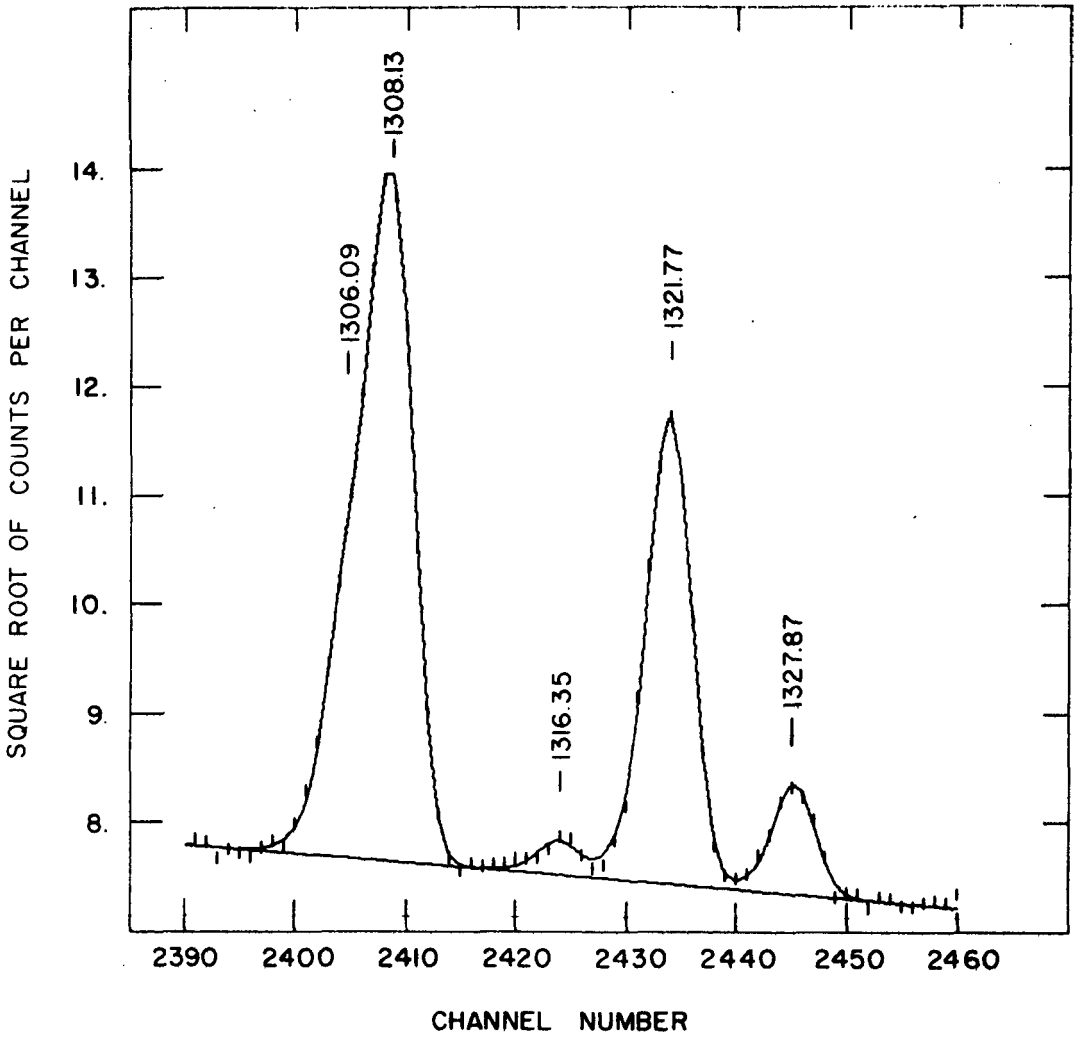

Figure 8. Typical SKEWGAUS fit for a multiplet

scribed in detail in ref. 37. The input required includes data on the detector relative efficiency, attenuation coefficients for any material between the source and detector, differential nonlinearity of the counting system, single-escape to photopeak and double-escape to photopeak ratios, and calibration pairs (gamma-ray energy and peak centroid).

The program calculates straight line parameters from the calibration pairs using a least-squares technique and then uses the nonlinearity information to determine the gamma-ray energy as a function of centroid location.

The attenuation data were taken from circular 583 of the National Bureau of Standards, and included only the data for the 0.16-cm aluminum wall of the MTC (44, 45). In all singles runs there was also a 6.3-mm thick plexiglass beta absorber on the face of the Ge(Li) detectors, but the relative efficiency measurements were made with this absorber in place and consequently the attenuation of this absorber is reflected in the relative efficiency tables used in the DRUDGE program. The data for the relative efficiency calibration were taken using ^{133}Ba, ^{152}Eu, ^{182}Ta and ^{56}Co sources. For the Ba, Eu, and Co sources the energies and relative intensities were those given in ref. 41. For the Ta source the intensities used were those reported by W. F. Edwards, *et al.* for the low energy transitions (46) and by J. J. Sapyta, *et al.* (47) for the high energy transitions.

In the analysis of each gamma singles measurement the DRUDGE program is used twice. The program is first used on the data of the calibration plus unknown run to determine the energies of the stronger transitions in the unknown spectrum, using the peaks of the calibration sources for the determination of the functional dependence of the energy on channel number. Then in the second DRUDGE application the stronger peaks of the unknown run are used with the data from the unknown run alone to determine the energies and intensities of the transitions of the unknown spectrum. The program provides punched card output listing the energy and intensity of each gamma-ray transition and the uncertainties in these quantities. These cards are then used as input data for two programs used in the construction of level schemes. Lists of possible Compton disturbed peaks and also lists of possible single- and double-escape peaks are printed out.

The analysis of the gamma-gamma coincidence data was carried out using the buffer tape system and plots of the coincidence spectra. Digital gates are set on the stronger peaks in the gating spectrum and as the tape is played back each coincidence event whose "B" address falls within a given gate will have its "A" address routed to the appropriate location in the memory of the 16384-channel analyzer. In this fashion a spectrum of all gamma-ray transitions in coincidence with the gating transition is obtained. However,

this spectrum also contains coincidences gated by Compton scattered gamma rays from higher energy gamma transitions which happen to fall within the selected gate, so these must be accounted for in the analysis. This is accomplished by setting another gate of the same width in a region close to the photopeak in question and the two spectra are then compared. If a peak in the photopeak gated spectrum is considerably enhanced over that displayed in the background gated spectrum, then the gamma-ray transition represented by this peak is regarded as definitely being in coincidence with the gating transition and the coincidence is indicated on the level scheme by a solid circle. For weaker peaks or for those where the enhancement over nearby gates is not as clearly indicated, the coincidence is regarded as being probable and is denoted on the level scheme by an open circle. Due to the large number of coincidence gates examined in both decays no attempt was made to submit these spectra to the fitting routines to determine intensities. The approximate numbers of coincidence spectra examined were 50 for the Cs decay and 30 for the Xe decay. Each of these was compared with the spectrum in coincidence with a nearby gate. An example of one of these spectra and that of the nearby gate is shown in Figure 9.

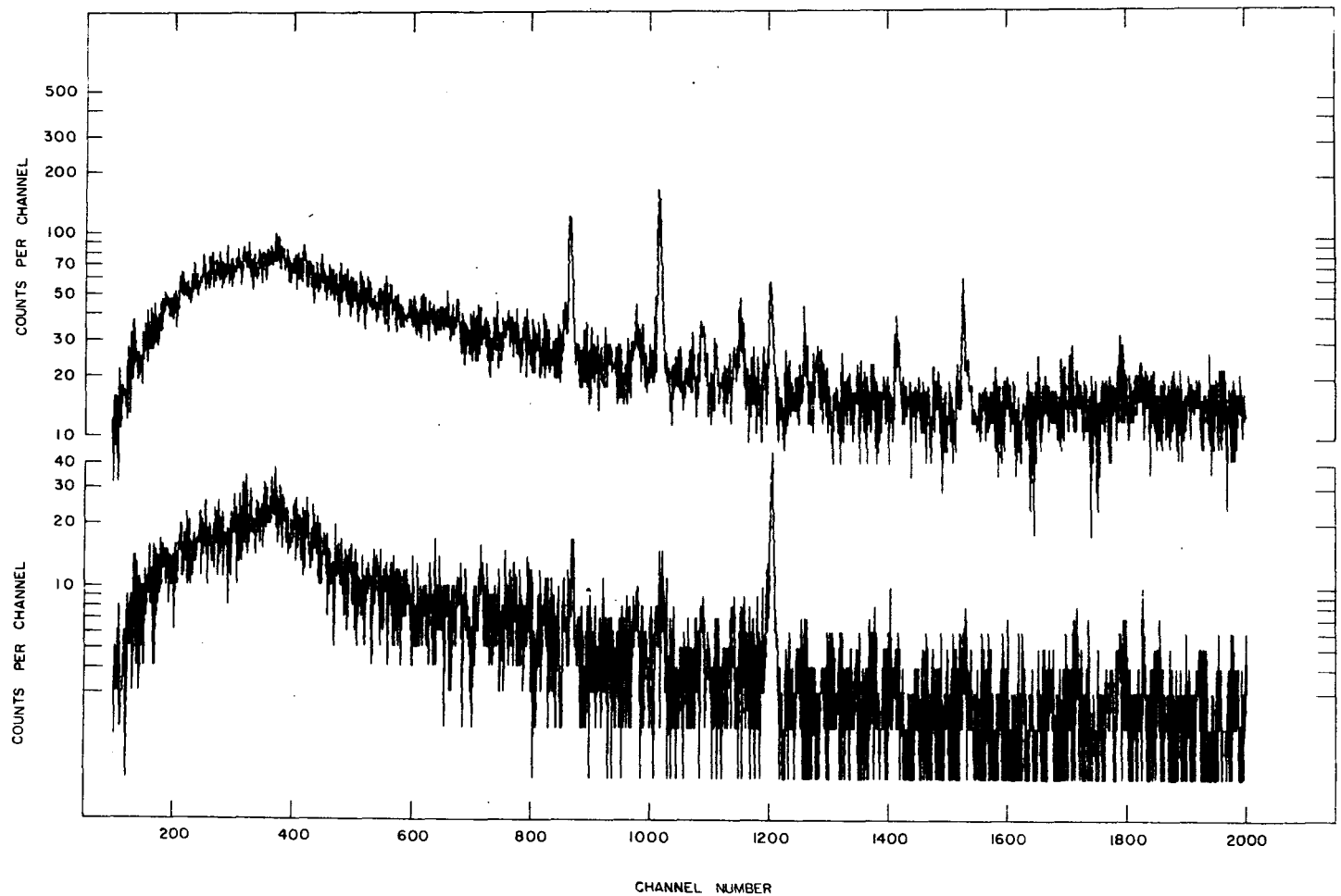

Figure 9. Typical coincidence gate and background slices

2. Beta-ray spectra

The procedures used in the analysis of the beta spectra have been described in ref. 40. A computer program called FERMI written by F. K. Wohn was used to determine the end-point energies of the various beta spectra. The program uses a "folding" technique which has been described by Rogers and Gordon (48). The technique involves first a distortion of the theoretical beta spectrum by the detector response function and then fitting the distorted spectrum to the measured spectrum by a least squares procedure. This technique avoids the distortions sometimes introduced when unfolding a spectrum and is particularly useful when the energy level scheme of the daughter nucleus is known. Knowledge of the differences in daughter energy levels allows constraints to be placed upon the differences between energies of the various beta groups so that the number of free parameters is reduced. This number is further reduced by applying additional constraints allowed by knowledge of the relative beta branching to excited states of the daughter nucleus. When these energy differences and branching ratios are all known, the only free parameters left are one end-point energy, the coefficient for one of the excited state branches, and the amplitude coefficient for the ground-state beta group.

The FERMI program goes through an iterative process, minimizing the square of the difference between the measured spectrum and the distorted spectrum. An initial estimate of the endpoint energy is required by the program and then a new value is calculated. If the new value differs from the initial estimate by more than one channel, the program uses the new value as an initial estimate and repeats the calculation. This procedure is repeated until the calculated value differs from the previous value by less than one channel, or about 40 keV. The error analysis carried out by the program has been described by J. R. Clifford (49).

III. RESULTS

The results of the studies of the decays of ^{139}Xe and ^{139}Cs are summarized in the graphs and tables which follow. For each decay a plot of the gamma-ray spectrum is presented in which the log of the number of counts per channel is plotted against the channel number. In these plots several of the peaks have been labelled with the energy of the corresponding gamma-ray transition. These plots are followed by a table which lists the observed gamma-ray energies and relative intensities along with the errors in these quantities as calculated by the DRUDGE program. The table for the Cs decay also includes values for the absolute intensities which are based upon an indirect calculation of the ground-state beta branching. The method used in these calculations has been reported in ref. 37. For the Xe decay these values are based upon the intensities of transitions observed in an equilibrium run on the Xe and Cs decays. The last column in this table gives the level placement for each of the transitions placed in the level scheme.

The level schemes presented are based upon the gamma-gamma coincidence results and upon gamma-ray energy sums. Due to the large number of gamma-ray transitions it was necessary to divide each of the level schemes into different energy regions.

The observed gamma-gamma coincidences are presented in the next table. These coincidences are listed as being either definite or probable. The definite coincidences are indicated on the level schemes by a solid circle while those regarded as probable are indicated by an open circle.

Log ft values were calculated for the various beta groups in each decay. The results of the ground-state beta branching calculation were used in these calculations.

For levels where no reaction data were available to aid in making spin and parity assignments, the log ft values were used to provide an indication of the limits on the range of spin values possible for each level. The rules used were those proposed by S. Raman and N. B. Gove (50). Briefly, the rules are as follows:

log ft < 5.9	$\Delta J = 0,1;\ \Delta\pi = +$
log f_1t < 8.5	$\Delta J = 0,1;\ \Delta\pi = \pm$
log ft < 11.0	$\Delta J = 0,1;\ \Delta\pi = \pm$. Or
	$\Delta J = 2;\ \Delta\pi = -$.
log ft < 12.8	$\Delta J = 0, 1, 2;\ \Delta\pi = \pm$.

In cases where several gamma-ray transitions depopulate a level it is assumed that these transitions have multipolarities E1, M1, or E2. It is assumed that M1 transitions will compete with E2, but that M2 transitions, as well as E3 transitions, are not likely to be observed.

Partial decay schemes showing the gamma-ray transitions used as gates in the beta-gamma coincidence experiments are presented. An example of the beta spectrum in coincidence with one of these transitions and the associated Fermi-Kurie plot are shown.

A. ^{139}Xe Decay

1. Gamma-ray decay scheme

Figure 10 shows the gamma-ray spectrum following the beta decay of ^{139}Xe. The spectrum covers an energy range from 0 - 4.5 MeV, and was taken with the MTC operating in a mode in which the counting was done while the beam was being deposited. Each sample was collected and counted for a period of 15.0 seconds. The integrated activity ratios calculated by ISOBAR for this run were 98.0% Xe and 2.0% Cs.

Table 4 lists the energies and intensities for the gamma-ray transitions observed following the Xe decay. The relative intensity values are based upon an assignment of a value of 1000 to the 218.59-keV transition. Also included are the absolute intensities in terms of the number of times each gamma-ray is emitted per 100 decays. The last column gives the level placement in the level scheme for ^{139}Cs. For the gamma-ray transitions which have been used twice due to uncertainty in their proper placement the intensities have been divided equally between the two placements.

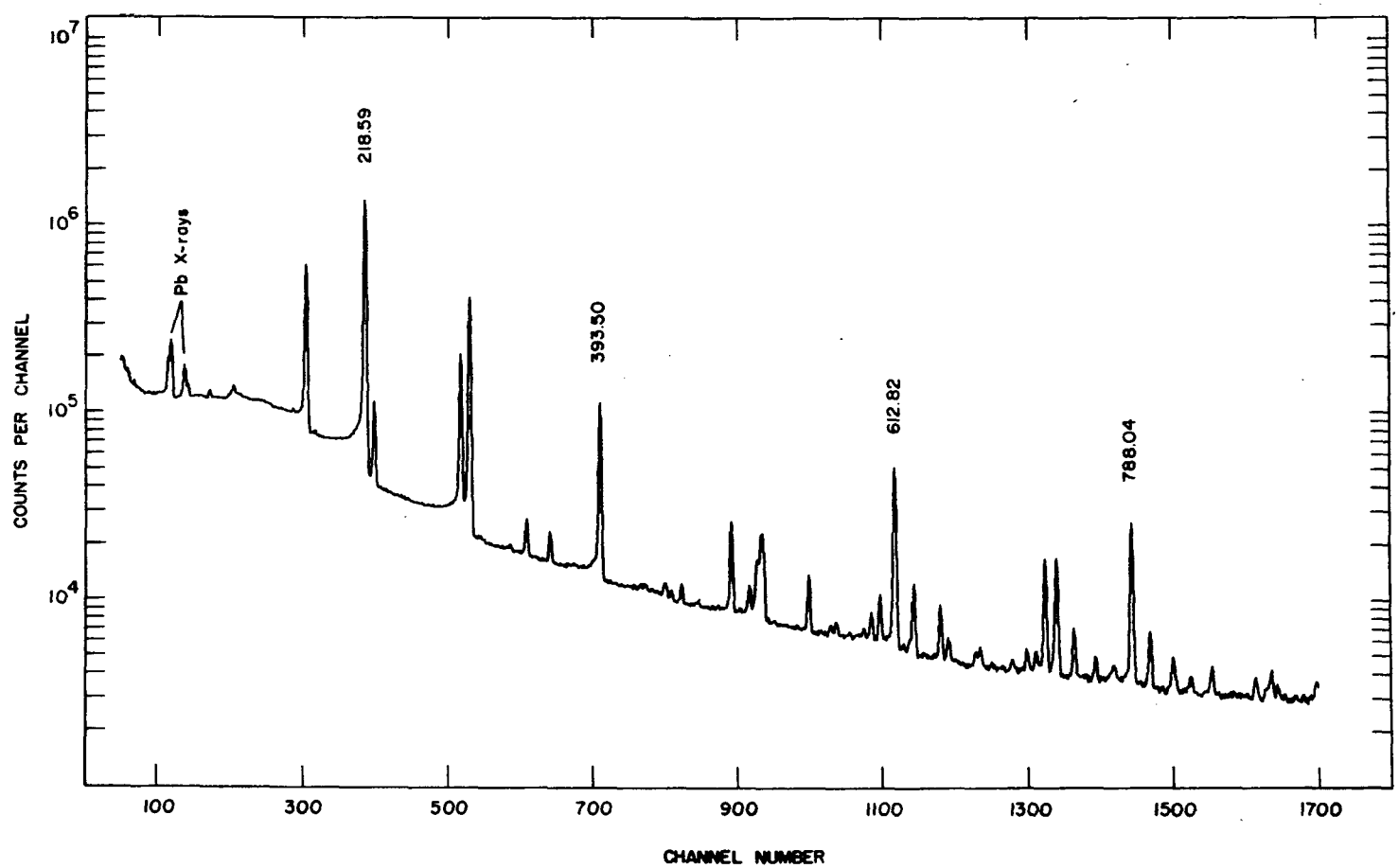

Figure 10. Gamma-ray spectrum for the decay of ^{139}Xe

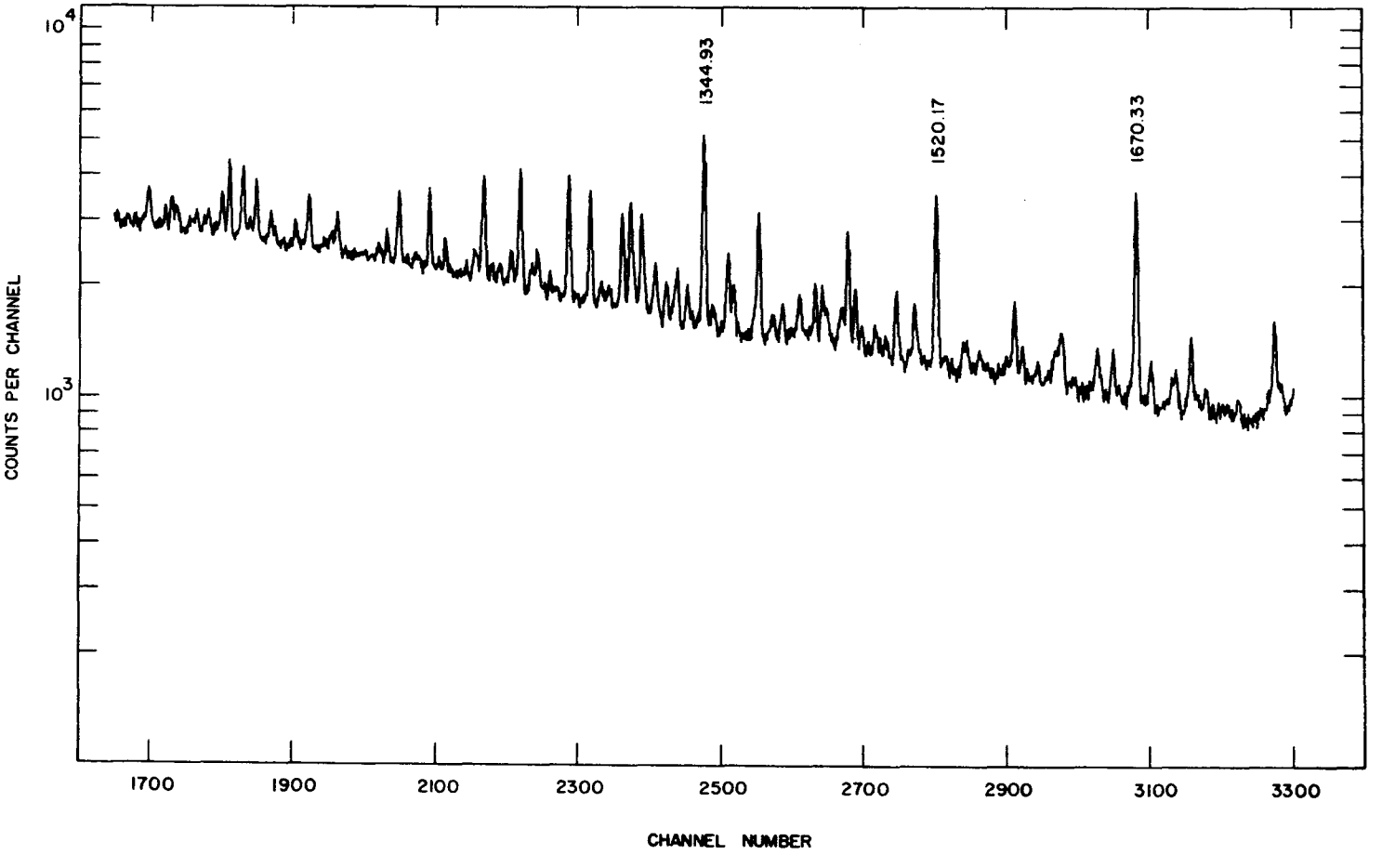

Figure 10. (Continued)

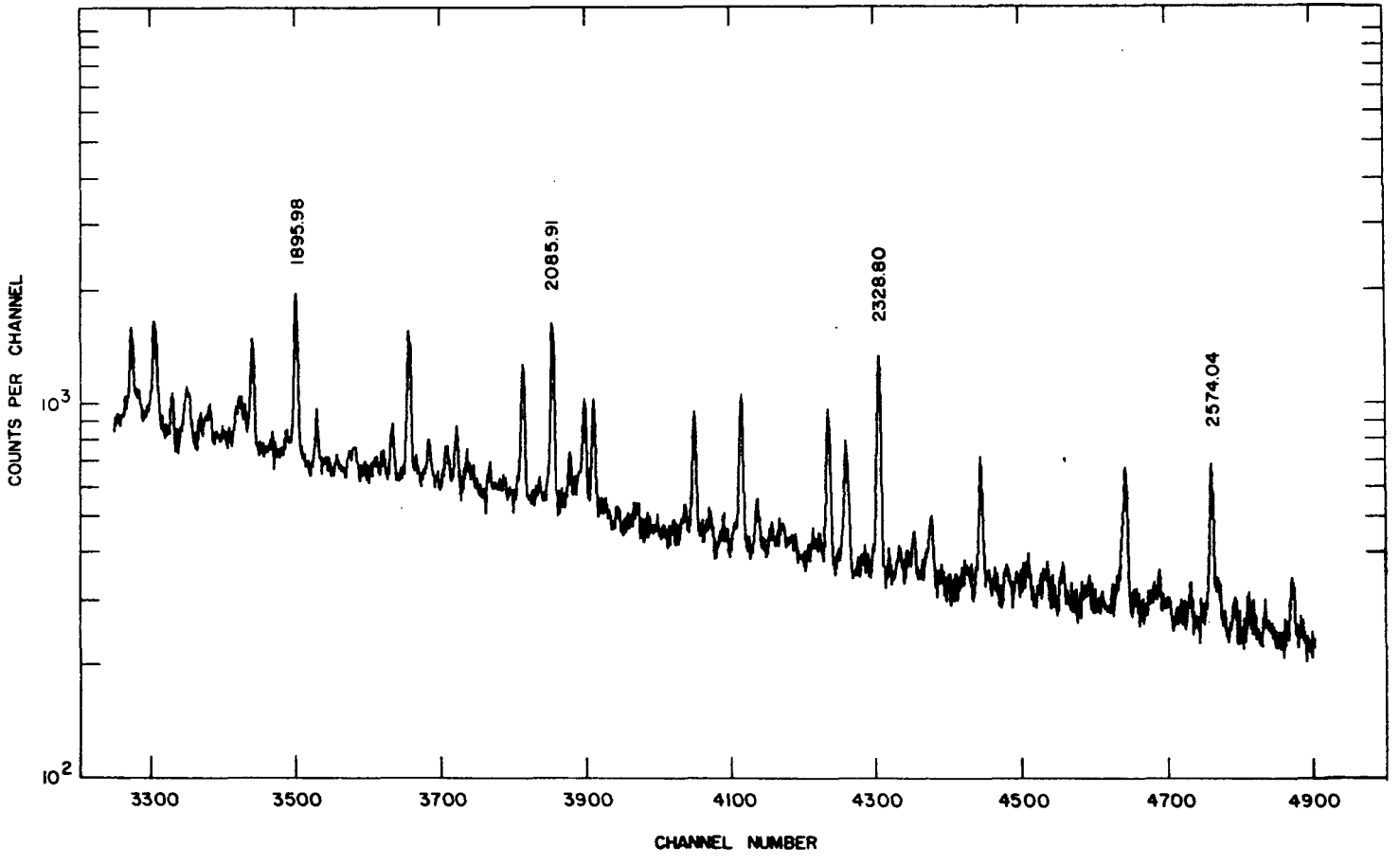

Figure 10. (Continued)

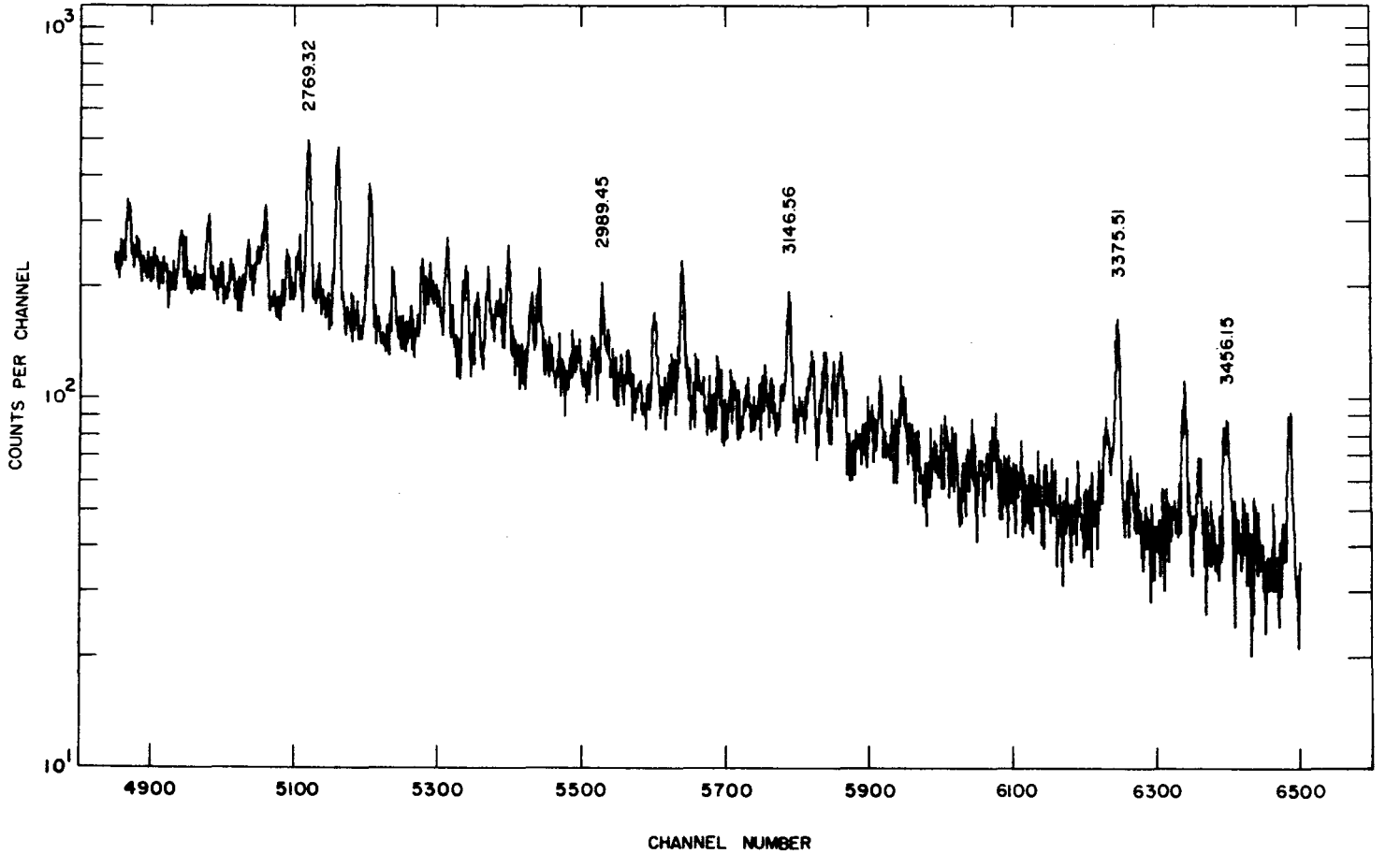

Figure 10. (Continued)

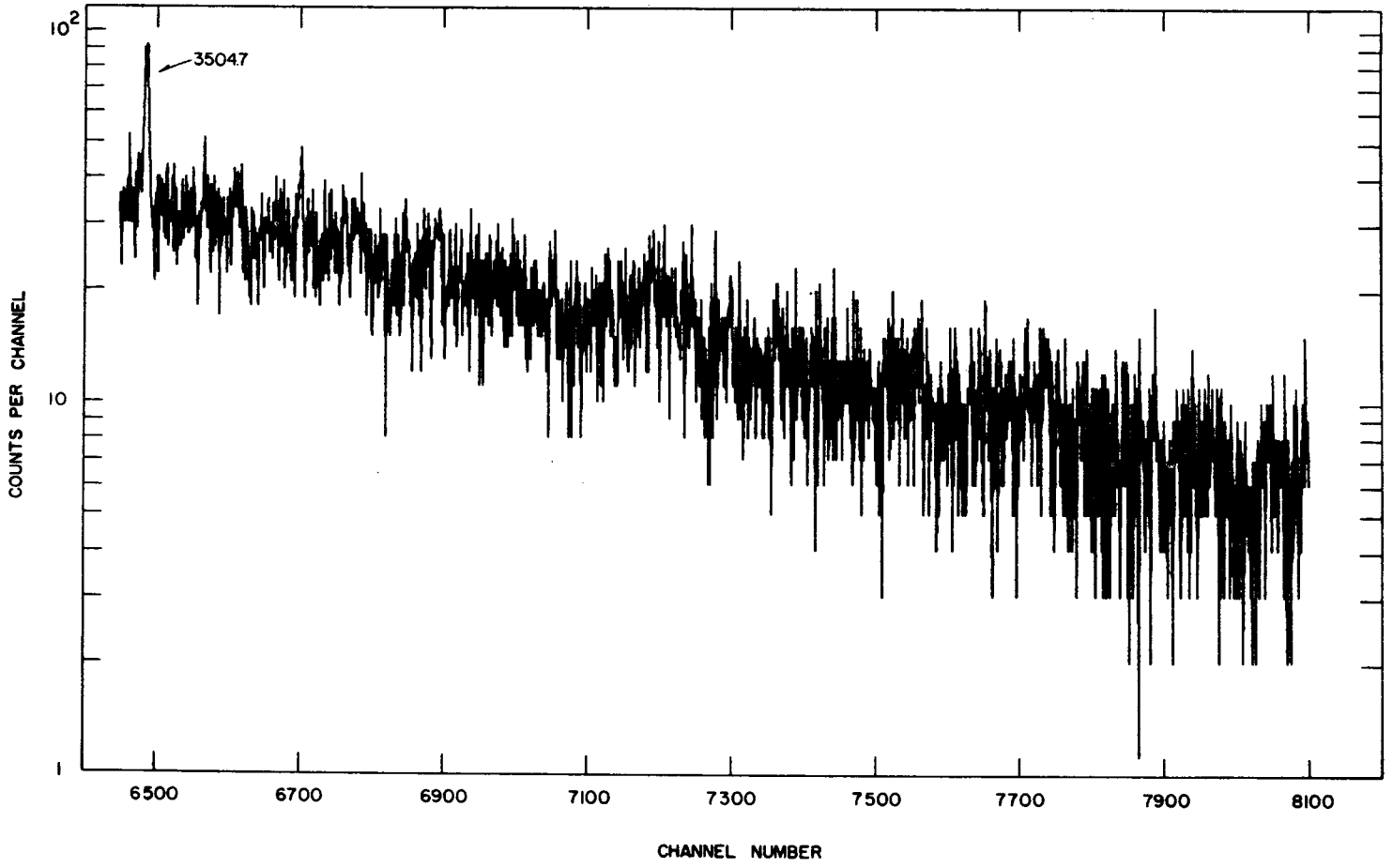

Figure 10. (Continued)

Table 4. Photopeaks observed in the decay of ^{139}Xe

Energy (keV)	Relative Intensity[1]	Intensity per 100 Decays[2]	Placement (keV)
55.74 ± 0.26	1.89 ± 0.54	0.10	
70.95 ± 0.39	4.63 ± 1.60	0.25	289 - 218
103.75 ± 0.06	5.65 ± 0.40	0.31	393 - 289
119.41 ± 0.38	1.24 ± 0.42	0.07	2304 - 2185
121.37 ± 0.08	6.90 ± 0.56	0.38	515 - 393
174.97 ± 0.04	355.76 ± 22.01	19.56	393 - 218
218.59 ± 0.03	1000.00 ± 56.03	54.98	218 - 0
225.38 ± 0.07	52.08 ± 4.92	2.86	515 - 289
289.78 ± 0.07	164.40 ± 9.78	9.04	289 - 0
296.53 ± 0.07	388.88 ± 21.62	21.38	515 - 218
326.77 ± 0.41	1.15 ± 0.42	0.06	
338.86 ± 0.07	10.71 ± 0.63	0.59	732 - 393
356.72 ± 0.08	8.84 ± 0.63	0.49	646 - 289
393.50 ± 0.06	120.29 ± 6.42	6.61	393 - 0
427.40 ± 0.36	1.06 ± 0.43	0.06	942 - 515
441.33 ± 0.70	1.65 ± 0.45	0.09	1461 - 1020
442.72 ± 0.45	2.76 ± 0.39	0.15	732 - 289
446.81 ± 0.32	1.24 ± 0.36	0.07	2099 - 1652
454.46 ± 0.13	3.47 ± 0.39	0.19	1461 - 1006
466.84 ± 0.30	1.31 ± 0.33	0.07	1652 - 1186
491.47 ± 0.04	25.78 ± 1.40	1.42	1006 - 515
498.18 ± 0.49	0.88 ± 0.36	0.05	891 - 393
505.07 ± 0.08	5.84 ± 0.49	0.32	1020 - 515
513.88 ± 0.11	15.01 ± 1.47	0.83	732 - 218
515.44 ± 0.14	9.21 ± 1.46	0.51	515 - 0
549.02 ± 0.04	10.34 ± 0.64	0.57	942 - 393
565.36 ± 0.32	1.08 ± 0.31	0.06	1508 - 942
569.64 ± 0.22	1.63 ± 0.32	0.09	1461 - 891
589.81 ± 0.38	1.07 ± 0.35	0.06	2328 - 1738
595.43 ± 0.13	3.49 ± 0.40	0.19	2103 - 1508
601.84 ± 0.07	9.30 ± 0.71	0.51	891 - 289
612.82 ± 0.04	98.30 ± 5.29	5.40	1006 - 393
624.33 ± 0.70	1.74 ± 0.88	5.40	
626.89 ± 0.11	14.03 ± 1.25	0.77	1020 - 393
646.50 ± 0.07	10.53 ± 0.76	0.58	646 - 0

[1]Measured relative to the 218.59-keV transition.

[2]Calculated from the ^{139}Cs level scheme with the 22% beta branching reported in Section III-A-2.

Table 4. (continued)

Energy (keV)	Relative Intensity[1]	Intensity per 100 Decays[2]	Placement (keV)
652.28 ± 0.13	4.17 ± 0.51	0.23	942 - 289
672.39 ± 0.18	2.49 ± 0.37	0.14	
675.79 ± 0.16	2.91 ± 0.38	0.16	2328 - 1652
699.64 ± 0.27	1.57 ± 0.36	0.09	1214 - 515
710.40 ± 0.18	3.19 ± 0.50	0.18	1652 - 942
716.96 ± 0.22	3.04 ± 0.49	0.17	1006 - 289
719.85 ± 0.55	1.18 ± 0.46	0.06	2373 - 1652
723.84 ± 0.06	32.21 ± 1.75	1.77	942 - 218
730.45 ± 0.27	4.10 ± 0.91	0.23	1020 - 289
732.42 ± 0.06	31.37 ± 1.87	1.72	732 - 0
745.16 ± 0.07	9.46 ± 0.57	0.52	1138 - 393
761.04 ± 0.16	3.55 ± 0.50	0.20	1652 - 891
773.39 ± 0.49	1.72 ± 0.56	0.09	2373 - 1599
775.61 ± 0.45	1.79 ± 0.56	0.10	1508 - 732
783.12 ± 0.54	1.10 ± 0.42	0.06	3156 - 2373
786.74 ± 0.65	3.87 ± 3.33	0.21	3372 - 2585
788.04 ± 0.08	60.22 ± 4.60	3.31	1006 - 218
801.62 ± 0.09	10.00 ± 0.71	0.55	1020 - 218
818.29 ± 0.15	4.98 ± 0.55	0.27	3147 - 2328
820.50 ± 0.44	1.56 ± 0.48	0.09	2328 - 1508
832.41 ± 0.24	1.86 ± 0.37	0.10	2936 - 2103
847.45 ± 0.12	4.49 ± 0.43	0.25	2586 - 1738
879.74 ± 0.18	2.66 ± 0.39	0.15	1395 - 515
888.60 ± 0.52	1.24 ± 0.57	0.07	1831 - 942
891.76 ± 0.18	3.83 ± 0.58	0.21	891 - 0
896.26 ± 0.31	1.93 ± 0.51	0.11	1186 - 289 [3]
896.26 ± 0.31	1.93 ± 0.51	0.11	2727 - 1831 [3]
924.48 ± 0.56	1.98 ± 1.10	0.11	1214 - 289
926.01 ± 0.61	1.80 ± 1.10	0.10	2620 - 1694
937.94 ± 0.35	1.26 ± 0.34	0.07	
942.61 ± 0.22	2.13 ± 0.37	0.12	942 - 0
946.46 ± 0.27	1.70 ± 0.38	0.09	1461 - 515
957.28 ± 0.39	1.31 ± 0.40	0.07	3937 - 2979
961.09 ± 0.39	1.35 ± 0.39	0.07	2099 - 1138
967.29 ± 0.47	1.17 ± 0.42	0.06	1186 - 218
970.32 ± 0.42	1.35 ± 0.44	0.07	3156 - 2185
980.59 ± 0.18	2.93 ± 0.44	0.16	
986.02 ± 0.11	5.99 ± 0.51	0.33	2585 - 1599

[3]Denotes multiple placement.

Table 4. (continued)

Energy (keV)	Relative Intensity[1]	Intensity per 100 Decays[2]	Placement (keV)
996.19 ± 0.11	5.79 ± 0.49	0.32	1214 - 218
1001.68 ± 0.35	1.42 ± 0.37	0.08	1395 - 393
1006.25 ± 0.14	2.07 ± 0.22	0.11	1652 - 646 [3]
1006.25 ± 0.14	2.07 ± 0.22	0.11	1738 - 732 [3]
1017.67 ± 0.33	2.35 ± 0.57	0.13	3815 - 2797
1021.38 ± 0.60	0.84 ± 0.39	0.05	2620 - 1599
1036.28 ± 0.29	1.76 ± 0.45	0.10	
1046.31 ± 0.15	4.83 ± 0.57	0.27	3374 - 2328
1067.56 ± 0.24	2.54 ± 0.48	0.14	1461 - 393
1099.45 ± 0.52	1.06 ± 0.46	0.06	
1105.57 ± 0.29	2.06 ± 0.44	0.11	1395 - 289
1114.48 ± 0.12	5.96 ± 0.57	0.33	1508 - 393
1137.52 ± 0.10	7.06 ± 0.54	0.39	1652 - 515
1149.23 ± 0.26	2.20 ± 0.45	0.12	
1171.50 ± 0.42	1.45 ± 0.45	0.08	1461 - 289
1176.27 ± 0.55	1.62 ± 0.59	0.09	1395 - 218
1178.73 ± 0.12	9.04 ± 0.79	0.50	1693 - 515
1190.59 ± 0.60	0.90 ± 0.42	0.05	2585 - 1395
1199.43 ± 0.23	2.39 ± 0.43	0.13	2852 - 1652
1206.45 ± 0.10	11.22 ± 0.87	0.62	1599 - 393
1214.89 ± 0.42	1.28 ± 0.40	0.07	1214 - 0
1219.33 ± 0.21	2.77 ± 0.45	0.15	2727 - 1508
1228.81 ± 0.51	1.05 ± 0.45	0.06	2967 - 1738
1242.88 ± 0.08	10.50 ± 0.75	0.58	1461 - 218
1259.26 ± 0.09	9.31 ± 0.70	0.51	1652 - 393
1273.14 ± 0.52	1.13 ± 0.47	0.06	3372 - 2099
1289.47 ± 0.19	7.77 ± 1.12	0.43	1508 - 218
1291.40 ± 0.42	3.10 ± 1.03	0.17	2799 - 1508
1297.85 ± 0.19	7.16 ± 1.10	0.39	2304 - 1006
1299.79 ± 0.88	1.46 ± 0.97	0.08	3130 - 1831
1309.39 ± 0.79	1.63 ± 1.02	0.09	1599 - 289
1316.35 ± 0.35	1.92 ± 0.50	0.11	3937 - 2620
1324.38 ± 0.21	3.32 ± 0.54	0.18	2510 - 1186
1344.93 ± 0.07	20.45 ± 1.21	1.12	1738 - 393
1351.64 ± 0.36	1.70 ± 0.50	0.09	3937 - 2586
1362.91 ± 0.12	5.11 ± 0.46	0.28	1652 - 289
1367.19 ± 0.16	3.31 ± 0.39	0.18	2099 - 732
1386.19 ± 0.11	10.33 ± 0.79	0.57	2328 - 942
1404.16 ± 0.25	2.18 ± 0.41	0.12	2799 - 1395
1416.94 ± 0.20	2.78 ± 0.43	0.15	2423 - 1006
1428.70 ± 0.21	3.17 ± 0.50	0.17	

Table 4. (continued)

Energy (keV)	Relative Intensity[1]	Intensity per 100 Decays[2]	Placement (keV)
1434.13 ± 0.24	2.95 ± 0.48	0.16	1652 - 218
1437.68 ± 0.66	1.32 ± 0.52	0.07	1831 - 393
1448.66 ± 0.32	1.94 ± 0.45	0.11	1738 - 289
1453.32 ± 0.10	8.64 ± 0.68	0.48	2185 - 732
1458.98 ± 0.22	2.85 ± 0.51	0.16	
1489.96 ± 0.39	4.37 ± 1.19	0.24	2510 - 1020
1503.12 ± 0.57	2.46 ± 1.24	0.14	3156 - 1652
1520.17 ± 0.08	14.67 ± 0.86	0.81	1738 - 218
1540.80 ± 0.54	1.20 ± 0.40	0.07	2936 - 1395
1543.59 ± 0.59	1.12 ± 0.30	0.06	3374 - 1831
1579.52 ± 0.45	3.65 ± 1.64	0.20	2586 - 1006
1584.69 ± 0.36	1.42 ± 0.37	0.08	2799 - 1214 [3]
1584.69 ± 0.36	1.42 ± 0.37	0.08	2979 - 1395 [3]
1609.33 ± 0.35	1.85 ± 0.39	0.10	
1612.45 ± 0.37	2.62 ± 0.51	0.14	1831 - 218
1614.97 ± 0.30	2.82 ± 0.52	0.16	2754 - 1138
1641.70 ± 0.29	2.71 ± 0.48	0.15	
1652.80 ± 0.32	2.03 ± 0.48	0.11	1652 - 0
1666.18 ± 0.63	0.83 ± 0.36	0.05	2852 - 1186
1670.33 ± 0.08	19.97 ± 1.12	1.10	2185 - 515
1681.13 ± 0.26	1.88 ± 0.35	0.10	3375 - 1693
1699.82 ± 0.34	1.87 ± 0.41	0.10	
1711.44 ± 0.17	4.13 ± 0.45	0.23	3815 - 2103
1722.59 ± 0.63	0.93 ± 0.37	0.05	3375 - 1652
1765.18 ± 0.63	0.77 ± 0.31	0.04	2979 - 1214
1773.84 ± 0.13	5.91 ± 0.50	0.32	2063 - 289
1776.91 ± 0.41	1.81 ± 0.38	0.10	2423 - 646 [3]
1776.91 ± 0.41	1.81 ± 0.38	0.10	2797 - 1020 [3]
1786.55 ± 0.45	1.13 ± 0.36	0.06	
1790.85 ± 0.18	6.81 ± 0.87	0.37	2797 - 1006
1792.96 ± 0.50	2.17 ± 0.75	0.12	2799 - 1006
1803.99 ± 0.25	2.20 ± 0.40	0.12	
1814.07 ± 0.36	2.16 ± 0.49	0.12	2103 - 289
1816.74 ± 0.36	2.22 ± 0.49	0.12	
1831.52 ± 0.45	1.35 ± 0.43	0.07	1831 - 0
1851.85 ± 0.49	1.98 ± 0.57	0.11	3504 - 1652
1854.51 ± 0.52	2.31 ± 0.55	0.13	2797 - 942
1857.64 ± 0.42	2.01 ± 0.47	0.11	2373 - 515
1862.40 ± 0.74	2.77 ± 1.99	0.15	2754 - 891
1864.03 ± 0.45	4.51 ± 2.00	0.25	2510 - 646
1895.98 ± 0.09	11.05 ± 0.73	0.61	2185 - 289

Table 4. (continued)

Energy (keV)	Relative Intensity[1]	Intensity per 100 Decays[2]	Placement (keV)
1911.42 ± 0.21	2.17 ± 0.32	0.12	2304 - 393
1935.07 ± 0.49	0.96 ± .29	0.05	2328 - 393
1939.48 ± 0.32	1.46 ± 0.32	0.08	2586 - 646
1967.27 ± 0.26	2.26 ± 0.41	0.12	2185 - 218
1979.57 ± 0.11	9.48 ± 0.75	0.52	2373 - 393
1994.18 ± 0.36	1.92 ± 0.49	0.11	4299 - 2304
2006.79 ± 0.37	1.82 ± 0.41	0.10	
2015.11 ± 0.17	2.80 ± 0.34	0.15	2304 - 289
2021.80 ± 0.40	1.31 ± 0.30	0.07	2754 - 732
2025.13 ± 0.47	1.27 ± 0.30	0.07	2967 - 942
2039.13 ± 0.40	1.28 ± 0.35	0.07	2328 - 289
2063.90 ± 0.12	7.51 ± 0.63	0.41	2063 - 0
2085.91 ± 0.10	12.02 ± 0.78	0.66	2304 - 218
2099.48 ± 0.20	2.28 ± 0.31	0.13	2099 - 0
2103.69 ± 0.56	1.04 ± 0.31	0.06	2103 - 0
2110.12 ± 0.13	5.22 ± 0.42	0.29	2328 - 218
2116.88 ± 0.11	5.85 ± 0.43	0.32	2510 - 393
2192.32 ± 0.13	6.08 ± 0.50	0.33	2585 - 393
2204.56 ± 0.64	0.80 ± 0.35	0.04	3147 - 942
2227.28 ± 0.25	6.59 ± 1.48	0.36	2620 - 393
2238.42 ± 0.55	1.30 ± 0.40	0.07	2754 - 515 [3]
2238.42 ± 0.55	1.30 ± 0.40	0.07	3130 - 891 [3]
2249.68 ± 0.40	1.24 ± 0.31	0.07	
2255.31 ± 0.69	0.81 ± 0.31	0.04	3908 - 1652 [3]
2255.31 ± 0.69	0.81 ± 0.31	0.04	3147 - 891 [3]
2291.61 ± 0.11	7.19 ± 0.52	0.40	2510 - 218
2304.97 ± 0.16	5.19 ± 0.47	0.29	2304 - 0
2328.80 ± 0.09	11.33 ± 0.69	0.62	2328 - 0
2366.97 ± 0.22	2.38 ± 0.31	0.13	2585 - 218
2403.75 ± 0.13	4.66 ± 0.41	0.26	2797 - 393
2423.62 ± 0.40	0.80 ± 0.20	0.04	2423 - 0
2430.28 ± 0.56	0.68 ± 0.22	0.04	3372 - 942
2437.75 ± 0.32	1.71 ± 0.29	0.09	2727 - 289
2451.65 ± 0.57	0.78 ± 0.28	0.04	2967 - 515
2464.61 ± 0.46	0.98 ± 0.26	0.05	2979 - 515 [3]
2464.61 ± 0.46	0.98 ± 0.26	0.05	2754 - 289 [3]
2507.65 ± 0.55	1.44 ± 0.43	0.08	2797 - 289
2510.41 ± 0.18	4.91 ± 0.53	0.27	2510 - 0
2534.98 ± 0.47	1.14 ± 0.32	0.06	2754 - 218
2574.04 ± 0.12	6.14 ± 0.46	0.34	2967 - 393
2578.93 ± 0.46	1.06 ± 0.28	0.06	2797 - 218

Table 4. (continued)

Energy (keV)	Relative Intensity[1]	Intensity per 100 Decays[2]	Placement (keV)
2613.71 ± 0.71	0.65 ± 0.27	0.04	3504 - 891
2633.75 ± 0.22	1.88 ± 0.26	0.10	2852 - 218
2640.13 ± 0.64	0.60 ± 0.25	0.03	3372 - 732
2673.40 ± 0.50	1.02 ± 0.30	0.06	
2693.40 ± 0.51	1.44 ± 0.42	0.08	3908 - 1214
2736.71 ± 0.31	2.12 ± 0.42	0.12	3130 - 393
2754.16 ± 0.36	1.21 ± 0.26	0.07	2753 - 0
2761.57 ± 0.36	1.22 ± 0.26	0.07	2979 - 218
2769.32 ± 0.12	5.33 ± 0.41	0.29	3908 - 1138
2790.89 ± 0.14	4.80 ± 0.44	0.26	4299 - 1508
2815.03 ± 0.15	4.04 ± 0.40	0.22	
2832.84 ± 0.37	1.12 ± 0.25	0.06	
2854.16 ± 0.40	1.57 ± 0.33	0.09	
2872.65 ± 0.25	2.15 ± 0.32	0.12	3815 - 942
2886.62 ± 0.36	1.46 ± 0.34	0.08	
2903.79 ± 0.39	1.41 ± 0.31	0.08	4299 - 1395
2911.70 ± 0.44	1.20 ± 0.31	0.07	3130 - 218
2918.32 ± 0.27	2.16 ± 0.35	0.12	
2936.25 ± 0.47	0.96 ± 0.26	0.05	2936 - 0
2941.85 ± 0.34	1.45 ± 0.29	0.08	
2989.45 ± 0.36	1.26 ± 0.27	0.07	3504 - 515
3028.55 ± 0.36	1.24 ± 0.27	0.07	
3110.80 ± 0.70	0.70 ± 0.40	0.04	3504 - 393
3130.63 ± 0.59	1.43 ± 0.53	0.08	3130 - 0
3146.56 ± 0.31	1.13 ± 0.19	0.06	3147 - 0
3156.28 ± 0.40	0.80 ± 0.20	0.04	3156 - 0
3168.66 ± 0.37	1.06 ± 0.20	0.06	3815 - 646
3214.84 ± 0.47	0.72 ± 0.20	0.04	3504 - 289
3375.51 ± 0.19	2.73 ± 0.28	0.15	3375 - 0
3424.78 ± 0.53	1.28 ± 0.36	0.07	
3504.71 ± 0.28	1.16 ± 0.19	0.06	3504 - 0

Figure 11 shows the level scheme deduced for ^{139}Cs from the gamma-gamma coincidence data and gamma-ray energy sums. A few transitions have been used twice in the level scheme and these are indicated with an asterisk. Weak coincidence data support the double placement of the 1006-keV transition but the other double placements are based only upon energy sums and more extensive coincidence data would be required to definitely assign these transitions to one or the other of the two placements. In this level scheme 195 of 221 observed gamma-ray transitions have been placed in 50 excited levels. The transitions placed account for more than 98% of the total gamma-ray intensity following the beta decay of ^{139}Xe.

A list of the observed gamma-gamma coincidences is given in Table 5. The first column gives the gating transition, the second column lists the transitions definitely established as being in coincidence with the gating transition and the last column contains those transitions for which there is some indication of coincidence with the gating transition but either the statistics are poor or there is not a dramatic enhancement over nearby background gates to definitely establish that a coincidence exists.

In the paragraphs which follow, arguments will be presented in support of the spin and parity assignments for the individual levels in ^{139}Cs. No reaction data are available which could provide information on the spins of these states,

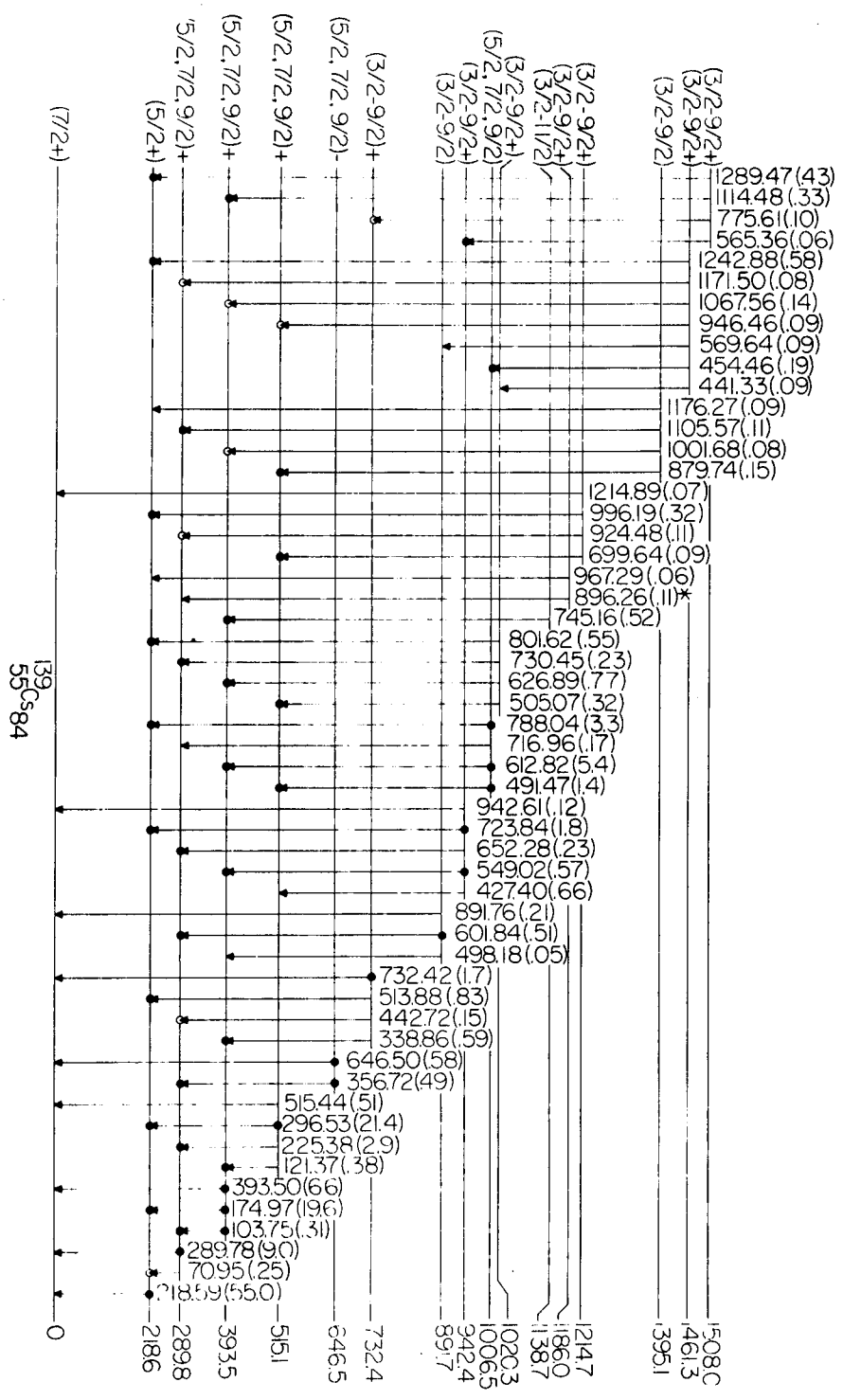

Figure 11. The ^{139}Cs level scheme deduced from the decay of ^{139}Xe

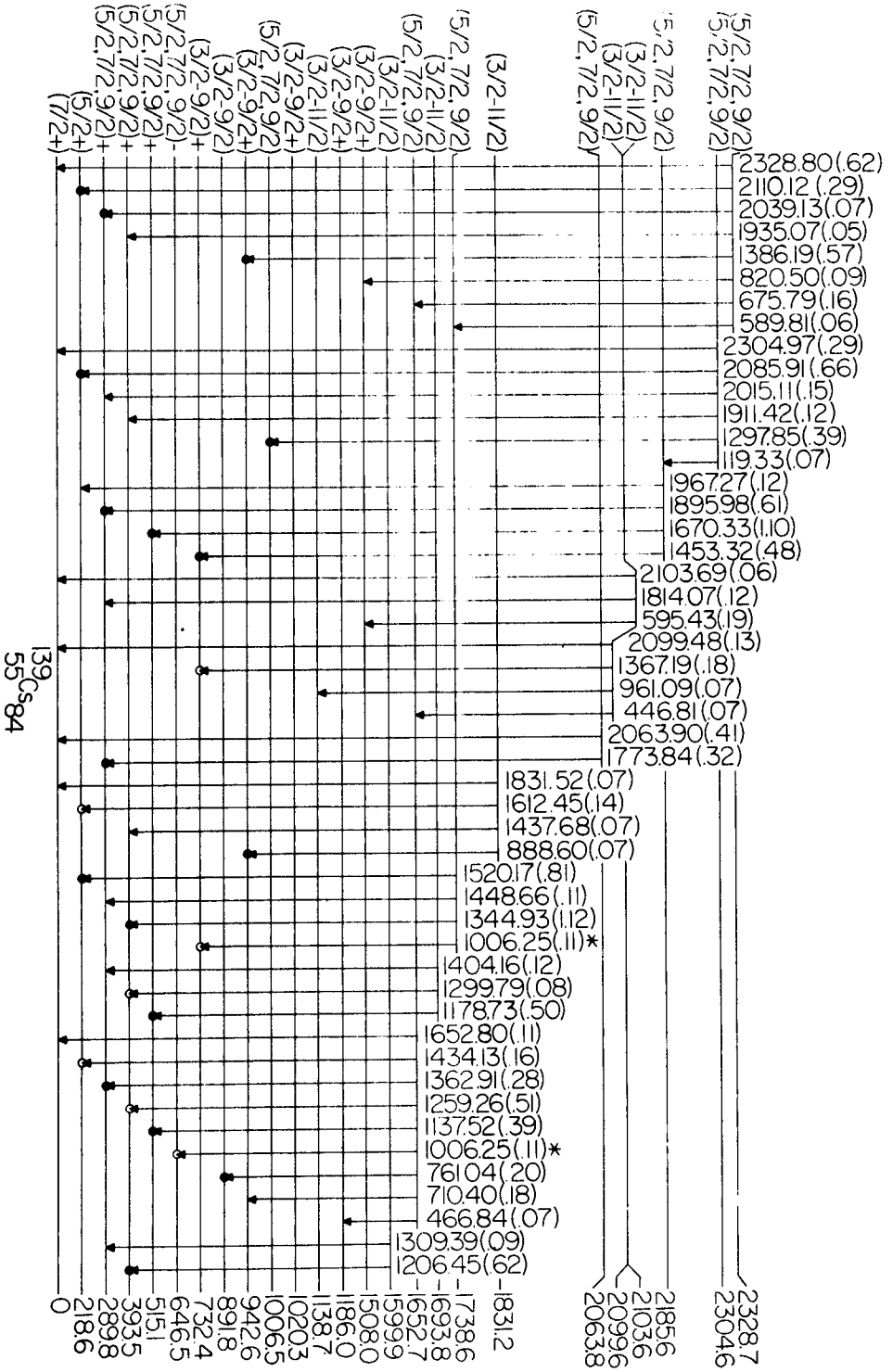

Figure 11. (Continued) Level spacing below 1831 keV is not to scale.

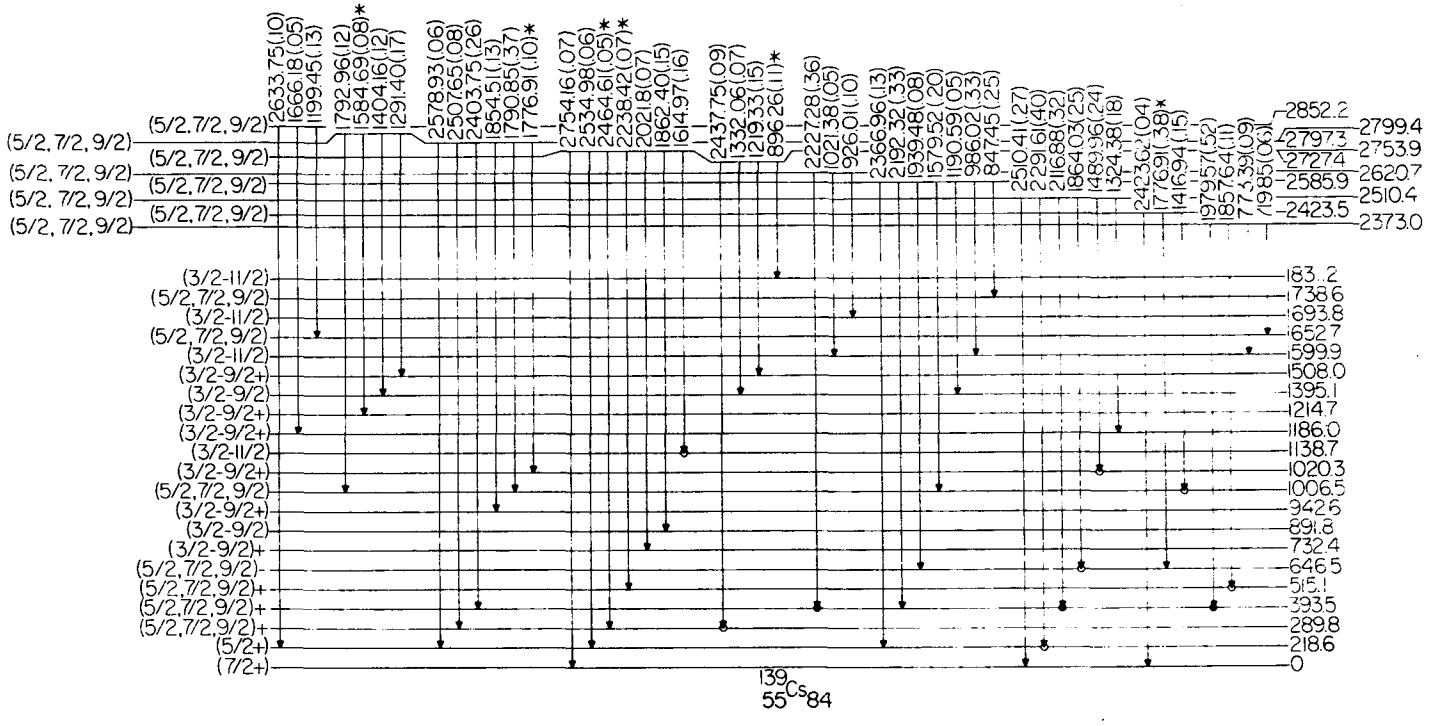

Figure 11. (Continued) Level spacing below 2373 keV is not to scale.

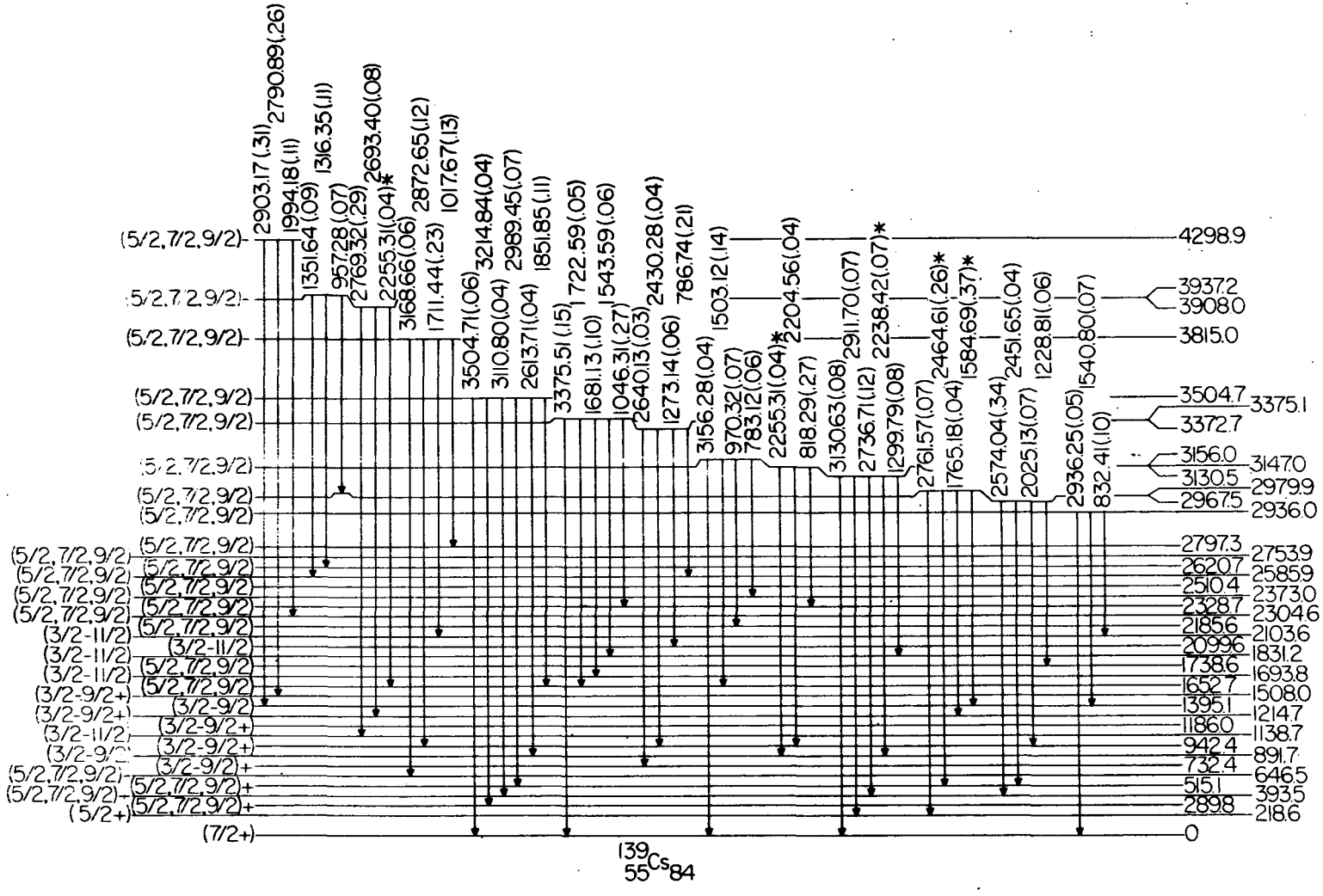

Figure 11. (Continued) Level spacing below 2936 keV is not to scale.

Table 5. Coincidence information for the decay of ^{139}Xe

Gate (keV)	Definite coincidences	Possible coincidences
121	103, 174, 218, 393	
174	121, 218, 338, 549, 612, 626, 745, 775, 1206, 1344, 1670, 1979, 2192, 2227, 2574	1259, 1297, 1614, 1699 1773, 1790
218	121, 174, 296, 338, 491, 505, 513, 549, 612, 626, 723, 745, 788, 801, 818, 847, 1114, 1137, 1178, 1206, 1289, 1297	71, 579, 672, 986, 996, 1046, 1162, 1242, 1259
289	103, 225, 356, 442, 491, 601, 612, 730, 1362, 1670, 1773, 1896, 2039	549, 652, 832, 924, 942, 1105, 1489, 2135, 2304, 2437
296	218, 491, 505, 612, 699, 1137, 1178, 1670	879, 1114, 1242, 1857, 1711, 2099
338	174, 218, 393, 1453	
356	289	1006, 1864
393	338, 549, 612, 626	1001, 1067, 1206, 1259 1297, 1344, 1386
491	225, 296, 515	121, 218, 533
549	174, 289, 393, 1386	565
601	289	761
612	103, 174, 218, 393, 454, 1297	1790
626	174, 393	296
646		1006
723	218, 1242, 1386	888

Table 5. (Continued)

Gate (keV)	Definite coincidences	Possible coincidences
732	1453	775, 1206
745	174, 393, 1046	601
788	103, 218	
1206	393	174, 732
1242	393, 549, 723	
1259	393	
1344	121, 174, 218, 393	847
1520	218, 847	
1579		466
1614		745
1670	174, 218, 225, 296, 393	
1773	289	
1790	788	174, 218, 491, 612
2192	174	218, 393
2574	121, 174, 218, 393	

so the arguments will be based primarily on the log ft values deduced in the present work.

Ground state: The results of an equilibrium run on the decays of ^{139}Xe and ^{139}Cs yielded a value of (22 ± 6)% for the ground state beta branching, leading to a log ft value of 6.6. The ground-state spin of ^{139}Cs appears to be 7/2+ based upon comparisons with the neighboring odd-A Cs isotopes (51). Using this value and the log ft value given above leads to possible spin and parity assignments of 5/2±, 7/2±, and 9/2± for the ^{139}Xe ground state. Among the other N = 85 isotones whose spins have been determined are ^{143}Ce with 3/2-, ^{145}Nd with 7/2-, ^{147}Sm with 7/2-, and ^{149}Gd with 7/2- (51). The ^{143}Ce nucleus has a closed $g_{7/2}$ proton shell, and the other nuclei mentioned above have Z > 58. Unfortunately, no spin measurements have been made for N = 85 nuclei with Z < 58, so it is not obvious whether the 3/2- spin of ^{143}Ce is associated with the shell closure at Z = 58 or whether it is indicative of a trend for N = 85 nuclei as Z decreases. For three identical spin 7/2 particles the possible total spin values are 3/2, 5/2, 7/2, 9/2, 11/2, and 15/2 (52). The overriding consideration in resolving this matter appears to be the existence of the 22% ground-state beta branch in the decay of ^{139}Xe to ^{139}Cs. If the ground-state spin of ^{139}Xe were 3/2-, the beta transition to the ground state of ^{139}Cs would require a spin change of 2, and a branching ratio as high as

22% would then be very unlikely. Consequently, the 7/2- assignment is favored for the ^{139}Xe ground state, and the spin and parity predictions for the levels in ^{139}Cs will be based on this assignment.

218.6-keV level: This level is assumed to be the first excited state because of the large gamma-ray intensity observed in the 218.59-keV transition and the large number of gamma-gamma coincidences observed with this transition. In previous studies of this decay (12 - 15) this level was also taken to be the first excited state. The level is populated with a 2.3% beta branch and the log f_1t value is 9.2, leading to possible spin and parity assignments ranging from 3/2+ to 11/2+. Achterberg et al. (15) have reported an internal conversion coefficient measurement leading to E2, M1 multipolarity for the 218.59-keV transition. This would eliminate the possibility of negative parity for this level, so the possible assignments are then limited to 5/2, 7/2, and 9/2 with positive parity. The systematics of the odd-A Cs isotopes below A = 139 favor the 5/2+ assignment for this level.

289.8-keV level: This level was established by the existence of a strong 289.78-keV transition, the observation of several coincidence relations involving this transition, and the fact that this transition is not in coincidence with the 218.59-keV transition. The level is populated with a beta

branch of 2.6% and the log f_1t value is 9.1. The internal conversion coefficient measurement of Achterberg et al. (15) indicate that the 289.78-keV transition has E2, M1 multipolarity. Thus the range of possible spin values could extend from 3/2 to 11/2, with positive parity. However, if the transition has some M1 mixture then the allowed range would only extend from 5/2 to 9/2.

393.5-keV level: This level was established by the existence of coincidence relations with the transitions depopulating the two lower lying excited states. The level is populated with a beta branch of 16.3% and the log ft value is 6.6. The ICC measurements of Achterberg et al. (15) indicate that the 174.97-kev transition to the 218.6-keV level has M1 (+E2) character and that the 103.75-keV transition to the 289.8-keV level has M1 character. These values rule out the possibility of negative parity for this level, so the possible assignments are 5/2, 7/2, and 9/2 with positive parity.

515.1-keV level: This level was established by the existence of coincidence relations involving transitions from each of the three lower lying excited states. The log ft value of 6.4 was calculated using the observed 20.8% beta branching ratio. The 296.53-keV transition has been reported to have E2-M1 character by Achterberg et al. (15). These considerations lead to possible spin assignments of 5/2, 7/2,

and 9/2, with positive parity.

646.5-keV level: This level was established on the basis of the coincidence relation observed between the 356.72-keV transition and the 289.78-keV transition. The level is fed by a 0.6% beta branch and the log f_1t value is 9.7. A measurement of the ICC for the 356.72-keV transition by Achterberg et al. (15) indicates that this transition has M2, E3 character. These considerations allow possible spin assignments ranging from 3/2 to 11/2, with negative parity for this level.

732.4-keV level: This level was established by the existence of three different coincidence relations with transitions depopulating lower lying levels. The level is fed with a beta branch of 2.2% and the log f_1t value is 8.9. The ICC values measured by Achterberg et al. (15) indicate that the ground-state transition has M1, E2 character and that the 338.86-keV transition to the 393.5-keV level has E2, M1 character. These results lead to possible spin and parity assignments ranging from 3/2 to 11/2, with positive parity. However, if the spin of the 218.6-keV first excited state is 5/2+, as the systematics suggest, then the upper limit of this range will be 9/2+.

891.7-keV level: This level was established by the coincidence observed between the 601.84-keV transition and the 289.78-keV transition. The level is fed by a beta branch

of 0.2% and the log f_1t value is 9.9, leading to possible spin and parity assignments of 3/2+, 5/2±, 7/2±, 9/2±, and 11/2+. Again, a 5/2+ assignment for the 218.6-keV level would make 9/2+ the highest possible assignment for this level.

942.4-keV level: This level was established using three different coincidence relations. The beta feeding is 1.4% and the log f_1t value is 9.0, which leads to possible spin and parity assignments of 3/2+, 5/2±, 7/2±, 9/2±, or 11/2+. However, the highest spin possible would be 9/2+ if the 218.6-keV level has the 5/2+ assignment.

1006.5-keV level: This level was established through the observation of three different coincidence relations. The log ft value of 6.6 is based on the observed 8.4% beta branching ratio. This leads to possible spin assignments including 5/2, 7/2, and 9/2,

Levels from 1020.3 keV to 1599.9 keV: Eight levels were established within this energy region, with indefinite parity. seven of which were established by coincidence relations. For each of these levels, the log f_1t value is between 8.7 and 10.3, which leads to possible spin and parity assignments of 3/2+, 5/2±, 7/2±, 9/2±, and 11/2+. The levels at 1020.3 keV, 1186.0 keV, 1214.7 keV, 1395.1 keV, 1461.3 keV, and 1508.0 keV all have depopulating transitions going to the 218.6-keV level, so the 11/2+ possibility hinges on

the uncertainty of the spin assignment for the 218.6-keV level. If, as is reasonable to assume, the spin assignment for the 218.6-keV level is 5/2+, then the upper limit is 9/2+ for these levels. Additional levels established in this region lie at energies of 1138.7 keV and 1599.9 keV. With the exception of the 1186.0-keV level, all of the levels in this region were established by using coincidence relations. The 1186.0-keV level was established by the energy agreement of three gamma-ray cascades, two of which depopulate the level.

1652.7-keV level: A total of nine gamma-ray transitions were placed from this level, six of these having been observed in coincidence with transitions depopulating lower levels. The log ft value is 7.1, which allows the possible spin and parity assignments to include 5/2±, 7/2±, and 9/2±.

1693.8-keV level: Two of the three transitions leaving this level were observed to be in coincidence with transitions depopulating lower lying levels. The log f_1t value is 9.0, which allows for a possible spin and parity assignment of 3/2+, 5/2±, 7/2±, 9/2±, or 11/2+.

1738.6-keV level: This level was established by the coincidence relations observed involving three of the four gamma-ray transitions placed leaving this level. The log ft value is 6.9, leading to possible spin assignments of 5/2, 7/2, and 9/2, with indefinite parity.

1831.2-keV level: This level was established by the existence of two coincidence relations. The log f_1t value of 9.4 leads to possible spin and parity assignments including 3/2+, 5/2±, 7/2±, 9/2±, and 11/2+.

2063.8-keV level: The coincidence between the 1773.84-keV transition and the 289.78-keV transition was used to establish this level. The log ft value is 7.1, so the possible spin assignment is included among the values 5/2, 7/2, and 9/2, with indefinite parity.

2099.6-keV level: This level was established by one weak coincidence and energy agreement in three other cascades. The log f_1t value is 8.6, indicating a range of possible spin values including 3/2+, 5/2±, 7/2±, 9/2±, and 11/2+.

2103.6-keV level: This level was established entirely on the basis of energy agreement with three depopulating transitions and three additional transitions to this level from higher lying levels. The beta branch is less than 0.05% and the log f_1t value is greater than 9.6, which leads to a range of possible spin and parity assignments including 3/2+, 5/2±, 7/2±, 9/2±, and 11/2+.

Levels between 2185.9 keV and 3504.7 keV: Several levels were established at energies within this range, and for each of these the log ft value was within the range from 6.0 to 7.2. The log f_1t value for each of the beta transi-

tions is less than 8.5, and consequently the possible spin assignments for these levels are 5/2, 7/2, and 9/2, with no information on the parity assignment. Coincidence relations were used in establishing the levels at energies of 2185.6 keV, 2304.6 keV, 2328.7 keV, 2373.0 keV, 2423.5 keV, 2510.4 keV, 2620.7 keV, 2727.4 keV, and 2967.5 keV. The other levels in this range were established entirely on the basis of energy agreement among at least three cascades involving transitions either populating or depopulating each level. These levels were established at energies of 2585.9 keV, 2797.3 keV, 2799.4 keV, 2852.2 keV, 2936.0 keV, 2979.9 keV, 3130.5 keV, 3147.0 keV, 3156.0 keV, 3372.7 keV, 3375.1 keV, and 3504.7 keV.

Levels above 3815 keV: The levels at energies of 3815.0 keV, 3908.0 keV, 3937.2 keV, and 4299.0 keV were established on the basis of energy agreement among at least three gamma-ray cascades originating on each level. The log ft values for the beta transitions to these levels range from 4.7 to 5.6, which is well below the the minimum of 5.9 for first-forbidden transitions. Consequently these transitions are allowed, and the spin and parity assignments for these levels are limited to the values 5/2-, 7/2-, and 9/2-.

2. Beta decay energy and branching

The Q-value for the beta decay of ^{139}Xe was measured to be 4.88 ± 0.06 MeV. For this measurement gates were set on

five different gamma-ray transitions and the endpoint energy of the coincident beta spectrum for each of these gating transitions was determined by the FERMI program. The Q-values obtained from these spectra were averaged with a least squares fit for a single variable (53). The individual Q-values and their associated gating transitions are contained in Table 6. Figure 12 shows the gating transitions and the ^{139}Cs levels involved in the Q-value measurement.

A beta-ray singles spectrum for the decay of ^{139}Xe was analyzed in an attempt to determine the ground-state beta branch. However, due to the finite resolution of the plastic scintillator, which is of the same order of magnitude as the separation between the ground state and the first excited state, it was not possible to assign a definite intensity value to the ground-state beta branching ratio.

The ground-state beta branching intensity was calculated from the gamma-ray equilibrium spectrum of ^{139}Xe and ^{139}Cs. The ground-state branch and the branch to the 1283-keV level in ^{139}Ba had previously been calculated from gamma-ray data using the ratio of the beta branches to the ground state and first excited state in the decay of ^{139}Ba as given in ref. 8. By comparing intensities of the stronger lines in the decays of ^{139}Xe and ^{139}Cs a value of (22 ± 6) % was obtained for the ground state beta branch in the ^{139}Xe decay. This value and the relative beta feeding for each level as determined from

Table 6. Beta endpoints for the decay of ^{139}Xe

Gating Peak (MeV)	Initial Level of Gating Peak (MeV)	Q (MeV)	ΔQ^1 (MeV)
0.225	0.515	4.90	0.06
0.296	0.515	4.89	0.05
0.393	0.393	4.84	0.06
0.612	1.006	4.88	0.06
0.788	1.006	4.89	0.07

Weighted Average Q = 4.88 ± 0.06 MeV.

[1] ΔQ is the geometrical sum of the error from the Fermi fit and the error from the calibration.

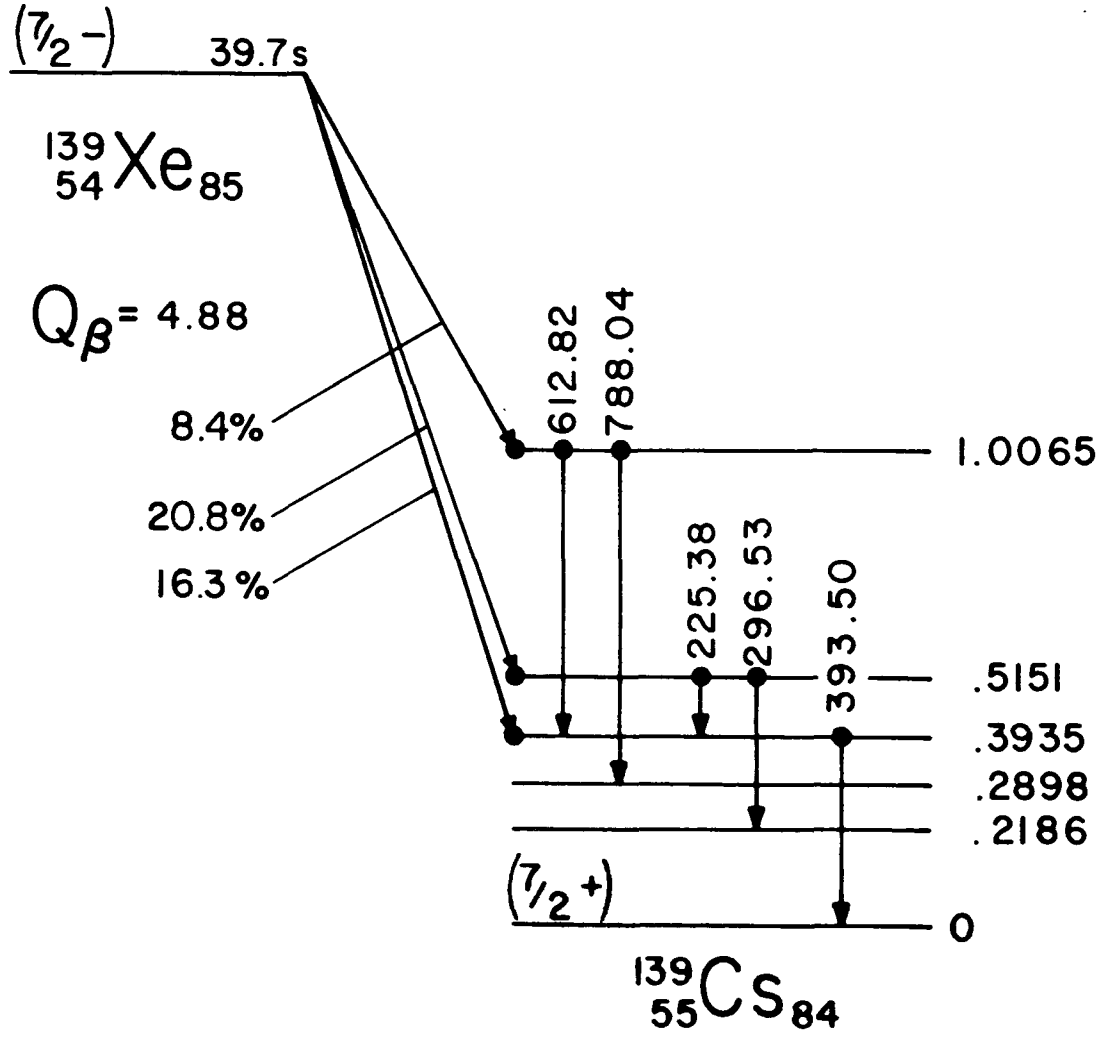

Figure 12. Gating transitions used in measurement of ^{139}Xe decay energy

the gamma-ray intensities were used to calculate the percent beta feeding to the excited levels of ^{139}Cs. These results were used in turn to calculate the log ft values for the various beta branches. The energy levels, the percent beta branching to each level, and the calculated log ft value for each branch are presented in Table 7. The measured Q-value of 4.88 MeV was also used in this calculation.

B. ^{139}Cs Decay

1. Gamma-ray decay scheme

The gamma-ray spectrum following the decay of ^{139}Cs is shown in Figure 13. This 8192-channel spectrum covers an energy range of 0 - 4.4 MeV. The data were accumulated at the daughter analysis port of the MTC using the optimum values of the MTC parameters as determined by ISOBAR. The use of these parameters resulted in integrated activity ratios of 0.2% Xe, 87.7% Cs and 12.1% Ba.

The gamma-ray energies and intensities and their errors as determined by DRUDGE are presented in Table 8. The relative intensity values are based upon an assignment of a value of 1000 for the 1283.23-keV transition. The absolute intensity values in this table are based upon the indirectly calculated value of (84 ± 6) % for the ground-state beta branching. The last column gives the placement in the ^{139}Ba level scheme.

Table 7. Beta branching and log ft's for the ^{139}Xe decay

^{139}Cs Levels (MeV)	Percent Beta Branching	Log ft	Log f_1t
0.0000	22. ± 6.	6.6 ± 0.1	8.4
0.2186	2.3 ± 3.7	7.5 ± 0.5	9.2
0.2898	2.6 ± 0.8	7.4 ± 0.1	9.1
0.3935	16.3 ± 1.5	6.6 ± 0.0	8.3
0.5151	20.8 ± 1.2	6.4 ± 0.1	8.1
0.6465	0.5 ± 0.1	8.0 ± 0.0	9.7
0.7324	2.2 ± 0.1	7.3 ± 0.0	8.9
0.8917	0.2 ± 0.1	8.3 ± 0.2	9.9
0.9424	1.4 ± 0.1	7.4 ± 0.1	9.0
1.0065	8.4 ± 0.4	6.6 ± 0.1	8.2
1.0203	1.4 ± 0.01	7.3 ± 0.1	9.0
1.1387	0.0 ± 0.05	10.0 ± 0.1	11.0
1.1860	0.1 ± 0.05	10.0 ± 0.1	11.0
1.2148	0.36 ± 0.08	7.8 ± 0.1	9.4
1.3951	0.03 ± 0.06	8.8 ± 0.5	10.3
1.4613	1.2 ± 0.1	7.2 ± 0.1	8.7
1.5080	0.05 ± 0.1	8.6 ± 0.5	10.1
1.5999	0.2 ± 0.1	7.8 ± 0.2	9.3
1.6527	1.2 ± 0.1	7.1 ± 0.1	8.5
1.6938	0.4 ± 0.1	7.6 ± 0.1	9.0
1.7386	1.7 ± 0.1	6.9 ± 0.1	8.3
1.8312	0.1 ± 0.08	8.0 ± 0.3	9.4
2.0637	0.69 ± 0.04	7.1 ± 0.1	8.4
2.0996	0.37 ± 0.05	7.3 ± 0.1	8.6
2.1036	0.04 ± 0.04	8.3 ± 0.4	9.6
2.1856	2.0 ± 0.1	6.5 ± 0.1	7.8
2.3049	1.5 ± 0.1	6.6 ± 0.1	7.8
2.3288	1.3 ± 0.1	6.6 ± 0.1	7.9
2.3730	0.7 ± 0.1	6.9 ± 0.1	8.4
2.5104	1.6 ± 0.1	6.4 ± 0.1	7.6
2.5858	1.0 ± 0.2	6.5 ± 0.1	7.7
2.6208	0.4 ± 0.1	6.9 ± 0.1	8.1
2.7274	0.3 ± 0.1	6.9 ± 0.1	8.0
2.7543	0.6 ± 0.1	6.6 ± 0.1	7.7
2.7973	0.8 ± 0.1	6.5 ± 0.1	7.6
2.7994	0.5 ± 0.1	6.7 ± 0.1	7.8
2.8523	0.3 ± 0.1	6.9 ± 0.1	8.0
2.9362	0.2 ± 0.1	6.9 ± 0.1	8.0
2.9675	0.5 ± 0.1	6.5 ± 0.1	7.6
2.9801	0.2 ± 0.1	7.0 ± 0.1	8.0
3.1303	0.4 ± 0.1	6.5 ± 0.1	7.4

Table 7. (Continued)

^{139}Cs Levels (MeV)	Percent Beta Branching	Log ft	Log f_1t
3.1471	0.4 ± 0.1	6.4 ± 0.1	7.4
3.1561	0.3 ± 0.1	6.6 ± 0.1	7.5
3.3727	0.3 ± 0.2	6.3 ± 0.2	7.2
3.3753	0.5 ± 0.1	6.1 ± 0.1	7.0
3.5047	0.3 ± 0.1	6.1 ± 0.1	6.9
3.8151	0.5 ± 0.1	5.5 ± 0.1	6.1
3.9082	0.4 ± 0.1	5.5 ± 0.1	6.0
3.9374	0.3 ± 0.1	5.6 ± 0.1	6.1
4.2990	0.4 ± 0.1	4.7 ± 0.1	4.9

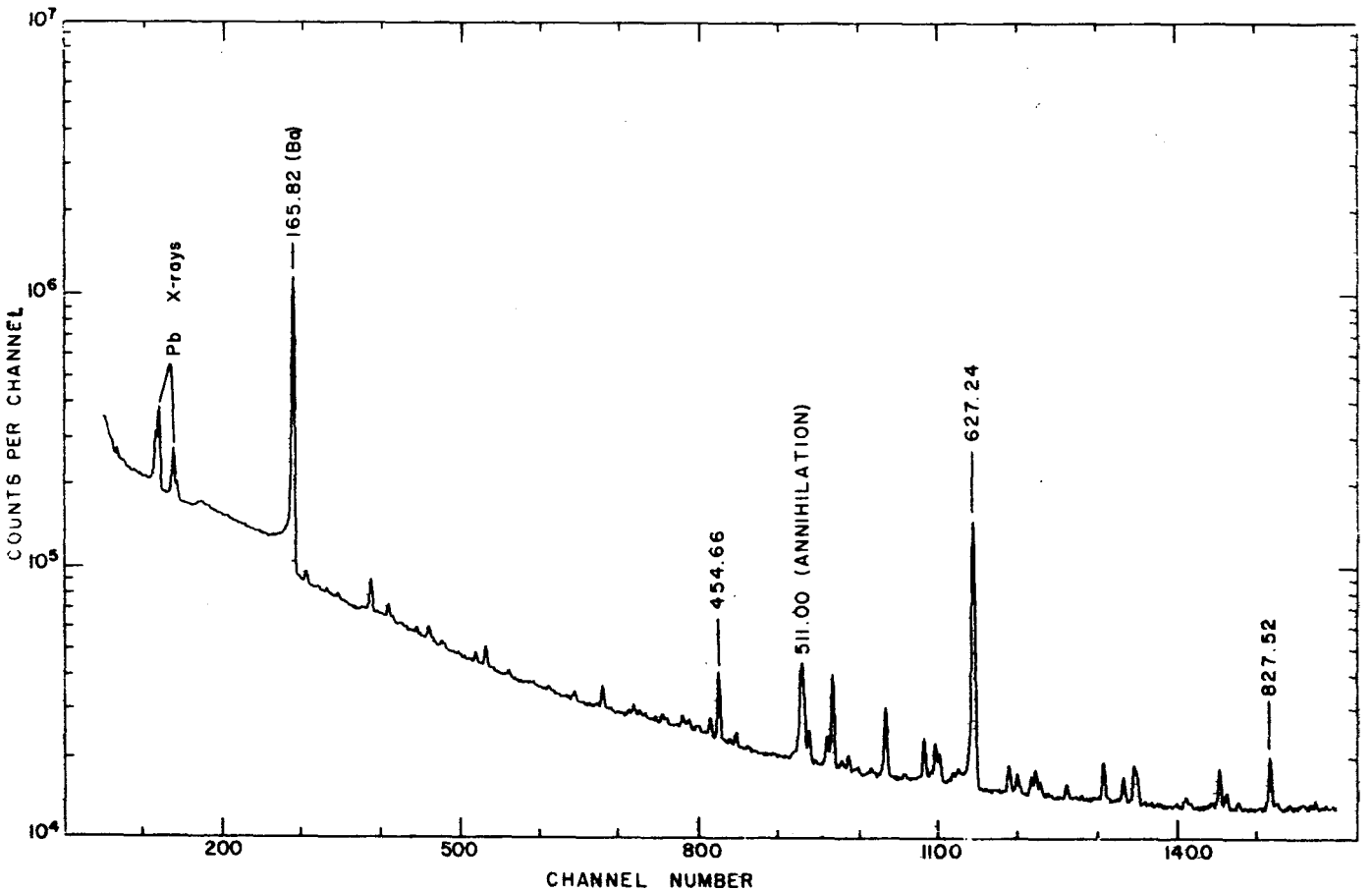

Figure 13. Gamma-ray spectrum for the decay of ^{139}Cs

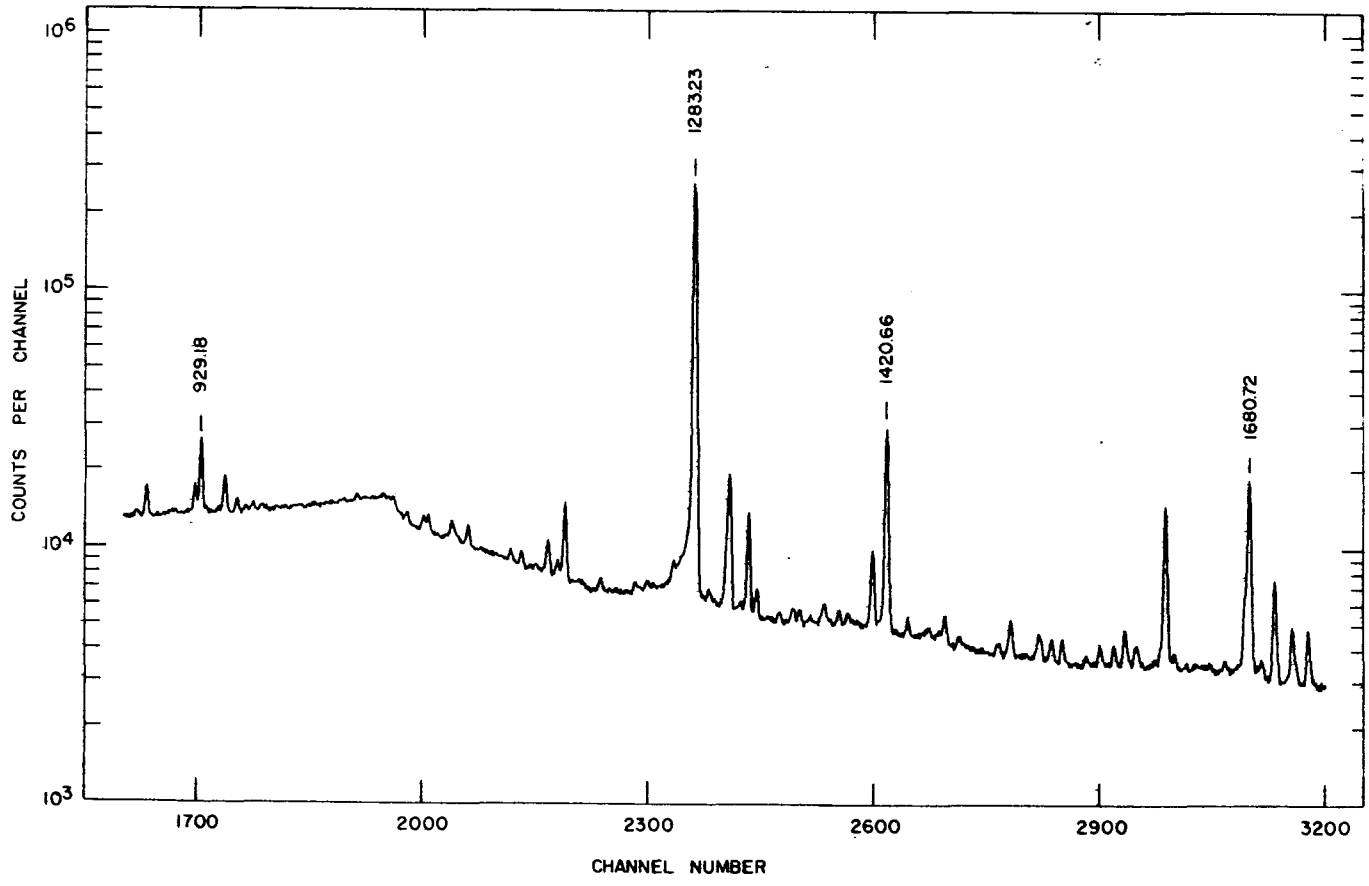

Figure 13. (Continued)

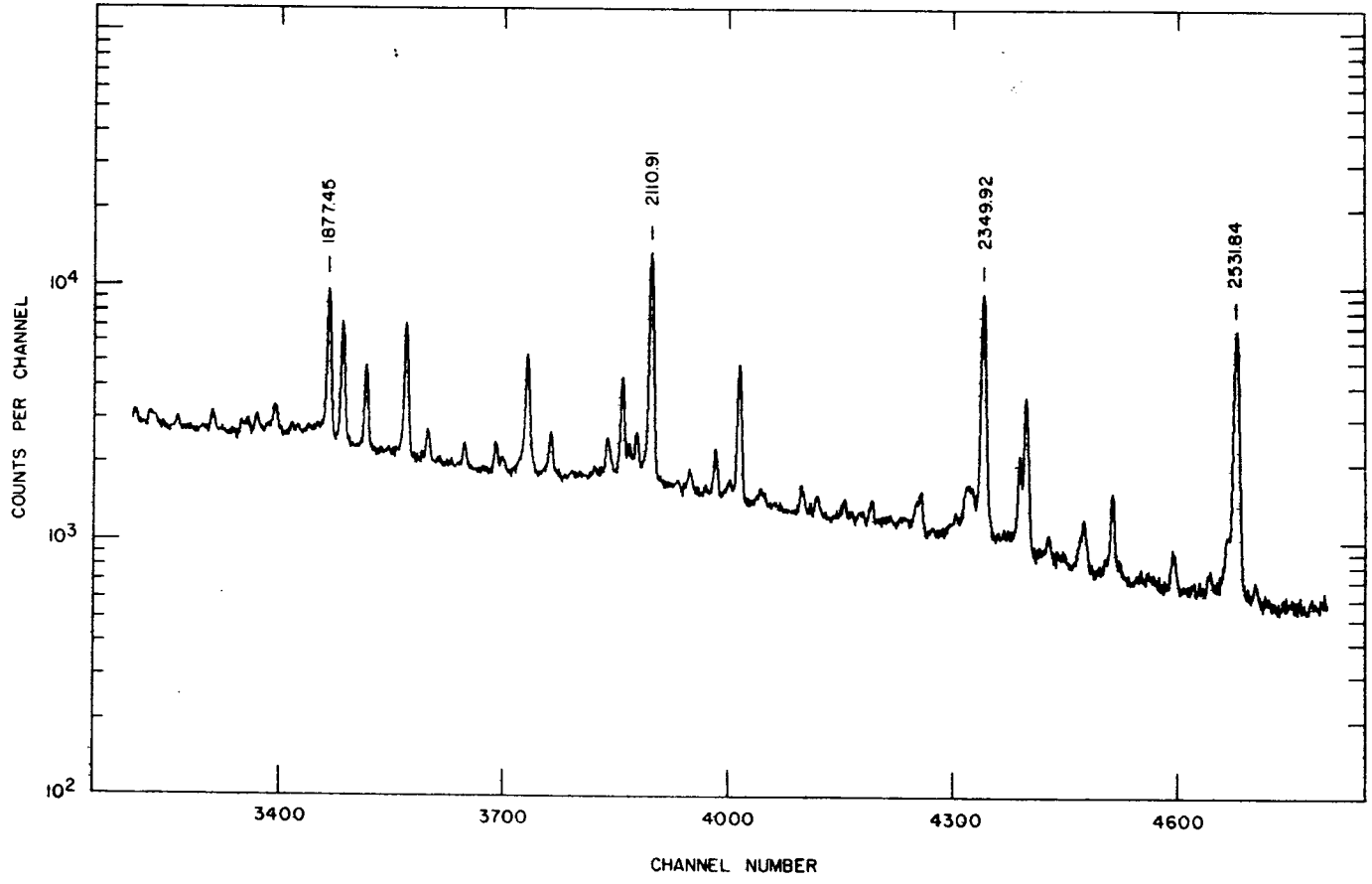

Figure 13. (Continued)

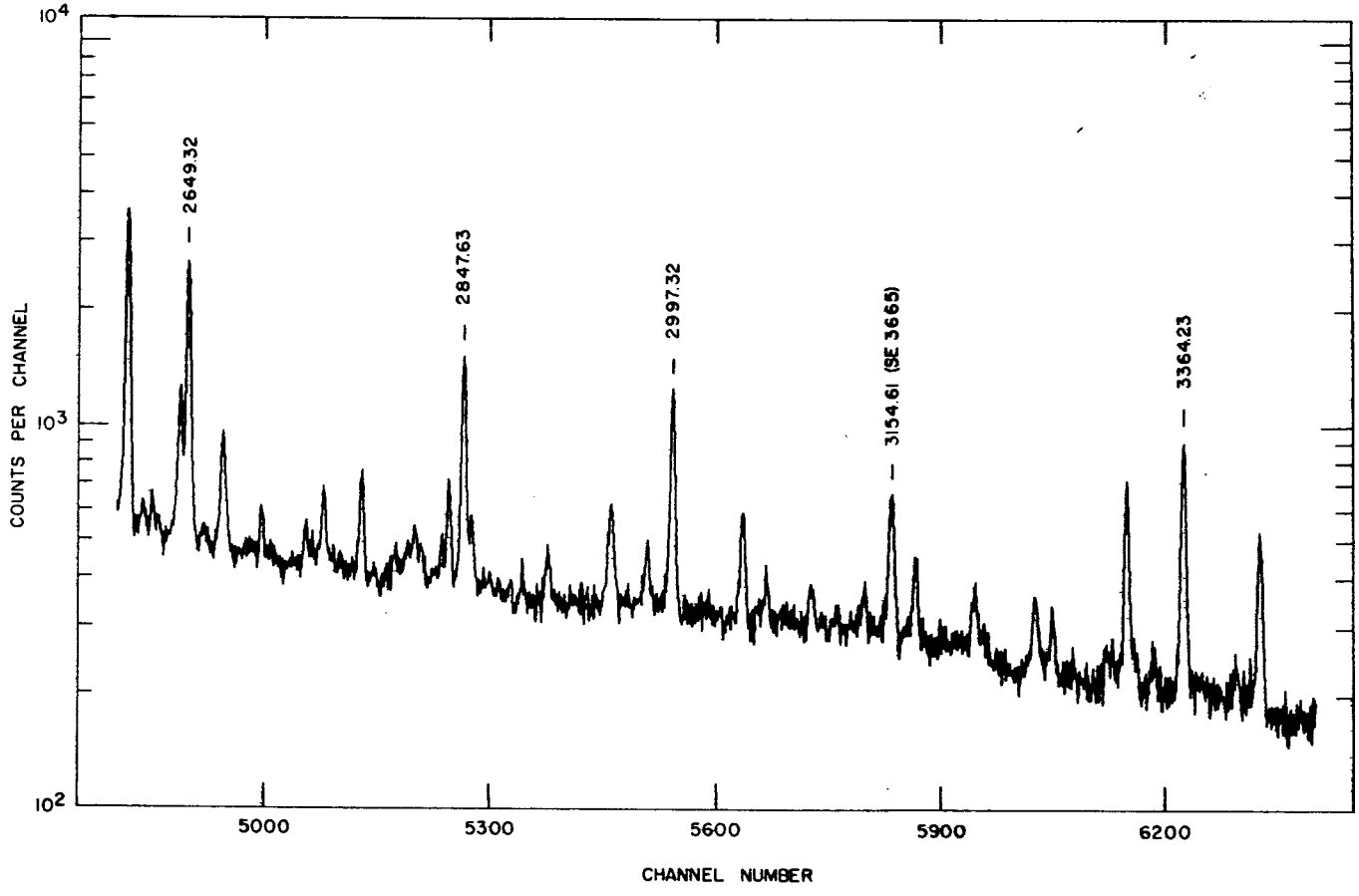

Figure 13. (Continued)

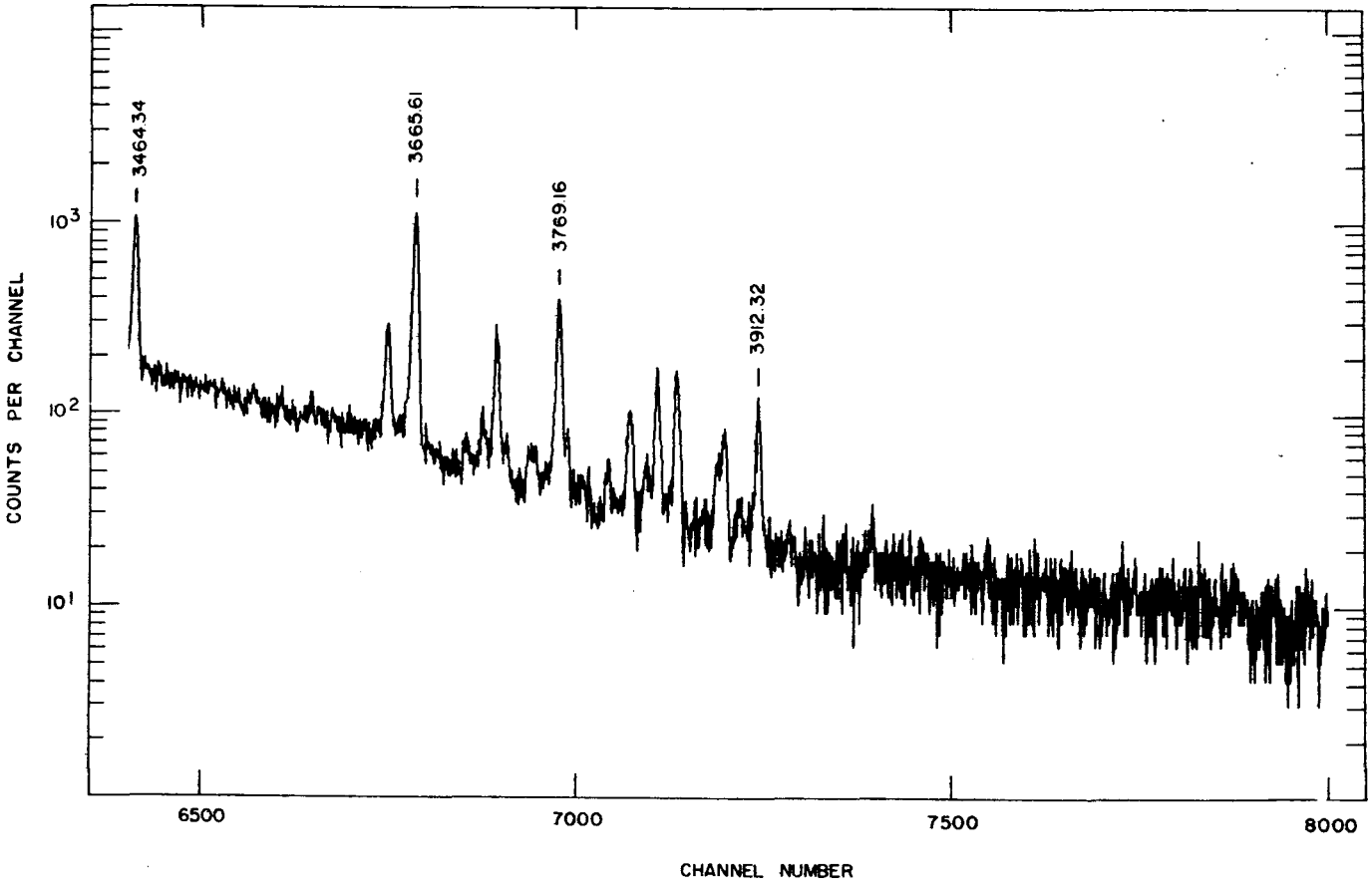

Figure 13. (Continued)

Table 8. Photopeaks observed in the decay of ^{139}Cs

Energy (keV)	Relative Intensity[1]	Intensity per 100 Decays[2]	Placement (keV)
188.88 ± 0.20	1.08 ± 0.24	0.01	1887 - 1698
196.51 ± 0.18	1.20 ± 0.24	0.01	1877 - 1680
230.76 ± 0.09	4.28 ± 0.38	0.03	1539 - 1308
233.45 ± 0.22	1.27 ± 0.29	0.01	2110 - 1877
249.89 ± 0.18	1.40 ± 0.28	0.01	2349 - 2100
260.57 ± 0.35	1.02 ± 0.34	0.01	1680 - 1420
267.59 ± 0.26	1.31 ± 0.35	0.01	
312.42 ± 0.21	1.08 ± 0.25	0.01	1620 - 1308
339.40 ± 0.41	0.75 ± 0.32	0.01	2156 - 1817
357.01 ± 0.16	1.92 ± 0.32	0.01	2037 - 1680
375.91 ± 0.07	5.35 ± 0.36	0.04	2605 - 2229
396.93 ± 0.26	2.16 ± 0.58	0.02	1817 - 1420
401.08 ± 0.22	1.38 ± 0.30	0.01	2218 - 1817
404.61 ± 0.25	1.14 ± 0.31	0.01	3769 - 3364
416.49 ± 0.22	1.71 ± 0.38	0.01	2349 - 1933
419.30 ± 0.28	1.32 ± 0.38	0.01	2100 - 1680
430.20 ± 0.16	2.52 ± 0.40	0.02	2110 - 1680 [3]
430.20 ± 0.16	2.52 ± 0.40	0.02	1850 - 1420 [3]
434.23 ± 0.20	1.93 ± 0.38	0.01	2524 - 2089
448.76 ± 0.12	4.22 ± 0.50	0.03	2605 - 2156
454.66 ± 0.06	18.20 ± 1.07	0.13	1081 - 627
466.70 ± 0.12	2.82 ± 0.33	0.02	1887 - 1420
505.45 ± 0.29	1.33 ± 0.38	0.02	
515.86 ± 0.07	7.22 ± 0.58	0.05	2605 - 2089
528.20 ± 0.10	5.04 ± 1.71	0.04	1949 - 1420
531.98 ± 0.04	29.71 ± 1.62	0.22	2349 - 1817
538.35 ± 0.24	1.81 ± 0.40	0.01	2218 - 1680
542.71 ± 0.15	3.15 ± 0.44	0.02	2847 - 2304
558.14 ± 0.30	1.24 ± 0.38	0.01	2375 - 1817
567.72 ± 0.05	18.67 ± 1.08	0.14	1850 - 1283
594.02 ± 0.05	9.78 ± 0.57	0.07	1877 - 1283
598.17 ± 0.18	1.59 ± 0.27	0.01	2218 - 1620
601.48 ± 0.05	8.94 ± 0.54	0.07	2349 - 1748

[1]Measured relative to the 1283.23-keV transition.

[2]Calculated from the ^{139}Ba level scheme with the 84% beta branching reported in Section III-B-2.

[3]Denotes multiple placement.

Table 8. (Continued)

Energy (keV)	Relative Intensity[1]	Intensity per 100 Decays[2]	Placement (keV)	
604.22 ± 0.06	5.91 ± 0.42	0.04	1887 - 1283	
613.39 ± 0.30	2.09 ± 0.62	0.02	2994 - 2380	
616.91 ± 0.21	3.28 ± 0.63	0.02	2037 - 1420	
619.70 ± 0.31	2.17 ± 0.60	0.02	3151 - 2531	
627.24 ± 0.03	213.63 ± 10.85	1.56	627 - 0	
651.08 ± 0.07	6.44 ± 0.53	0.05	2349 - 1698	
656.58 ± 0.13	4.26 ± 0.50	0.03	2605 - 1949	
666.07 ± 0.11	3.98 ± 0.42	0.03	1748 - 1081	
668.97 ± 0.08	5.76 ± 0.48	0.04	2349 - 1680	
672.21 ± 0.15	2.68 ± 0.40	0.02	2605 - 1933	
690.04 ± 0.09	2.96 ± 0.28	0.02	1998 - 1308	
714.90 ± 0.06	9.88 ± 0.63	0.07	1998 - 1283	
728.38 ± 0.09	5.61 ± 0.49	0.04	2605 - 1877	
735.68 ± 0.09	8.89 ± 0.72	0.06	1817 - 1081	
737.60 ± 0.12	6.05 ± 0.63	0.04	2020 - 1283	
770.56 ± 0.19	2.31 ± 0.39	0.02	2079 - 1308	
773.50 ± 0.33	1.33 ± 0.38	0.01		
788.33 ± 0.36	1.21 ± 0.40	0.01	2605 - 1817	
793.28 ± 0.07	10.49 ± 0.69	0.08	1420 - 627	
798.01 ± 0.14	3.59 ± 0.47	0.03	2218 - 1420	
806.32 ± 0.21	1.67 ± 0.33	0.01	2089 - 1283	
827.52 ± 0.07	15.23 ± 0.98	0.11	2110 - 1283	
832.17 ± 0.34	1.69 ± 0.57	0.01	3364 - 2531	
849.72 ± 0.33	1.45 ± 0.40	0.01		
858.44 ± 0.30	1.65 ± 0.42	0.01	2166 - 1308	
883.48 ± 0.28	1.79 ± 0.47	0.01	2994 - 2110	
890.54 ± 0.08	10.22 ± 0.69	0.07	2173 - 1283	
924.96 ± 0.08	9.20 ± 0.67	0.07	2605 - 1680	
929.18 ± 0.06	31.95 ± 1.70	0.23	2349 - 1420	
933.03 ± 0.30	1.75 ± 0.47	0.01	3151 - 2218	
946.46 ± 0.08	13.66 ± 0.97	0.10	2229 - 1283	
955.19 ± 0.19	3.99 ± 0.63	0.03	2375 - 1420	
966.61 ± 0.31	2.36 ± 0.61	0.02	2249 - 1283	
973.03 ± 0.40	1.83 ± 0.63	0.01		
1040.93 ± 0.22	2.18 ± 0.43	0.02	2461 - 1420	[3]
1040.93 ± 0.22	2.18 ± 0.43	0.02	3151 - 2110	[3]
1059.89 ± 0.29	2.07 ± 0.67	0.02	3364 - 2304	
1063.72 ± 0.41	1.45 ± 0.69	0.01	2997 - 1933	
1067.06 ± 0.19	3.25 ± 0.63	0.02		
1076.94 ± 0.17	3.57 ± 0.66	0.03		
1092.23 ± 0.12	2.87 ± 0.30	0.02	3622 - 2529	[3]

Table 8. (Continued)

Energy (keV)	Relative Intensity[1]	Intensity per 100 Decays[2]	Placement (keV)
1092.23 ± 0.12	2.87 ± 0.30	0.02	2173 - 1081 [3]
1108.93 ± 0.18	5.61 ± 0.77	0.04	2529 - 1420
1110.90 ± 0.41	2.67 ± 0.69	0.02	2531 - 1420
1120.89 ± 0.10	6.53 ± 0.59	0.05	1748 - 627
1159.30 ± 0.17	3.70 ± 0.54	0.03	3464 - 2304
1178.35 ± 0.09	9.33 ± 0.76	0.07	2461 - 1283
1185.21 ± 0.17	4.09 ± 0.58	0.03	2605 - 1420
1190.42 ± 0.06	25.55 ± 1.47	0.19	1817 - 627
1216.14 ± 0.19	2.90 ± 0.46	0.02	2524 - 1308
1240.93 ± 0.25	2.05 ± 0.39	0.01	2524 - 1283
1249.41 ± 0.22	2.09 ± 0.38	0.02	3270 - 2020
1283.23 ± 0.05	1000.00 ± 52.89	7.30	1283 - 0
1306.09 ± 0.11	14.66 ± 1.32	0.11	1933 - 627
1308.13 ± 0.06	52.17 ± 2.90	0.38	1308 - 0
1316.36 ± 0.35	1.84 ± 0.51	0.01	2997 - 1680
1321.77 ± 0.06	32.48 ± 1.78	0.24	1949 - 627
1344.38 ± 0.35	1.74 ± 0.49	0.02	
1353.92 ± 0.19	3.00 ± 0.47	0.02	3734 - 2380
1386.85 ± 0.24	2.59 ± 0.51	0.02	
1393.18 ± 0.30	2.13 ± 0.52	0.02	3769 - 2375
1410.58 ± 0.07	20.86 ± 1.22	0.15	2037 - 627
1420.66 ± 0.06	110.19 ± 5.67	0.80	1420 - 0
1462.43 ± 0.19	4.98 ± 0.81	0.04	2089 - 627
1472.64 ± 0.52	1.61 ± 0.68	0.01	3171 - 1698
1500.53 ± 0.34	1.98 ± 0.51	0.01	3674 - 2173
1529.34 ± 0.28	3.61 ± 0.81	0.03	2156 - 627
1531.18 ± 0.34	2.97 ± 0.79	0.02	3151 - 1620
1539.09 ± 0.14	4.00 ± 0.44	0.03	1539 - 0
1546.63 ± 0.13	4.24 ± 0.47	0.03	2173 - 627
1563.91 ± 0.38	1.40 ± 0.42	0.01	
1573.84 ± 0.15	3.47 ± 0.41	0.03	2994 - 1420
1591.73 ± 0.11	7.30 ± 0.62	0.05	2218 - 627
1600.70 ± 0.46	2.72 ± 0.98	0.02	3819 - 2218
1620.74 ± 0.06	57.99 ± 3.05	0.42	1620 - 0
1677.44 ± 0.10	12.38 ± 0.93	0.09	2304 - 627
1680.72 ± 0.06	83.63 ± 4.31	0.61	1680 - 0
1689.04 ± 0.25	2.70 ± 0.50	0.02	2997 - 1308
1698.66 ± 0.07	24.61 ± 1.40	0.18	1698 - 0
1711.09 ± 0.11	10.89 ± 0.83	0.08	2994 - 1283
1713.64 ± 0.39	2.23 ± 0.58	0.02	3887 - 2173
1722.55 ± 0.09	10.38 ± 0.74	0.08	2349 - 627

Table 8. (Continued)

Energy (keV)	Relative Intensity[1]	Intensity per 100 Decays[2]	Placement (keV)
1737.91 ± 0.27	2.09 ± 0.42	0.02	3418 - 1680 [3]
1737.91 ± 0.27	2.09 ± 0.42	0.02	3912 - 2173 [3]
1748.58 ± 0.30	2.10 ± 0.41	0.02	1748 - 0
1768.19 ± 0.21	1.87 ± 0.30	0.01	3645 - 1877
1793.63 ± 0.17	2.98 ± 0.39	0.02	3950 - 2156
1814.65 ± 0.41	1.66 ± 0.47	0.01	3665 - 1850
1818.51 ± 0.33	2.08 ± 0.48	0.02	
1850.69 ± 0.37	1.42 ± 0.37	0.01	1850 - 0
1877.45 ± 0.07	47.30 ± 2.55	0.35	1877 - 0
1887.57 ± 0.07	30.46 ± 1.74	0.22	1887 - 0
1904.50 ± 0.07	17.11 ± 1.01	0.12	2531 - 627
1933.48 ± 0.07	33.93 ± 1.85	0.25	1933 - 0
1949.26 ± 0.14	4.60 ± 0.50	0.03	1949 - 0
1998.46 ± 0.15	3.99 ± 0.44	0.03	3418 - 1420
2003.43 ± 0.29	1.96 ± 0.39	0.01	3853 - 1850
2020.76 ± 0.25	18.37 ± 6.01	0.13	2020 - 0
2022.09 ± 0.49	9.25 ± 5.93	0.07	2649 - 627
2038.10 ± 0.11	5.94 ± 0.50	0.04	2038 - 0
2079.33 ± 0.19	5.79 ± 0.73	0.04	2079 - 0
2089.91 ± 0.09	18.91 ± 1.25	0.14	2089 - 0
2100.13 ± 0.17	6.51 ± 0.77	0.05	2100 - 0
2110.91 ± 0.06	90.63 ± 4.77	0.66	2110 - 0
2156.94 ± 0.13	5.73 ± 0.57	0.04	2156 - 0
2166.72 ± 0.40	1.66 ± 0.50	0.01	2166 - 0
2173.98 ± 0.07	27.85 ± 1.54	0.20	2174 - 0
2218.91 ± 0.23	2.90 ± 0.45	0.02	2218 - 0
2229.88 ± 0.34	1.89 ± 0.44	0.01	2229 - 0
2249.66 ± 0.35	1.61 ± 0.39	0.01	2249 - 0
2269.52 ± 0.33	1.96 ± 0.45	0.02	
2304.97 ± 0.16	4.18 ± 0.47	0.03	2305 - 0
2330.19 ± 0.62	1.43 ± 0.59	0.01	3950 - 1620
2339.43 ± 0.50	3.94 ± 0.88	0.03	3622 - 1283
2349.92 ± 0.06	77.45 ± 4.20	0.57	2349 - 0
2352.64 ± 0.56	3.08 ± 1.09	0.02	
2375.95 ± 0.11	9.61 ± 0.76	0.07	2375 - 0
2380.66 ± 0.07	25.96 ± 1.49	0.19	2380 - 0
2418.93 ± 0.41	1.70 ± 0.42	0.01	3839 - 1420
2422.16 ± 0.18	3.99 ± 0.48	0.03	
2524.47 ± 0.22	3.93 ± 0.58	0.03	2524 - 0
2529.88 ± 0.26	11.41 ± 2.69	0.08	2529 - 0
2531.84 ± 0.07	58.38 ± 4.02	0.43	2531 - 0

Table 8. (Continued)

Energy (keV)	Relative Intensity[1]	Intensity per 100 Decays[2]	Placement (keV)
2605.75 ± 0.06	33.81 ± 1.87	0.25	2605 - 0
2649.32 ± 0.07	23.18 ± 1.28	0.17	2649 - 0
2673.98 ± 0.18	4.82 ± 0.60	0.03	
2774.04 ± 0.13	4.07 ± 0.36	0.03	3401 - 627
2836.88 ± 0.16	3.77 ± 0.41	0.03	3464 - 627
2847.63 ± 0.08	13.77 ± 0.83	0.10	2847 - 0
2978.99 ± 0.24	1.81 ± 0.25	0.01	
2997.32 ± 0.09	11.92 ± 0.75	0.09	2997 - 0
3047.29 ± 0.16	4.14 ± 0.41	0.03	3674 - 627
3096.36 ± 0.39	1.18 ± 0.26	0.01	3724 - 627
3171.57 ± 0.23	2.48 ± 0.34	0.02	3171 - 0
3270.23 ± 0.32	1.41 ± 0.25	0.01	3270 - 0
3323.66 ± 0.15	6.93 ± 0.66	0.05	3950 - 627
3364.23 ± 0.11	10.95 ± 0.75	0.08	3364 - 0
3418.77 ± 0.15	5.53 ± 0.48	0.04	3418 - 0
3464.34 ± 0.09	15.06 ± 0.90	0.11	3464 - 0
3645.70 ± 0.13	3.83 ± 0.32	0.03	3645 - 0
3665.61 ± 0.08	18.92 ± 1.08	0.14	3665 - 0
3724.20 ± 0.15	3.62 ± 0.32	0.03	3724 - 0
3769.16 ± 0.11	6.24 ± 0.44	0.05	3769 - 0
3819.99 ± 0.24	1.51 ± 0.21	0.01	3819 - 0
3839.78 ± 0.17	2.50 ± 0.23	0.02	3839 - 0
3853.87 ± 0.16	2.68 ± 0.24	0.02	3853 - 0
3887.75 ± 0.31	1.14 ± 0.17	0.01	3887 - 0
3912.32 ± 0.21	1.67 ± 0.22	0.01	3912 - 0

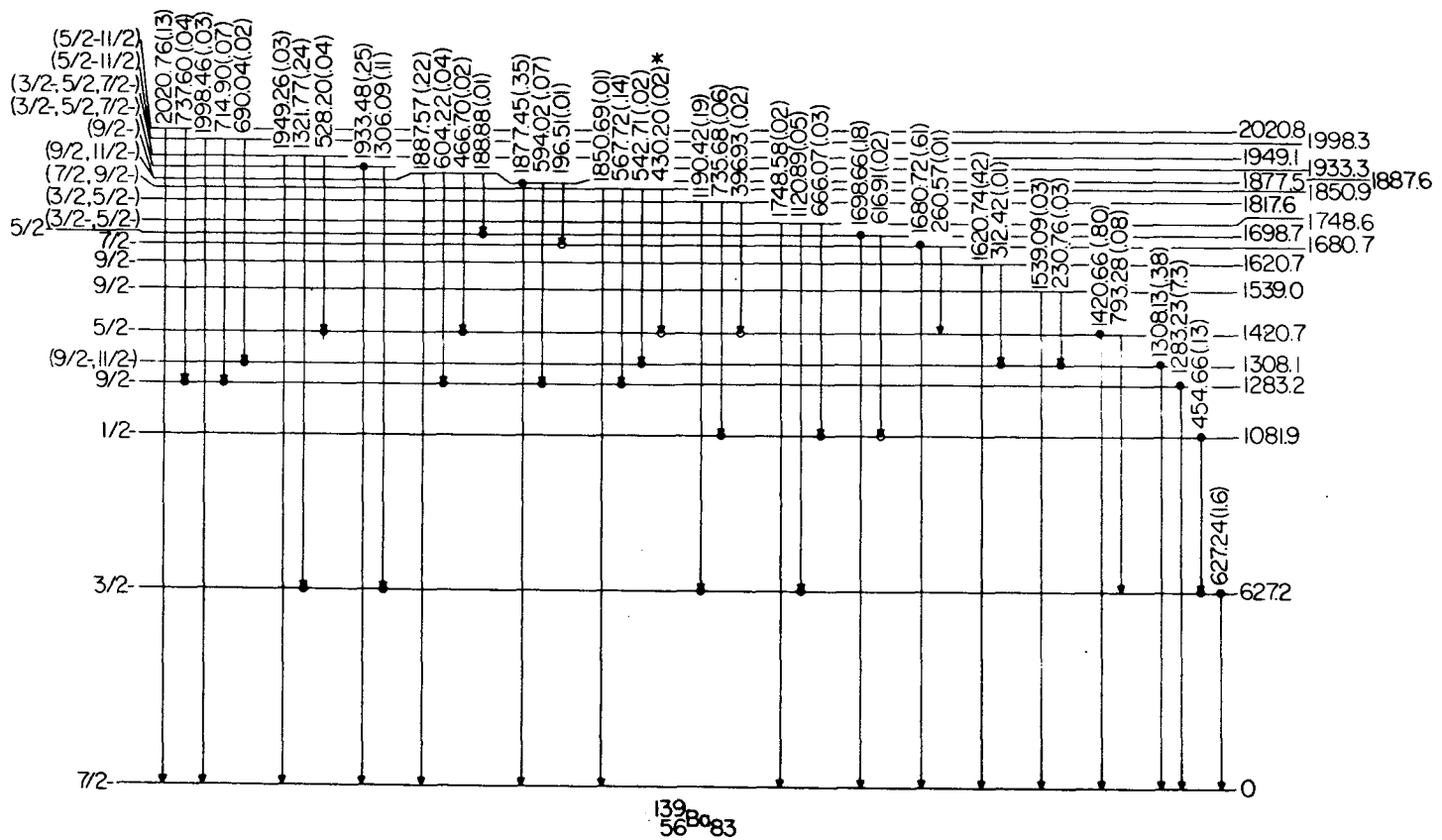

Figure 14. The ^{139}Ba level scheme deduced from the decay of ^{139}Cs

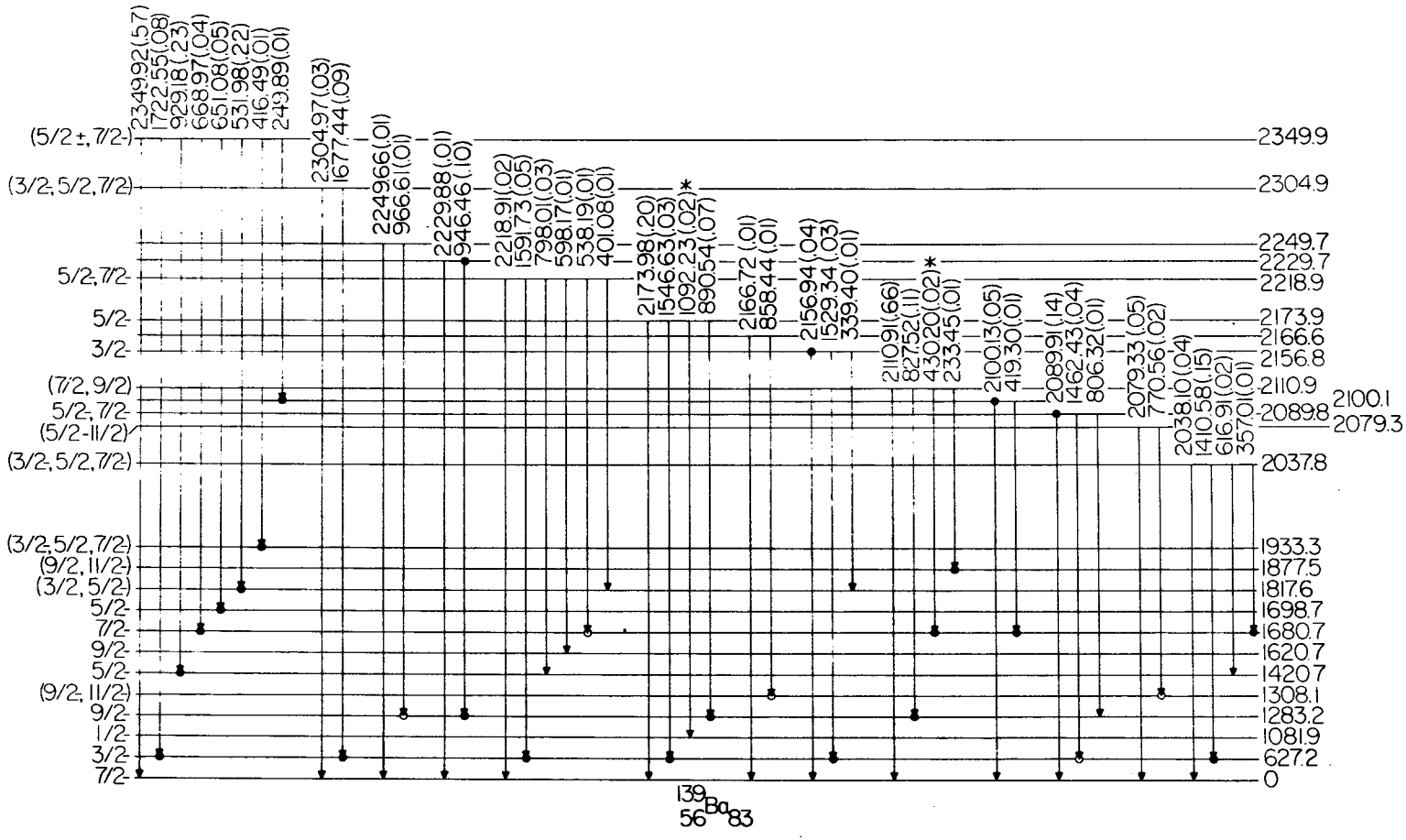

Figure 14. (Continued) Level spacing below 2037 keV is not to scale.

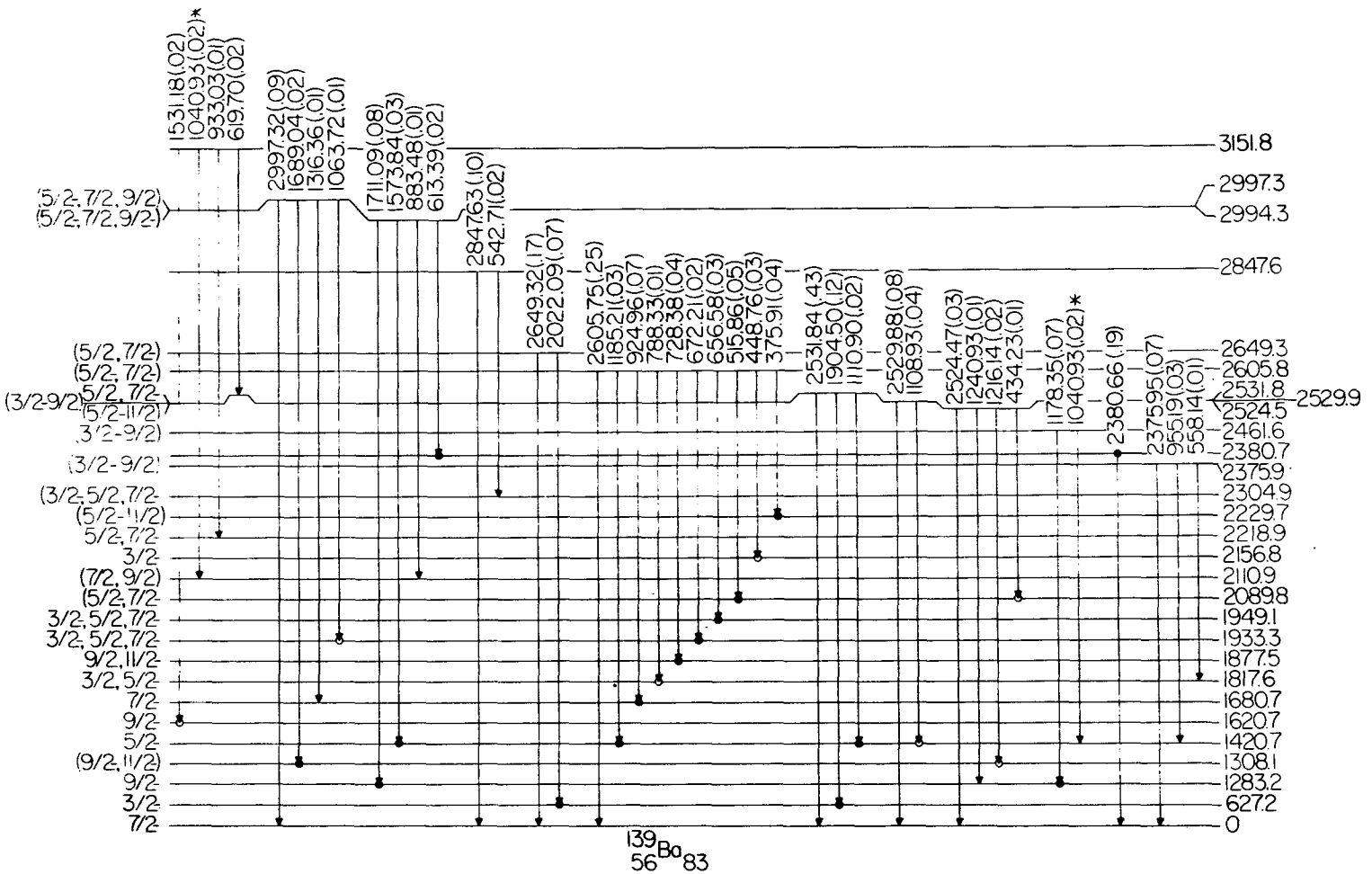

Figure 14. (Continued) Level spacing below 2375 keV is not to scale.

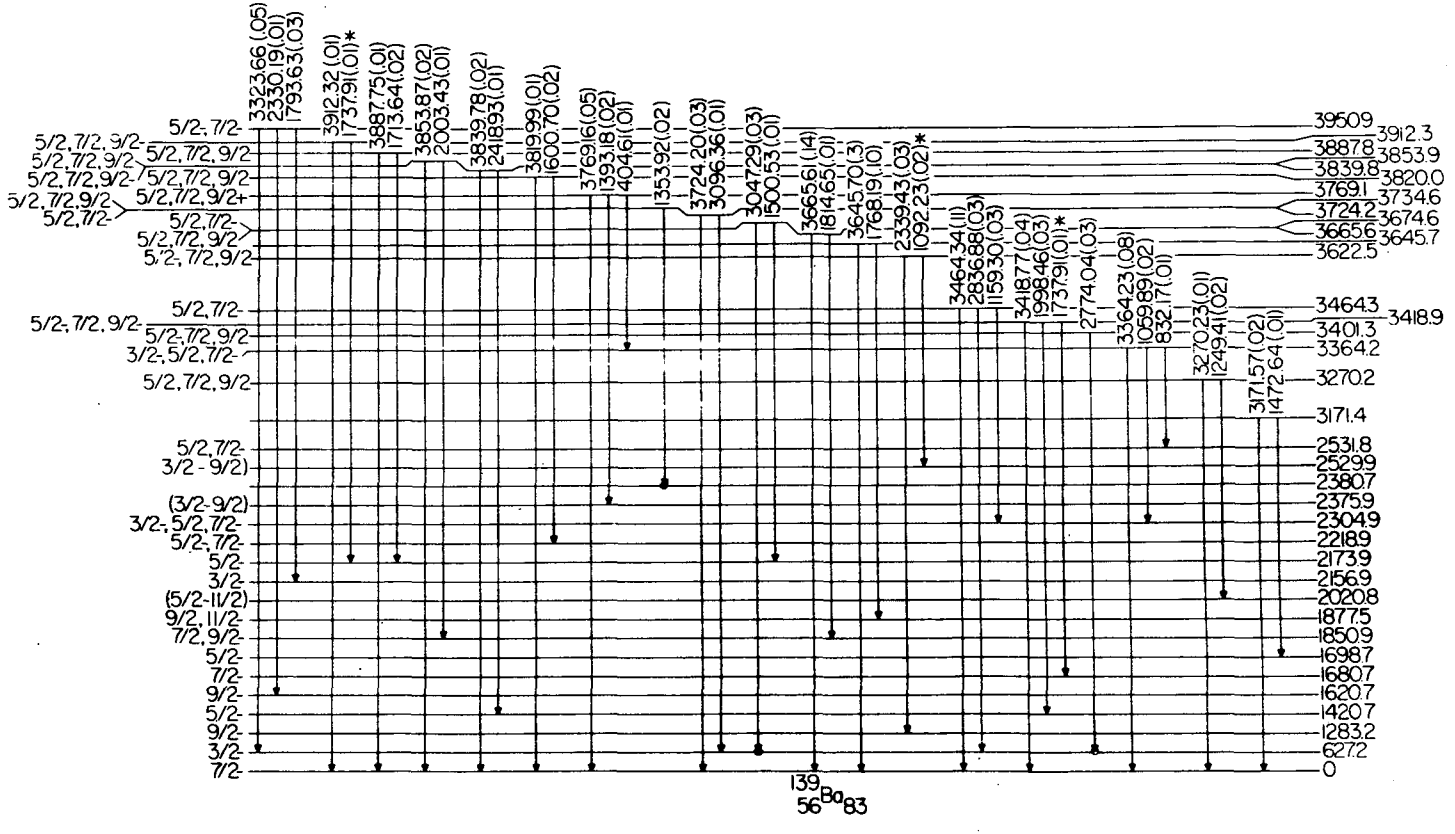

Figure 14. (Continued) Level spacing below 3171 keV is not to scale.

The level scheme deduced for ^{139}Ba is shown in Figures 14. This level scheme contains 161 of the 177 observed gamma-ray transitions. These transitions are placed among 62 excited levels and constitute more than 98% of the gamma-ray intensity. Four transitions have been used twice each in this level scheme, and the lack of any coincidence information on these transitions precludes an unambiguous level assignment. For these double placements the observed intensity has been divided equally between the two placements.

The gamma-gamma coincidence relationships observed following the Cs decay are presented in Table 9. As in the previous section, these are divided into two categories--definite and probable.

The spins and parities of several of the levels have been determined from the results of the (d,p) reaction work on ^{138}Ba carried out by D. von Ehrenstein *et al.* as reported in references 22 and 23. The log ft values measured in the present work will be used to make possible spin and parity assignments for those levels for which no reaction results are available.

For the beta transitions to most of the excited levels up to 2500 keV the calculated log f_1t values lie in the range from 9.2 to 10.5. For these values, the rules presented by Raman and Gove (50) indicate $\Delta J = 0, 1$ and $\Delta\pi = \pm$, or $\Delta J = 2$ and $\Delta\pi = -$. Consequently, it is not possible to place a very

Table 9. Coincidence information for the decay of ^{139}Cs

Gate (keV)	Definite coincidences	Possible coincidences
375	946, 1283	
454	531, 627, 666, 735, 1076	1190
531	454, 627, 735, 1190	396, 714, 793, 1283, 1420
567	1283, 1410	
627	454, 531, 567, 601, 656, 735, 793, 1076, 1120, 1190, 1306, 1321, 1410, 1531, 1591, 1677, 1722, 1904, 2022	448, 666, 929, 1159, 1462, 1546
666	627	454, 601
668	1680	
714	567, 1283	
735	454, 531, 627	
793	627, 929	1573
827	357, 1283, 1420	
946	375, 531, 567, 1283	
1108	1420	
1120	601, 627	
1178	1283	
1190	531, 627	
1283	375, 567, 594, 604, 714, 735, 827, 890, 946, 1178, 1711	666, 966

Table 9. (Continued)

Gate (keV)	Definite coincidences	Possible coincidences
1306	627	
1308	230, 312, 542, 690, 1689	770, 858, 1216
1321	627, 656	
1410	627	
1420	528, 567, 616, 929, 1110, 1185, 1573	396, 430, 466, 668
1677	627	
1680	357, 419, 430, 538, 668 924	1316
1698	188, 651	
1711	1283	
1877	233, 728	466
1904	627	
1933	672	416, 1063
2022	627	
2089	515	434
2100	249	
2156	448	
2774	627	
3047	627	

narrow limitation on the possible spin and parity assignments for ^{139}Ba levels. The range of possible assignments based on the log f_1t values in this range includes 3/2-, 5/2±, 7/2±, 9/2±, and 11/2-. In some cases it is possible to place a further restriction on the possible assignment by using ratios of the Weisskopf estimates for the gamma-ray transitions depopulating a level.

Ground state: The ground-state spin and parity appear to be well established at 7/2-. The (p,p) elastic scattering work of Veeser and Haeberli (25) on ^{138}Ba targets and the (d,p) experiments reported in references 17 - 22 all indicated an angular momentum transfer of 3, which leads to a spin and parity assignment of 7/2- for the ground state. The log ft value of 6.9 for the ground-state beta branching of 84% measured in this work is consistent with this assignment and a 7/2+ assignment for the ^{139}Cs ground state.

627.2-keV level: The (p,p) experiments and the (d,p) experiments mentioned above all indicate a 3/2- assignment for this level. The gamma-ray decay scheme deduced in this work indicates that this level has a beta branching ratio less than 0.05%, with a minimum log ft value of 10.0. This spin and parity assignment together with the 7/2+ value for the parent ^{139}Cs ground state indicates that the beta transition would have a high degree of -forbiddenness, and thus the beta transition to this level would likely be hindered.

1081.9-keV level: A spin and parity assignment of 1/2- is indicated by the results of the reaction experiments mentioned above. However, the beta branching value is equal to 0.04% ± 0.04%, and the log f_1t value is 11.1, with a log ft value of 9.7. This leads to spin assignments in the range from 3/2 to 11/2, in contrast to the 1/2- value assigned from reaction data. One of the double placements of a gamma-ray transition terminates on this level. If the entire transition intensity were assigned to the placement terminating on this level the resulting beta intensity could be zero, a value which would be expected for a spin 1/2 level.

1283.2-keV level: This level has the largest beta branching intensity of the excited levels in ^{139}Ba with 6.4% of the total beta intensity going to this level. The log ft value is 7.3, indicating that the beta transition is either allowed or first forbidden. This level was populated in the (d,p) reaction experiments of von Ehrenstein (22) and of Rapaport and Kerman (21). In ref. 22 an angular momentum transfer of 5 is reported for this level, which leads to an assignment of 9/2-. This assignment is consistent with the log ft value measured in the present work.

1292.6-keV level (?): Wiedner et al. (20) and Moragues et al. (26) have reported a level at 1292.6 ± 1.5 keV and tentatively assigned a spin of 1/2 or 3/2. No evidence was found that such a level is populated in the ^{139}Cs decay. In

the gamma-ray spectrum a photopeak occurs at 1293.6 keV, but this photopeak also appears in the background spectrum with the same intensity so it is not attributed to the ^{139}Cs decay but rather to the decay of 1.8-hr ^{41}Ar.

1308.1-keV level: This level has not been previously reported. Its existence is established on the basis of the 1308.1-keV transition which is in coincidence with several other transitions but which is not in coincidence with any of the transitions either to or from the first three excited states. Definite coincidences were observed with five transitions and possible coincidences were observed with three additional transitions. The log ft value calculated for the beta branching to this level is 8.7, which only restricts the possible spin assignment to the range from 3/2 to 11/2. The fact that no gamma-ray transitions were observed from this level to the 3/2- level at 627.2 keV nor to the 1/2- level at 1081.9 keV would tend to rule out assignments from the lower values in this range. An assignment of either 3/2 or 5/2 seems unlikely because of the lack of gamma-ray transitions to these lower levels, thus leaving a range from 7/2 to 11/2. Two of the gamma-ray transitions populating this level come from levels at 1539.0 keV and at 1620.7 keV, both of which have been found to have spin and parity assignments of 9/2- by von Ehrenstein et al. (22, 23). If the spin assignment for this level were 7/2- one would expect to see an E2 tran-

sition to the 3/2- state at 627.2 keV but no such transition was observed. Thus it seems likely that the spin of this level is either 9/2- or 11/2-.

1420.7-keV level: This level is fed with a beta branch of 0.3% and the calculated log ft value is 8.6. The reaction experiments (17 - 22) yield an angular momentum transfer of 3, leading to a spin and parity assignment of 5/2- for this state. The log ft value obtained in the present work is consistent with this assignment.

1539.0-keV level: This level is rather weakly fed in the beta decay of ^{139}Cs, with a branching ratio of 0.06% and a corresponding log ft value of 9.2. In the (d,p) reaction experiments (17 - 22) a level at 1540 keV is populated with angular momentum transfer of 5, and a 9/2- assignment is made for this level. The log ft value obtained in the present work would allow a spin change of 0, 1, or 2, with a range of possible spin assignments for this level then extending from 3/2 to 11/2. The 9/2- assignment is consistent with the results of this work.

1620.7-keV level: This level is populated with a beta branch of 0.39% and the calculated log f_1t value is 9.7. In the (d,p) reaction work of von Ehrenstein (22) a spin and parity assignment of 9/2- is tentatively made for a level at 1625 keV. The log ft value determined in this work is consistent with that assignment.

1680.7-keV level: A beta-branching ratio of 0.41% populates this level and leads to a log f_1t value of 9.6. D. von Ehrenstein and M. C. Tsangarides have reported a measured value of 7/2- for the spin and parity of a level at 1682 ± 13 keV (23). This assignment is consistent with the results of the present work.

1698.7-keV level: The calculated log ft value for the beta transition feeding this level is 8.9, based upon an observed beta branching ratio of 0.11%. In ref. 22 a spin and parity of 5/2- are reported for a level at 1700 keV. This is consistent with the log ft value found in the present work.

1748.6-keV level: The establishment of this level is based upon the observation of gamma-gamma coincidences of the 666.07-keV transition with the 454.66-keV transition depopulating the 1/2- state at 1081.9 keV and of the 1120.89-keV transition with the 627.24-keV transition from the 3/2- first excited state. The beta branching ratio is 0.03% and the log ft value is 9.5. In the (d,p) reaction studies (20 - 22) a level at this energy has been reported, but no spin assignments were made. The higher values of the spin allowed by the log ft value may be ruled out on the basis of the gamma rays depopulating the level. The only transitions leaving this level go to the 7/2- ground state, to the 3/2- first excited state, and to the 1/2- state at 1081.9 keV. Again assuming that these gamma-ray transitions

do not have a multipolarity higher than E2 limits the possible assignment of spin and parity to 3/2- or 5/2-.

1817.6-keV level: This level was established on the basis of observed gamma-gamma coincidences, and has not been previously reported. The level is populated by a beta branch of 0.02%, and the log ft value is 9.5, which allows a range of spin assignments from 3/2 to 11/2. The gamma-ray transitions depopulating the level go to levels having spin and parity assignments of 1/2-, 3/2-, and 5/2-. By using the same line of reasoning as was used in the preceding paragraph one can limit the assignment to 3/2± and 5/2-.

1850.9-keV level: This level has not been reported in any of the reaction studies. Its establishment is based upon the observation of two gamma-gamma coincidence relations. The beta branching ratio is 0.14% and the log ft value is 8.7. The gamma-ray transitions depopulating the level go to levels having spins of 5/2-, 7/2-, 9/2-, and (9/2-, 11/2-), but no transitions were observed going to the 3/2- first excited state nor to the 1/2- second excited state. This rules out the possibility of a 3/2- assignment and also makes the 5/2- assignment unlikely. Consequently, the assignment for this level is 7/2± or 9/2-.

1877.5-keV level: This level has not been reported in any of the published reaction studies, but was established on the basis of observed gamma-gamma coincidences. The level is

populated with a beta branch of 0.36%, and the log f_1t value is 9.5. Of the gamma-ray intensity depopulating the level, 81% goes directly to the ground state, with the remainder going to levels having spin and parity assignments of 9/2-. This limits the possible spin and parity assignment for this level to one of the values 5/2-, 7/2±, 9/2±, or 11/2-. If the spin were 5/2- or 7/2- one would expect to see a transition to the 3/2- first excited state, but no such transition was observed. This would indicate a probable assignment of 9/2± or 11/2-.

1887.6-keV level: A level at 1898 keV has been reported in ref. 22 and in ref. 21 a level is reported at 1893 keV. These levels could correspond to this level, but no spin assignment was reported in either study. The level is populated by a beta branch of 0.30% and the log f_1t value is 9.5. The gamma-ray transitions depopulating the level go to levels having spin and parity assignments of 5/2-, 7/2-, and 9/2-, but no transition was observed to a lower spin state. An assignment of 11/2- would require that the transition to the 5/2- state at 1420.7 keV have multipolarity of at least E3, which is unlikely. The arguments used in the preceding paragraph would then yield a probable assignment of 9/2- for this level.

1933.5-keV level: This level was established by the observation of a coincidence relation between the 1306.09-keV

transition and the 627.24-keV transition from the 3/2- first excited state. In (d,p) reaction studies (21, 22) levels have been reported at energies of 1934 keV and 1930 keV, but no spin assignment was made in either report. The level is populated with a beta branch of 0.31%, and the log f_1t value is 9.5. The gamma-ray transitions depopulating this level proceed to to the 7/2- ground state (69%) and to the 3/2- first excited state (31%). An assignment of 9/2- would require that the 1306.09-keV transition have E4 or M3 multipolarity, with the ground-state transition then possibly E2 or M1. However, the ratio of the Weisskopf estimates for these two transitions is not consistent with the ratio of the observed gamma-ray intensities so the 9/2- assignment appears unlikely. Consequently, the assignment for this level is either 3/2-, 5/2±, or 7/2-.

1949.3-keV level: This level was established by the existence of two gamma-gamma coincidence relations. The 1321.97-keV transition carries 76% of the depopulating intensity and was observed in coincidence with the 627.24-keV transition. The 528.20-keV transition is in coincidence with the 1420.66-keV transition and carries 12% of the intensity. The remaining 12% of the intensity is carried by the ground-state transition. In the (d,p) reaction study of ref. 21 a level at 1943 keV is reported, and in ref. 22 a level at 1952 keV is reported, also in a (d,p) experiment. Also, in ref.

26 a level is reported at 1952.3 keV in a neutron capture gamma-ray experiment. None of these studies yielded a spin assignment for this level. The level is populated by a beta branch of 0.28% and the log f_1t value is 9.5. The existence of the transition to a 3/2- state would tend to rule out any spin assignment greater than 7/2, so the likely spin and parity assignment for this level is among the values 3/2-, 5/2±, and 7/2-.

1998.5-keV level: This level has not been reported previously, but its existence was established on the basis the coincidence observed between the 714.90-keV transition and the 1283.23-keV ground-state transition. The level is populated with a beta branch of 0.09% and the log ft value is 8.7. The gamma-ray transitions depopulating the level go to levels having spin and parity assignments of 7/2-, 9/2-, and (9/2-,11/2-). Thus the 3/2- assignment is unlikely so the possible spin and parity assignments include 5/2-, 7/2±, 9/2±, and 11/2-.

2020.8-keV level: This level also has not been reported previously, but was established on the basis of the the coincidence observed between the 737.60-keV transition and the 1283.24-keV transition. The level is populated with a beta branch of 0.16%, and the log f_1t value is 9.6. A ground state transition carries 75% of the depopulating gamma-ray intensity with the remaining 25% carried by the 737.60-keV

transition. The existence of the transition to the 9/2- state at 1283.2 keV would tend to rule out the possibility of a 3/2- or 5/2+ assignment for this level. Thus the possible assignments are 5/2-, 7/2±, 9/2±, and 11/2-.

2037.8-keV level: This level, previously unreported, was established on the basis of two gamma-gamma coincidence relations. The beta branching ratio for the transition populating this level is 0.23%, and the log f_1t value is 9.5. The gamma-ray transitions depopulating the level go to the 3/2- level at 627.2 keV and to the 5/2- level at 1680.7 keV. The existence of the strong transition to the 3/2- level would rule out the possibility of a 9/2- or a 7/2+ assignment, so the remaining possibilities are 3/2-, 5/2±, and 7/2-.

2079.3-keV level: This level was established by the coincidence relation between the 770.56-keV transition and the 1308.13-keV ground-state transition. The other gamma-ray transition depopulating the level is a ground-state transition. The level is fed with a beta branch of 0.02% and the log ft value is 9.4. The gamma-ray transitions go to levels with spin and parity assignments of 7/2- and (9/2-, 11/2-) so the 3/2- and the 5/2+ assignments may be ruled out. Thus the possible assignments are 5/2-, 7/2, 9/2, and 11/2-.

2089.9-keV level: This level was established on the coincidence relation observed between the 1462.43-keV transi-

tion and the 627.24-keV ground-state transition from the first excited state. The level is fed with a beta branch of 0.12% and the log ft value is 8.6 The gamma-ray transitions depopulating the level go to levels with spin and parity assignments of 3/2-, 7/2-, and 9/2-. Assuming that the highest multipolarity among these transitions is E2, the only possible assignments for the spin and parity for this level are 5/2- and 7/2-.

2100.1-keV level: This level was established by the coincidence observed between the 419.30-keV transition and the 1680.72-keV ground-state transition. One other transition depopulates this level, proceeding to the ground state. The level is fed with a beta branch of 0.05%, and the log ft value is 9.0. Since both depopulating gamma-ray transitions go to levels having spin and parity of 7/2-, no additional limitation on the possible spin and parity assignment can be made.

2110.9-keV level: von Ehrenstein et al. (22) have reported a level at 2112 keV and Rapaport and Kerman (21) have reported a level at 2106 keV. In the present work the existence of this level was supported by three gamma-gamma coincidence relations. The level is fed with a beta branch of 0.77% and the log f_1t value is 8.9. This leads to possible spin and parity assignments of 3/2 to 11/2. The gamma-ray transitions depopulating this level go only to levels

having spin and parity of 7/2- and 9/2-. The absence of any transitions from this level to the low lying excited states, which have spins of 3/2- and 1/2-, tends to favor an assignment of 7/2±, 9/2±, or 11/2- for this level.

2156.9-keV level: The existence of a coincidence relation between the 1524.34-keV transition and the 627.24-keV transition from the first excited state was used in establishing this level. Rapaport and Kerman (21) reported a level at 2153 keV and von Ehrenstein et al. (22) reported a level at 2162 keV in (d,p) reaction studies on ^{138}Ba. Also, Moragues et al. (26) have reported a level at 2156.0 keV in the report of their neutron capture work with ^{138}Ba, and they have assigned a spin of 1/2 or 3/2 to this level. In the present work the level was found to be fed with a beta branch of 0.04% with a corresponding log ft value of 9.0. Of the gamma-ray intensity from this level, 57% goes to the ground state and 35% to the 3/2- first excited state. This transition to the 3/2- state would tend to rule out the possibility of a 9/2 or 11/2 assignment for this level, and the transition to the 7/2- level would rule out the possibility of the 1/2 assignment of Moragues et al. Consequently, the 3/2- assignment is the only possible assignment consistent with both the log ft value of this work and the work of Moragues et al.

2166.6-keV level: This level was established by the existence of a coincidence between the 858.44-keV transition

and the 1308.13 keV ground-state transition. The level is fed by a 0.02% beta branch, leading to a log ft value of 9.2. The depopulation of the level is carried by two gamma-ray transitions of approximately equal intensities which go to the 7/2- ground state and to the (9/2-, 11/2-) state at 1308.1 keV. This makes a 3/2- assignment unlikely, so the possible spin and parity assignments then include 5/2-, 7/2±, 9/2±, and 11/2-.

2174.0-keV level: The existence of this level was established by two gamma-gamma coincidence relations. The beta branch feeding this level has a strength of 0.26% and the log f_1t value is 9.3. The gamma-ray transitions depopulating the level go to to levels having spins ranging from 1/2 to 9/2. Assuming that none of these transitions has a multipolarity higher than E2, the only possible spin and parity assignment is then 5/2-.

2218.9-keV level: This level was established by the observation of one definite coincidence relation and a possible coincidence relation. The level is fed with a beta branch of 0.10%, leading to a log f_1t value of 9.6. The depopulating gamma-ray transitions go to levels having spins ranging from 3/2 to 9/2, so if one again assumes no multipolarity higher than E2, the only possible spin and parity assignments are 5/2- and 7/2-.

2229.9-keV level: This level is populated with a beta branch of 0.07%, leading to a log ft value of 8.6. The level was established by a coincidence relation. The depopulating gamma-ray transitions go to the 9/2- state at 1283.2 keV and to the 7/2- ground state. The transition to the 9/2- state renders a 3/2- assignment as well as a 5/2+ assignment unlikely, so the possible spin and parity assignments include 5/2-, 7/2±, 9/2±, and 11/2-.

2249.7-keV level: This level was established on the basis of a coincidence relation between the 966.61-keV transition and the 1283.23-keV transition. The level has a beta branching ratio of 0.03%, and the log ft value is 9.0. The two gamma-ray transitions depopulating this level are of approximately equal intensity and go to levels with spins of 9/2- and 7/2-. The arguments used in the preceding paragraph apply to this level and lead to the same range of possible spin and parity assignments.

2305.0-keV level: This level was established on the basis of a definite coincidence observed between the 1677.44-keV transition and the 627.24-keV transition. In (d,p) reaction studies a level at 2300 keV is reported in ref. 21, and in ref. 22 a level is reported at 2308 keV, but no spin assignments were given. In the present work the log ft value of 8.7 was calculated, based on a beta branching ratio of 0.06%. The existence of a gamma-ray transition to

the 3/2- level at 627.2 keV would tend to rule out the possibility of either the 7/2+, the 9/2, or the 11/2 assignment, so the possible spin and parity assignments include 3/2-, 5/2±, and 7/2-.

2349.9-keV level: This level was established by the observation of seven different gamma-gamma coincidence relations. This level has not been reported in any of the published reaction studies. The level is populated with a beta branch of 1.3% and the log ft value is 7.3, which leads to possible spin assignments of 5/2, 7/2, and 9/2. The gamma-ray transitions from this level proceed to levels having spin assignments of 3/2-, 5/2-, and 7/2-, but no transitions to spin 9/2 levels were observed. The existence of the transition to a 3/2- level eliminates the possibility of a 9/2 assignment. If the spin of this level were 5/2- or 7/2± one might expect to see transitions to one or more of the 9/2- levels. The absence of such transitions indicates that the 5/2+ assignment is the most probable one for this level, but the 5/2- and 7/2- assignments cannot be ruled out completely.

2375.9-keV level: This level was established on the basis of energy sum agreements among four gamma-ray cascades. In reports of (d,p) experiments with ^{138}Ba targets von Ehrenstein et al. (22) have indicated a level at 2368 keV and Rapaport and Kerman (21) have indicated a level at 2378 keV, and these levels could correspond to the level found in the

present work. This level is populated with a beta branch of 0.09% and the log f t value is 9.5. The gamma-ray transitions depopulating this level go to levels with spins of 7/2-, 5/2-, and (3/2-, 5/2-). Thus the possible spin and parity assignments are 3/2-, 5/2±, 7/2±, and 9/2-.

2380.7-keV level: In reference 22 a level at 2381 keV is reported. In the present work a gamma ray of 2380.66 keV was observed to be in coincidence with a gamma ray of 1353.92 keV. The 2380.66-keV transition was placed as a ground-state transition in this cascade because of the agreement with the level populated in the (d,p) experiment of ref. 22. The level is fed with a beta branch of 0.15% and the log f_1t value is 9.2. Since there is only one gamma-ray transition depopulating the level, no further restriction can be placed on the possible spin and parity assignments for this level.

2461.6-keV level: This level was established by the gamma-gamma coincidence observed between the 1178.90-keV transition and the 1283.23-keV ground-state transition. The log f_1t value for the beta transition to this level is 9.4, based on the 0.08% beta branching ratio. The existence of a gamma-ray transition from this level to a 5/2- level renders the 11/2- and 9/2+ assignments unlikely due to the high multipolarity which would be required. Consequently, the possible assignments include 3/2-, 5/2±, 7/2±, and 9/2-.

2524.5-keV level: Two weak coincidences were used in establishing this level, together with energy agreement with two additional transitions. The level is populated with a beta branch of 0.05% and the log ft value is 8.6. The gamma-ray transitions depopulating the level go to levels having spin assignments of (5/2, 7/2) and (9/2, 11/2). This makes the 3/2- and 5/2+ values unlikely assignments but leaves as possible spin and parity assignments the values 5/2-, 7/2±, 9/2±, and 11/2-.

2529.5-keV level: This level is populated with a 0.08% beta branch which leads to a log f_1t value of 9.3. The establishment of the level is based upon a weak coincidence relation between the 1108.93-keV transition and the 1420.66-keV ground-state transition. The 1420.7-keV level has been established as having a spin and parity of 5/2-, so the 11/2- and 9/2+ assignments permitted by the log ft value appear to be unlikely choices. The possible assignments then are 3/2-, 5/2±, 7/2±, and 9/2-.

2531.8-keV level: This level was established by the observation of coincidences with the ground-state transitions from the 3/2- state at 627.2 keV and with the 5/2- state at 1420.7 keV. In the (d,p) reaction experiments there was a level at 2534 keV reported in ref. 22, and in ref. 21 a level at 2527 keV has been reported. Since the energy resolution obtained in these (d,p) reaction experiments was of the order

of 10 to 15 keV, the levels reported in these experiments could correspond to one or more of the three levels near 2530 keV populated in the beta decay of ^{139}Cs. This level at 2531.8 keV is fed with a beta branch of 0.54% and the log ft value is 7.5, which leads to possible spin and parity assignments of 5/2±, 7/2±, and 9/2±. The transitions from this state go to levels having spin and parity assignments of 3/2-, 5/2-, and 7/2-. The existence of the transition to the 3/2- state makes the 9/2± and 7/2+ assignments unlikely, so the remaining possibilities are 5/2± and 7/2-.

2605.8-keV level: This level was established by the observation of nine gamma-gamma coincidences in addition to the ground-state transition. The log ft value is 7.4 and the level is fed with a 0.57% beta branch. The gamma-ray transitions depopulating the level go to levels with spins ranging from 3/2- to (9/2-, 11/2-). Consequently, the only possible spin and parity assignments consistent with both the log ft value and the assumption of no multipolarity higher than E2 are the 5/2- and 7/2- assignments.

2649.3-keV level: This level was established on the basis of the coincidence observed between the 2022.09-keV transition and the 627.24-keV transition. The log f_1t value of 8.7 is based on the beta branching ratio of 0.24%. The existence of the transition to a 3/2- level makes the 7/2+ and the 9/2 assignments unlikely, so the possible assignments

are 3/2, 5/2, and 7/2-.

2847.6-keV level: In the gamma-ray spectrum a transition of energy 2847.63 keV was observed. This was placed as a ground-state transition even though only one additional depopulating transition could be placed at this level. The justification for considering this to be a level lies in the energy agreement with a level at 2857 keV found in the (d,p) reaction study of ref. 22. The depopulating gamma-ray transitions do not provide any information which can be used to further limit the range of possible spin and parity assignments.

Levels above 2900 keV: With the exception of the 3171.6-keV level and the 3950.8-keV level, all levels above 2900 keV have log $f_1 t$ values less than 8.5 and log ft values greater than 5.9, so the spin and parity assignments all fall within the range 5/2±, 7/2±, and 9/2±. In the discussion of these higher levels this range will not be quoted, but arguments for placing further limitations on the possible spin and parity assignments will be presented.

2994.3-keV level: This level was established by the existence of three different coincidence relations. The gamma rays depopulating this level lead to levels having spins of 5/2-, 7/2-, and 9/2-, and to the 2380.7-keV level for which the spin assignment is not known. However, the existence of the transitions to the 5/2- and 9/2- levels would restrict

the spin and parity assignment for this level to 5/2-, 7/2±, or 9/2-.

2997.3-keV level: Two gamma-gamma coincidence relations were used to establish this level. The depopulating transitions go to levels with spin assignments of 7/2- and (9/2-, 11/2-). This rules out the possibility of a spin assignment of 5/2+ but does not allow any further restriction to be made. Consequently, the possible assignments for this level are 5/2-, 7/2±, and 9/2±.

3151.8-keV level: This level was established by the observation of a weak coincidence and energy agreement with three additional depopulating transitions. These transitions go to levels having possible spin assignments (5/2±, 7/2-) and (7/2-, 9/2-). This information does not allow any further restriction on the spin and parity assignment beyond that furnished by the log ft value.

3171.4-keV level: von Ehrenstein *et al.* (22) have reported a level at 3175 keV and Rapaport and Kerman (21) gave the energy of this level at 3177 keV. In the present work a gamma-ray transition of energy 3171.57 keV was observed, and this was taken to be a ground-state transition. One additional gamma-ray transition was placed at this level. The log f_1t value for the beta transition to this level was calculated to be 8.6, just slightly greater than the minimum required for a first-forbidden unique transition. Consequent-

ly, the possible spin and parity assignments for this level include 3/2-, 5/2±, 7/2±, 9/2±, and 11/2-.

3270.2-keV level: The 3270.23-keV transition observed in this work was placed as a ground-state transition, defining a level corresponding to the level at 3270 keV reported in ref. 22 and given as 3264 keV in ref. 21. The gamma-ray transitions depopulating this level do not furnish any information which would allow any further restriction to be placed on the possible spin assignment beyond the (5/2, 7/2, 9/2) provided by the log ft value.

3364.2-keV level: The 3364.23-keV transition has only two possible placements in the level scheme. Since the first excited state is at 627.2 keV and the second excited state is at 1081.9 keV, this transition could be placed either as a direct ground-state transition or as a transition to the first excited state. The decay energy of 4.29 MeV will not allow a higher placement. The choice to place this as a ground-state transition was based on the energy sum agreements with two additional depopulating transitions from this level, whereas no such agreements were found for the other possible placement. The level is fed with a beta branch of 0.13% and the log ft value is 7.1. The gamma-ray transitions go to levels with possible spins of 3/2-, 5/2±, and 7/2-. Consequently, the spin and parity of this level must be among the values 3/2-, 5/2±, and 7/2-.

3401.3-keV level: This level was established by the observation of a weak coincidence between the 2774.04-keV transition and the 627.24-keV transition. No other transitions were found to depopulate this level. The possible spin assignments are 5/2, 7/2, and 9/2.

3418.9-keV level: The 3418.77-keV transition was placed as a ground-state transition rather than as a transition to the first excited state primarily due to the report of a level at 3409 keV in ref. 22. The gamma-ray transitions depopulating the level go to the 7/2- ground state and to the 9/2- state at 1620.7 keV. The possible spin and parity assignments are then limited to 5/2-, 7/2±, and 9/2±.

3464.3-keV level: This level was established by the energy agreement among three cascades. The depopulating transitions go to the 7/2- ground state and to the 3/2- first excited state. This limits the possible spin and parity assignments to 5/2± and 7/2-.

3622.1-keV level: In ref. 22 a level is reported at 3614 keV which may correspond to this level. In the present work two gamma-ray transitions were placed depopulating this level, one of which goes to the 9/2- state at 1283.2 keV. The possible spin and parity assignments are 5/2-, 7/2±, and 9/2±.

3645.7-keV level: The transition of energy 3645.70 keV was tentatively placed as a ground-state transition. The

only other possible placement would be as a transition to the first excited state, and this would require a level at 4272.9 keV, an energy which is only 20 keV less than the measured value of the decay energy. The uncertainty in the measured value of the decay energy is 70 keV, so the placement of the 3645.70-keV transition as a ground-state transition is the more likely placement.

Levels above 3650 keV: Several levels above 3650 keV were established on the basis of observed gamma-ray transitions which could not be placed as transitions to excited states by decay energy limitations. Subtracting the first excited state energy of 627.2 keV from the measured decay energy value of 4290 keV leaves a value of 3663 keV as the upper limit on the energy of a transition which could be placed as a transition to the first excited state.

3665.6-keV level: This level was established by the existence of the 3665.61-keV transition. An additional depopulating transition goes to the 1850.9-keV level. The possible spin assignments, based on the log ft value, are 5/2, 7/2, and 9/2.

3674.6-keV level: This level was established by the coincidence observed between the 3047.29-keV transition and the 627.24-keV transition. There is also a transition to the 5/2- state at 2174 keV. Assuming that these depopulating transitions do not have multipolarity higher than E2 leads to

possible assignments of 5/2± and 7/2-.

3724.2-keV level: This level was established by the existence of the 3724.20-keV transition. An additional transition goes to the 3/2- level at 627.2 keV. This leads to possible assignments of 5/2± and 7/2-.

3734.6-keV level: This level was established by the observation of a weak coincidence between the transitions of 1353.92 keV and 2380.66 keV. The possible spins are 5/2, 7/2, and 9/2.

3769.1-keV level: This level was established by the existence of the 3769.17-keV transition. Two additional transitions depopulate the level, with one of these going to the (5/2+) level at 2349 keV. This leads to possible spin and parity assignments of 5/2±, 7/2±, or 9/2+.

3820.0-keV level: This level was established by the existence of the 3819.99-keV transition. An additional transition was placed between this level and the (5/2-, 7/2-) level at 2218 keV. The possible spin assignments are 5/2, 7/2, and 9/2.

3839.8-keV level: This level was established by the existence of the 3839.78-keV transition. An additional transition goes to the 5/2- level at 1420.7 keV. The possible spin and parity assignments are 5/2±, 7/2±, and 9/2-.

3853.9-keV level: A transition of energy 3853.88 keV was used to establish this level. An additional transition

depopulates the level but does not furnish any further restriction on the spin and parity assignment. The spin may be 5/2, 7/2, or 9/2.

3887.8-keV level: This level was established by the existence of the 3887.8-keV transition. No additional depopulating transitions were observed. The possible spin assignments are 5/2, 7/2, and 9/2.

3912.3-keV level: This level was established by the existence of the 3912.32-keV transition, with an additional transition to the 5/2- level at 2174.0 keV. The possible spin and parity assignments are 5/2±, 7/2±, and 9/2-.

3950.9-keV level: This level was established by energy sum agreement among three gamma-ray cascades. The depopulating transitions go to levels with spins of 3/2- and 9/2-. This limits the possible spin and parity assignment to either 5/2- or 7/2-.

2. Beta decay energy and branching

The beta-gamma coincidence experiments in the ^{139}Cs decay yielded a value of 4.29 ± 0.07 MeV for the Q-value of this decay. A total of eight different gating transitions were used in obtaining the beta spectra. The decay energy results ranged from 4.20 to 4.36 MeV, with a rms spread of 0.06 MeV. Adding an uncertainty of 0.04 MeV in the calibration data leads to the error of 0.07 MeV quoted above. The beta branching and the gating transitions used are shown in

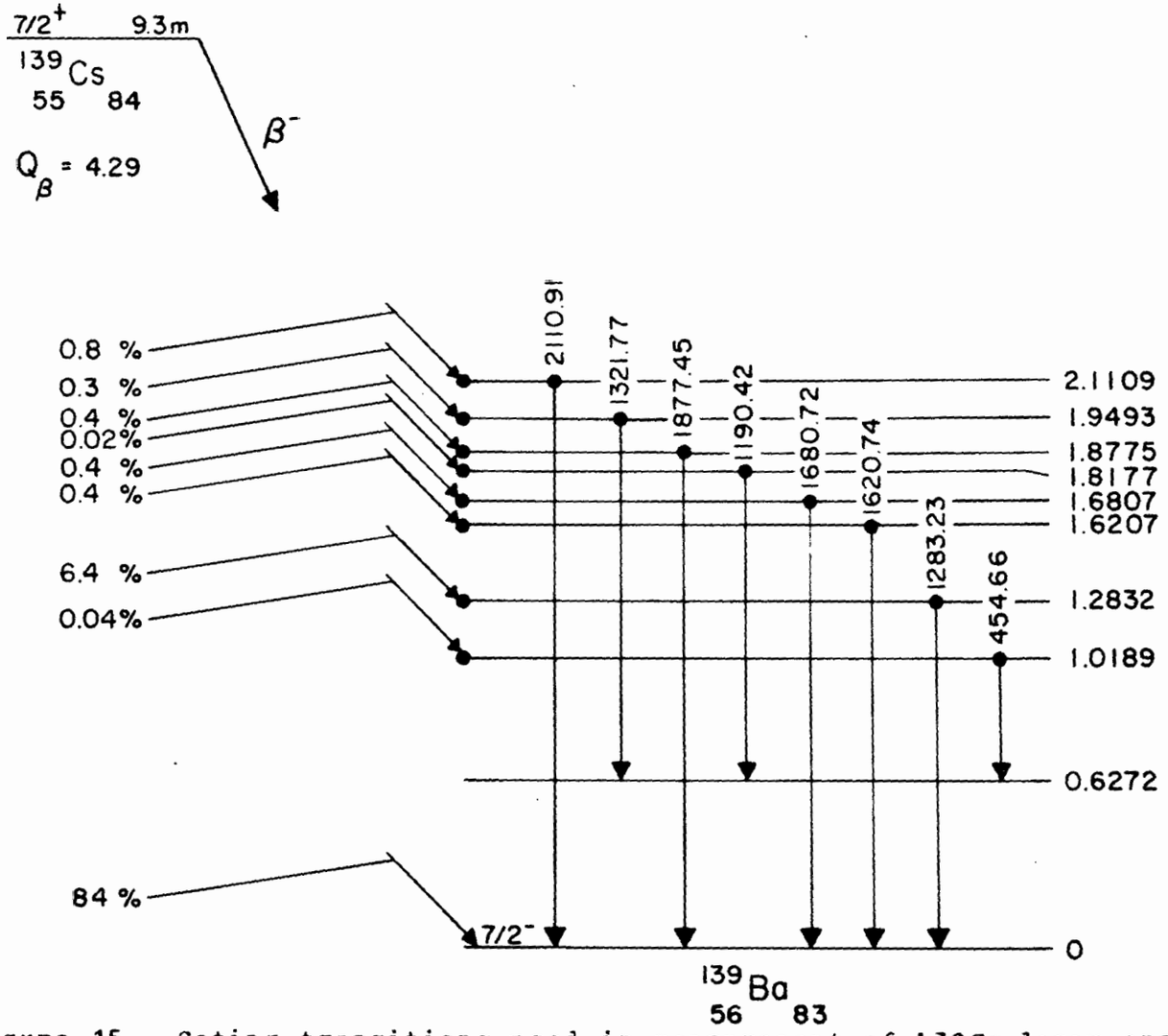

Figure 15. Gating transitions used in measurement of ^{139}Cs decay energy

Figure 15. Table 10 contains a list of the gating transitions used along with the Q-value obtained from each gated beta spectrum. These Q-values were averaged using the least squares fit for a single variable of ref. 53.

Following the same procedure as for the Xe decay, the log ft values were calculated using the observed gamma-ray intensities and the calculated value of 84% for the ground-state beta branching. The percent beta branching and the log ft values for the ^{139}Ba levels are listed in Table 11.

Table 10. Beta endpoints for the decay of ^{139}Cs

Gating Peak (MeV)	Initial Level of Gating Peak (MeV)	Q (MeV)	ΔQ^1 (MeV)
0.454	1.081	4.29	0.06
1.190	1.817	4.24	0.09
1.283	1.283	4.30	0.05
1.321	1.949	4.35	0.09
1.620	1.620	4.36	0.09
1.680	1.680	4.21	0.07
1.877	1.877	4.20	0.06
2.110	2.110	4.29	0.06

Weighted Average $Q = 4.29 \pm 0.07$ MeV.

[1] ΔQ is the geometrical sum of the error from the Fermi fit and the error from the calibration.

Table 11. Beta branching and log ft's for the ^{139}Cs decay

^{139}Ba Levels (MeV)	Percent Beta Branching	Log ft	Log $f_1 t$
0.0000	84. ± 6.	6.9 ± .2	8.6
0.6272	.05 ± .1	10.0 ± .2	11.0
1.0819	.04 ± .01	9.7 ± .2	11.1
1.2832	6.4 ± .4	7.4 ± .2	8.8
1.3081	.25 ± .02	8.7 ± .2	10.2
1.4207	.29 ± .05	8.6 ± .2	10.0
1.5390	.06 ± .01	9.2 ± .2	10.6
1.6207	.39 ± .02	8.4 ± .2	9.7
1.6807	.41 ± .03	8.3 ± .2	9.6
1.6987	.11 ± .01	8.9 ± .2	10.5
1.7486	.03 ± .01	9.5 ± .2	10.7
1.8177	.02 ± .02	9.5 ± .4	10.8
1.8507	.14 ± .01	8.7 ± .2	9.9
1.8774	.36 ± .02	8.2 ± .2	9.5
1.8876	.30 ± .01	8.3 ± .2	9.5
1.9335	.31 ± .02	8.3 ± .2	9.5
1.9493	.28 ± .02	8.3 ± .2	9.5
1.9985	.09 ± .01	8.7 ± .2	9.9
2.0208	.16 ± .04	8.5 ± .2	9.6
2.0378	.23 ± .01	8.3 ± .2	9.5
2.0793	.02 ± .01	9.4 ± .2	10.6
2.0899	.12 ± .01	8.6 ± .2	9.7
2.1001	.05 ± .01	9.0 ± .2	10.1
2.1109	.77 ± .04	7.7 ± .2	8.9
2.1569	.04 ± .01	9.0 ± .2	10.1
2.1666	.02 ± .01	9.2 ± .2	10.3
2.1740	.26 ± .01	8.1 ± .2	9.3
2.2189	.10 ± .01	8.5 ± .2	9.6
2.2299	.07 ± .01	8.6 ± .2	9.7
2.2497	.03 ± .01	9.0 ± .2	10.1
2.3050	.06 ± .01	8.7 ± .2	9.8
2.3499	1.27 ± .04	7.3 ± .2	8.4
2.3759	.09 ± .01	8.4 ± .2	9.5
2.3807	.15 ± .01	8.2 ± .2	9.2
2.4616	.08 ± .01	8.4 ± .2	9.4
2.5245	.05 ± .01	8.6 ± .2	9.5
2.5299	.08 ± .02	8.3 ± .2	9.3
2.5318	.54 ± .03	7.5 ± .2	8.5
2.6058	.57 ± .02	7.4 ± .2	8.4
2.6493	.24 ± .04	7.8 ± .2	8.7
2.8476	.12 ± .01	7.8 ± .2	8.6
2.9943	.13 ± .01	7.6 ± .2	8.3

Table 11. (Continued)

^{139}Ba Levels (MeV)	Percent Beta Branching	Log ft	Log f_1t
2.9973	.13 ± .01	7.6 ± .2	8.3
3.1519	.10 ± .01	7.5 ± .2	8.2
3.1716	.03 ± .01	8.0 ± .2	8.6
3.2702	.03 ± .01	7.9 ± .2	8.5
3.3642	.10 ± .01	7.2 ± .2	7.7
3.4013	.03 ± .01	7.6 ± .2	8.1
3.4188	.09 ± .01	7.2 ± .2	7.6
3.4643	.16 ± .01	6.8 ± .2	7.2
3.6221	.07 ± .01	6.8 ± .2	7.1
3.6457	.04 ± .01	7.0 ± .2	7.2
3.6656	.15 ± .01	6.4 ± .2	6.6
3.6746	.05 ± .01	6.9 ± .2	7.1
3.7242	.04 ± .01	6.9 ± .2	7.0
3.7346	.02 ± .01	7.0 ± .2	7.2
3.7692	.07 ± .01	6.5 ± .2	6.6
3.8200	.03 ± .01	6.7 ± .2	6.7
3.8398	.03 ± .01	6.6 ± .2	6.6
3.8539	.03 ± .01	6.5 ± .2	6.5
3.8878	.03 ± .01	6.5 ± .2	6.4
3.9123	.03 ± .01	6.4 ± .2	6.3
3.9508	.06 ± .01	5.9 ± .2	5.7

IV. DISCUSSION

In the previous chapter the log ft values deduced in this work, along with the observed gamma-ray transitions, were used to establish spin and parity assignments for the levels in the nuclides ^{139}Cs and ^{139}Ba. In the present chapter an attempt will be made to interpret some of these levels in terms of shell-model states available to the nucleons in the mass 139 region. For neutrons above N = 82 the shell-model states are $1h_{9/2}$, $2f_{7/2}$, $2f_{5/2}$, $3p_{3/2}$, $3p_{1/2}$, and $1i_{13/2}$, with all having negative parity except for the $1i_{13/2}$ state. The protons above Z = 50 have shell-model states $1g_{7/2}$, $2d_{5/2}$, $2d_{3/2}$, $2s_{1/2}$, and $1h_{11/2}$, with all but the $1h_{11/2}$ state having positive parity.

The excited states of an odd-A nucleus may be interpreted from several viewpoints. One can think of the nucleus being excited from its ground state by the elevation of the odd particle from one single-particle state to another, a picture which is expected to be valid for only the first few excited states of odd nuclei close to major shell closures. Another excitation mechanism which might occur in nuclei with several nucleons outside a major shell would involve a recoupling of these nucleons to a different angular momentum and energy from that of the ground state, but with these nucleons still remaining in the same shell-model orbits. An additional mode of excitation for odd-A nuclei is the

coupling of the various single-particle states of the odd nucleon to the vibrational excitations of the even-even core.

In the case of ^{139}Cs the only experimental information available in addition to the results of this work consists of the values of some internal conversion coefficients presented in ref. 15. There is no direct information on the ground-state spin and parity of the parent ^{139}Xe so all spin assignments in ^{139}Cs are based on the deduced 22% ground-state beta branching value. No reaction work has been reported which could provide information on the levels in ^{139}Cs.

For the levels in ^{139}Ba there exists a great deal of information derived from reaction experiments, particularly from the (d,p) reaction on ^{138}Ba. In addition, the excited states of ^{138}Ba are well known from the work of Carlson et al. (54). This information will be used along with the results of the present work in an attempt to interpret some of the levels in ^{139}Ba.

Since the information obtained in this study came from observation of the beta decays of ^{139}Xe and ^{139}Cs and the subsequent gamma-ray de-excitations, it is important to consider the nature of the beta interaction when attempting to interpret the levels populated through this beta decay. The beta decay process involves the decay of a single neutron into a proton and beta particle, along with the associated neutrino, but without the excitation of other nucleons to

higher excited states. This rules out the possibility of multiple processes where, for example, one member of a pair of neutrons decays to a proton and the remaining member of the pair is simultaneously promoted to a higher single-particle state.

A. The Levels of ^{139}Ba

The states in ^{139}Ba studied in this work are those populated following beta decay from the ground state of ^{139}Cs, which has five protons outside the major shell Z = 50 and two neutrons outside the major shell N = 82. The neutrons in ^{139}Cs presumably couple to zero angular momentum in the ground state so that the ground-state spin is determined by the protons. In analogy with the nearby odd-A Cs isotopes the ground-state spin is assumed to be 7/2+. The probable shell-model configuration is $\pi(g_{7/2})^5 \nu(f_{7/2})^2$, with possible admixtures of other states. The beta decay to the ground state of ^{139}Ba could then be considered as the decay of one of the $f_{7/2}$ neutrons to a $g_{7/2}$ proton with the other neutron remaining in the $f_{7/2}$ state. This would constitute a first-forbidden transition, and is consistent with the 84% ground-state beta branching observed in this decay. The ground state of ^{139}Ba appears to be a rather pure neutron $f_{7/2}$ state. This contention is supported by the the observation that more than 99% of the beta decay of ^{139}Ba goes to the 7/2+ ground state and 5/2+ first excited state in ^{139}La, as

indicated in ref. 8. Further support for this contention lies in the large spectroscopic factors found in the (d,p) reaction experiments.

In the decay of ^{139}Cs there are excited states populated in ^{139}Ba which appear to be largely single particle in character. These states have spins of 5/2- and 9/2-. This would indicate that the ground state of ^{139}Cs has some configuration mixing because the nature of the beta interaction would not allow all of these levels to be populated if the ground state of ^{139}Cs were a pure $\pi(g_{7/2})^5\nu(f_{7/2})^2$ configuration. Consequently, there is likely some mixing of the $\pi(g_{7/2})^5\nu(h_{9/2})^2$, the $\pi(g_{7/2})^5\nu(f_{7/2})^1\nu(h_{9/2})^1$, and the $\pi(g_{7/2})^5\nu(d_{5/2})^2$ configurations in the ^{139}Cs ground state. In ref. 54, Carlson discusses mixing in the ground state of ^{138}Xe in terms of the configurations which could give rise to the allowed beta decay observed in that work. His discussion is closely related to the present problem since ^{138}Xe can be considered as an even-even core to which one proton is added to obtain ^{139}Cs. With these configurations mixed in with the $\pi(g_{7/2})^5\nu(f_{7/2})^2$ configuration in the ^{139}Cs ground state it becomes plausible for the beta decay to occur to several of the states in ^{139}Ba and still be consistent with the nature of the beta interaction.

The first excited state in ^{139}Ba, at an energy of 627.2 keV, has a spin and parity of 3/2-. There is little or no

beta feeding to this level, but the level is populated in (d,p) reactions with $\ell_n = 1$, indicating p-wave neutron transfer. The configuration is likely $\pi(g_{7/2})^6 \nu(p_{3/2})^1$. The small upper limit to the beta branching to this level is understandable in terms of the large change in ℓ-value which would be required for the decay of a $p_{3/2}$ neutron to a $g_{7/2}$ proton. This fact would greatly hinder any beta decay to this level even if there were a substantial $\nu(p_{3/2})^2$ component in the ^{139}Cs ground-state wave function.

The second excited state occurs at an energy of 1081.9 keV and has spin and parity of 1/2-. The likely configuration is $\pi(g_{7/2})^6 \nu(p_{1/2})^1$, which would be consistent with the $\ell_n = 1$ neutron transfer observed in (d,p) experiments. As with the first excited state, beta decay to this state would be highly hindered due to the large spin change required.

The level at 1283.2 keV is the most strongly fed of the excited states in ^{139}Ba from the beta decay of ^{139}Cs. In the (d,p) reaction experiments this level is populated with $\ell_n = 5$, and has been assigned a spin and parity of 9/2- on the basis of available shell-model states. The likely configuration is $\pi(g_{7/2})^6 \nu(h_{9/2})^1$. The relatively large beta feeding of this level suggests that the ground state of ^{139}Cs should have a substantial $\pi(g_{7/2})^6 \nu(h_{9/2})^2$ component. Then the beta decay to this level could be described as the decay of a $h_{9/2}$ neutron to a $g_{7/2}$ proton, with the remaining

neutron staying in the $h_{9/2}$ orbit. This transition would involve angular momentum change of one unit, and would be classified as first forbidden, a designation supported by the log ft value of 7.4 found in this work.

Another level which may be interpreted as primarily a single-particle excitation occurs at an energy of 1420.7 keV. This level is populated in (d,p) reaction experiments by $\ell_n = 3$ neutron transfer, and is given a spin and parity assignment of 5/2-, a designation which is supported by the log ft value observed in the present work. A likely configuration is $\pi(g_{7/2})^6\nu(f_{5/2})^1$. The beta decay to this level could be described as the decay of a $f_{5/2}$ neutron to a $g_{7/2}$ proton, assuming that there is a $(f_{5/2})^2$ component in the ^{139}Cs wave function.

Some aspects of particle-core coupling in odd-A nuclei have been discussed by de-Shalit (55) and by Kisslinger (56). More recently, Henry et al. (57) and in ref. 54 Carlson et al. have used particle-core coupling to describe levels populated in the daughters of gaseous fission products.

If one thinks of the ^{139}Ba nucleus as being composed of a ^{138}Ba core plus an additional neutron, then one might look for a sequence of levels based on the first 2+ vibrational state in ^{138}Ba, which occurs at an energy of 1435.9 keV (54). Coupling a $f_{7/2}$ neutron to this 2+ core excitation would result in states with spins ranging from 3/2- to 11/2-. The

weighted average energy of these states would be approximately the energy of the 2+ excitation in the ^{138}Ba core.

The level at 1308.1 keV has not been reported previously, and the log ft value indicates a spin and parity of 9/2- or 11/2-. There are no gamma-ray transitions from this state to any of the lower lying single-particle states. This level may be one of the particle-core coupled states in this nucleus, and if so, a possible configuration would be a coupling of the $f_{7/2}$ neutron to the 2+ one-phonon vibration in the ^{138}Ba core. If one assumes a 11/2- designation for this level and uses the 1539-keV 9/2- level, the 1680-keV 7/2- level, the 1698-keV 5/2- level, and the 1748-keV 3/2- level as a multiplet, the weighted average energy is 1542 keV, as compared with the 1436 keV energy for the 2+ excitation in ^{138}Ba. There is no hard evidence that these states are indeed members of a particle-core coupled multiplet, but it is quite likely that such coupling is present in this region.

The second excited state of ^{138}Ba occurs at an energy of 1899 keV, as reported in ref. 54, and has a spin and parity of 4+. The coupling of this excitation to the $f_{7/2}$ neutron could give rise to a sequence of levels with spins ranging from 1/2 to 15/2, all with negative parity. The results of the present work give no indication of any population of levels with spin greater than 11/2, which is understandable for beta decay from a spin 7/2 parent, so there is no indica-

tion where levels of spin 13/2 or 15/2 might lie. However, if one takes as members of this multiplet the 1620-keV 9/2- level, the 1850-keV level assuming a spin of 7/2-, the 1933-keV level with spin 5/2-, and the 2100-keV level with spin 3/2-, the resulting weighted average energy is 1821 keV, as compared with the 1899-keV energy for the 4+ excitation in ^{138}Ba.

An additional set of particle-core coupled levels could arise from a coupling of the $p_{3/2}$ neutron with the 2+ one-phonon excitation. The center of gravity of such a sequence might be expected to lie at an energy equal to the sum of the energies of the single-particle and core excitations, or 2063 keV. The spins possible in such a sequence would range from 1/2- to 7/2-. Again, the ℓ-forbiddenness would hinder the population of a 1/2- state in the beta decay from a 7/2+ parent. But using the 1949-keV level with spin 7/2, the 2020-keV level with spin 5/2, and the 2037-keV level with spin 3/2 leads to a weighted average energy of 1993 keV. Inclusion of a spin 1/2 level would raise the average energy somewhat closer to the 2063-keV value.

In this energy region there are other couplings which could presumably be involved in the structure of ^{139}Ba. At these energies it is also possible for proton pairs to be broken so that other excitations of the core could be involved. In ref. 54 there are additional levels reported in

^{138}Ba at 2217 keV, 2307 keV, 2445 keV, and 2369 keV which are fed by relatively strong beta branches in the decay of ^{138}Cs. Coupling of these excitations with the neutron single-particle excitations could lead to a large number of states in this region, and the complexity of this structure is such that one would need firm and definite spin and parity assignments in order to sort out the various multiplets possible.

The multiplet groupings of the levels presented in the preceding paragraphs must be regarded with some skepticism in the absence of better experimental information on the spin and parity assignments for these levels.

B. The N = 83 Nuclides

Figure 16 is a plot of the energy levels of some of the even-odd nuclides with N = 83. For ^{137}Xe the energies have been determined by P. A. Moore et al. by observing isobaric analog states populated in (p,p) elastic scattering experiments on ^{136}Xe (58). The levels shown for ^{139}Ba are from the present work. For ^{141}Ce the level energies have been determined by J. Cook and W. L. Talbert, Jr. from a study of the ^{141}La decay (59). The data used for ^{143}Nd are from a report on a ^{142}Nd(d,p) reaction experiment by P. Christensen et al. (60). The energies for ^{145}Sm were determined by E. Newman et al. in a study of the ^{145}Eu decay (61) and by P. Christensen et al. in a (d,p) reaction study on ^{144}Sm as reported in ref. 60.

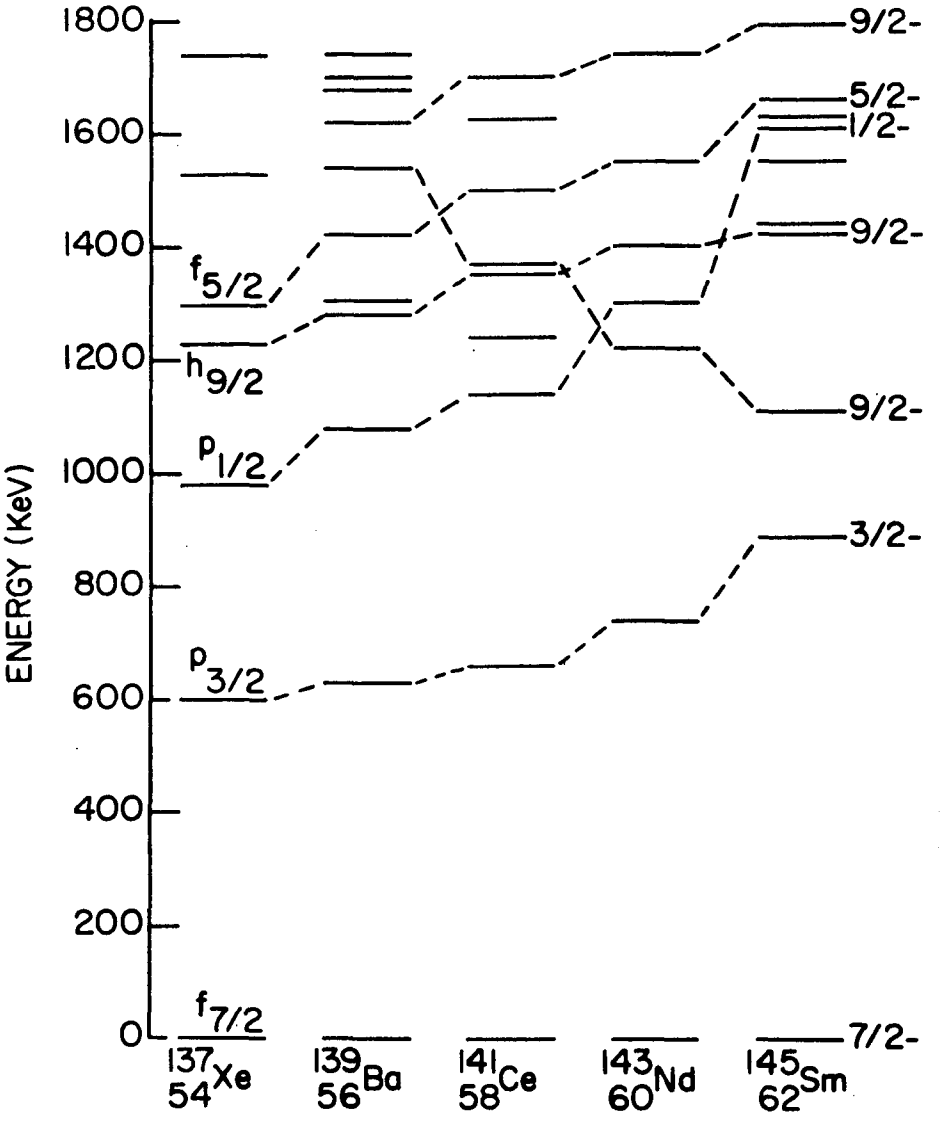

Figure 16. Energy levels of N = 83 nuclides

The single particle designations for several of the levels are shown at the left in the figure, and dashed lines connect levels in adjacent nuclides which are believed to have the same single-particle designation. The ground-state spin and parity for each of these nuclides is 7/2-, corresponding to a $f_{7/2}$ shell-model state for the 83rd neutron. The results of the reaction studies indicate that the ground state of each of these nuclides is a rather pure $f_{7/2}$ neutron configuration.

The energy of the first excited state varies smoothly from 600 keV for ^{137}Xe to 893 keV for ^{145}Sm. The results of the reaction experiments have led to a $p_{3/2}$ designation for this state, based on the $\ell_n = 1$ neutron transfer observed in these experiments and the conventional spin orbit splitting of the shell model.

A similar trend may be observed in the figure for the $p_{1/2}$ state. However, the rate of increase in energy with increasing Z is greater for the $p_{1/2}$ state, increasing from 980 keV in ^{137}Xe to 1607 keV in ^{145}Sm. This would indicate that the spin-orbit splitting increases as the number of protons in the nucleus increases.

The $h_{9/2}$ level occurs at an energy of 1230 keV in ^{137}Xe, and shows a relatively moderate rate of increase in energy with increasing Z, reaching an energy of 1423 keV in ^{145}Sm.

A somewhat larger increase in energy occurs with the $f_{5/2}$ state. For ^{137}Xe this level lies at 1300 keV and for ^{145}Sm the energy of this state is 1658 keV.

There are two additional sets of levels in the figure, both of which have spin and parity values of 9/2-. One of these sets begins at 1620 keV in ^{139}Ba and increases to 1788 keV in ^{145}Sm. The other sequence begins at 1539 keV in ^{139}Ba, but decreases in energy with increasing Z rather than increasing as the single-particle levels do. This 9/2- excitation drops below the $p_{1/2}$ and $h_{9/2}$ levels between ^{141}Ce and ^{143}Nd so that it becomes the second excited state for ^{143}Nd and ^{145}Sm. This behavior would seem to indicate that these levels arise from a different type of interaction with the protons in the nucleus.

C. The Levels of ^{139}Cs

The ^{139}Cs nucleus has five protons outside the closed shell at Z = 50, so the shell-model orbits accessible to these protons are the $1g_{7/2}$, $2d_{5/2}$, $2d_{3/2}$, $3s_{1/2}$, and $1h_{11/2}$ states, all having positive parity except the $1h_{11/2}$ state. There are two neutrons outside the major shell closure at N = 82, and the shell-model states available for these neutrons are the negative parity $2f_{7/2}$, $2f_{5/2}$, $1h_{7/2}$, $3p_{3/2}$, and $3p_{1/2}$ states and the $1i_{13/2}$ positive-parity state. With the large number of nucleons outside the major shells one might expect that the structure of this nucleus would not ex-

hibit much in the way of single-particle excitations.

The ground state of ^{139}Cs likely has a spin and parity of 7/2+, in analogy with the nearby odd-A Cs isotopes. Figure 17 shows the lower lying excited states of odd-A Cs isotopes for A = 133 through A = 141. The data for A = 139 is taken from the present work, the levels in ^{141}Cs are from J. Cook and W. L. Talbert, Jr. (59). For A = 133 the energies are taken from V. R. Dave et al. (62). P. Alexander and J. P. Lau (63) and J. P. Op de Beeck and W. B. Walters (64) have reported level energies for A = 135. For A = 137 the data are from G. Holm (65). A likely configuration for the ground state of ^{139}Cs is $\pi(g_{7/2})^5\nu(f_{7/2})^2$. The beta decay to this state would involve the decay of a $f_{7/2}$ neutron in ^{139}Xe to a $g_{7/2}$ proton, a first-forbidden transition. The 22% ground-state beta branch determined in this study leads to a log ft value of 6.6 which is in agreement with this classification.

As indicated in the figure, the first excited state of the odd-A Cs isotopes in this region generally has a spin and parity assignment of 5/2+. Assuming that this designation also holds for ^{139}Cs, a possible configuration for this state at 218.6 keV would be $\pi(g_{7/2})^4\pi(d_{5/2})^1\nu(f_{7/2})^2$. The beta decay to this state would then involve the decay of a $f_{7/2}$ neutron to a $d_{5/2}$ proton.

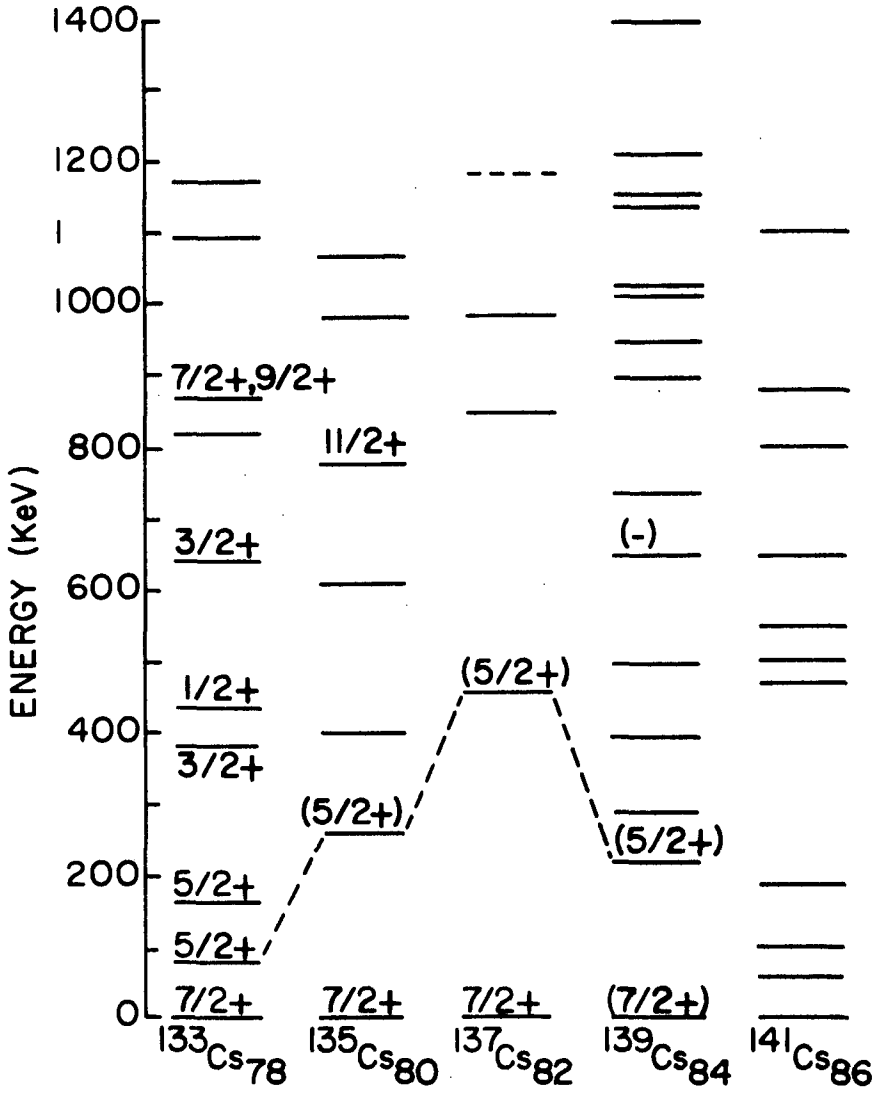

Figure 17. Energy levels of odd-A Cs nuclides

The second excited state occurs at an energy of 289.8 keV, and the results of this work establish the spin only to within 5/2, 7/2, or 9/2+ so it is difficult to make a case for any particular mode of excitation for this state. This level is populated with a beta branch of approximately the same value as that of the first excited state, so this may indicate that there is some similarity in the beta decay to these states, particularly since they are separated by only 71 keV. One possible configuration for this state is $\pi(g_{7/2})^3\pi(d_{5/2})^2\nu(f_{7/2})^2$. This would be consistent with the nature of the beta interaction if the ground state of ^{139}Xe contains a $\pi(g_{7/2})^3\pi(d_{5/2})^1\nu(f_{7/2})^3$ component. Then the beta decay to the 289.8-keV level would involve the decay of a $f_{7/2}$ neutron to a $d_{5/2}$ proton.

To examine the effects of particle-core coupling in this nucleus one can think of the nucleus as being composed of a ^{138}Xe core plus an additional proton. The excitation energies of the states in ^{138}Xe have not been measured but one can appeal to the systematics of even-even nuclei in this region and get some indication of the magnitudes of the energies involved. In Figure 18 are shown the lower lying excited states of the other N = 84 nuclei ^{140}Ba (66), ^{142}Ce (67), ^{144}Nd, and ^{146}Sm (51). The excitation energies of the 2+ one-phonon vibration, the 4+ and 2+ two-phonon vibrations, and the 3- octupole vibration vary quite smoothly in this

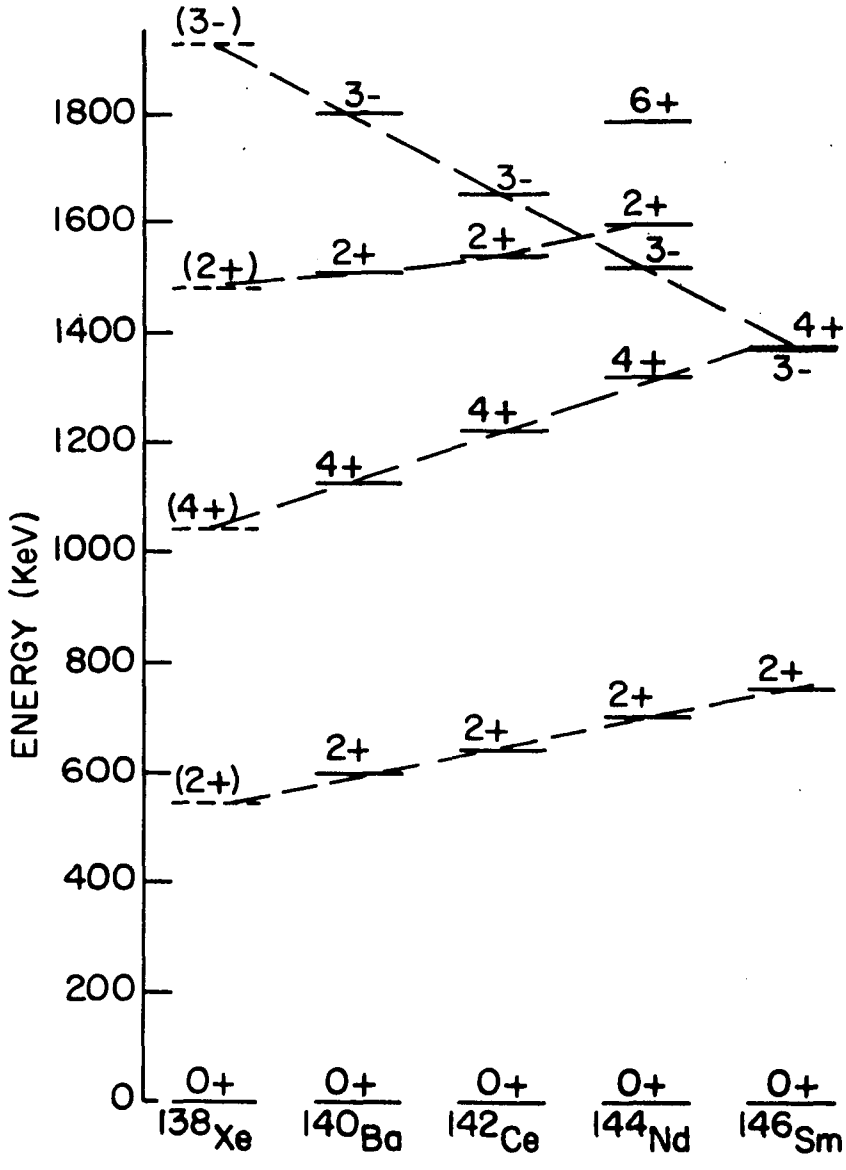

Figure 18. Energy levels of N = 84 nuclides

picture. The dotted lines show the shift from nuclide to nuclide and an extrapolation back to the ^{138}Xe nuclide. From this extrapolation it appears that in ^{138}Xe the first 2+ state should appear at approximately 580 keV, the 4+ state at 1040 keV, the second 2+ state at 1480 keV, and the 3- state at 1940 keV. The relatively low value for the first 2+ excitation indicates that particle-core coupling could be involved in even the low-energy excited states of ^{139}Cs.

For a coupling of the odd $g_{7/2}$ proton to the one-phonon excitation of the core, the possible spin and parity values of the resulting states would range from 3/2+ to 11/2+ and the weighted average of the energies should be approximately 580 keV. A coupling of this 2+ excitation to the $d_{5/2}$ proton could result in a sequence of levels centered around 800 keV having spins ranging from 1/2+ to 9/2+. An additional sequence could arise from the coupling of the 4+ excitation with the $g_{7/2}$ proton, for which the average energy should be approximately 1040 keV. Negative parity states could arise from a coupling of the 3- octupole vibration with the $g_{7/2}$ single proton, and these states should occur at energies around 1980 keV. An additional source for negative parity states would be the $1h_{11/2}$ orbit, which is among the shell-model states available to protons in this region. However, population of this state in the beta decay from ^{139}Xe would require a second-forbidden beta transition and thus it is not

likely that it would be observed.

With the large number of low-lying levels in ^{139}Cs and the various particle-core couplings multiplets possible it becomes very difficult to separate the levels into these various groups. This is particularly so because of the lack of good definition of the spins of these levels. For most of these levels the spins have only been identified to within a range of four units, or in some cases from 5/2 to 9/2. The results of this work indicate that the higher spin states of these multiplets are not populated in beta decay, so one can only look at the members of these multiplets having spins between 3/2 and 9/2.

If one takes as members of the $g_{7/2}$ proton plus one-phonon multiplet the 393-keV level with spin 9/2, the 515-keV level with spin 7/2, the 732-keV level with spin 5/2, and the 1020-keV level with spin 3/2, the weighted average energy is 590 keV. This value agrees very well with the 580-keV value obtained for the excitation energy of the first 2+ state in ^{138}Xe.

For the coupling of the $g_{7/2}$ proton with the 4+ excitation one might expect to find states which de-excite by gamma-ray transitions to members of the proton plus one-phonon multiplet, but which do not have crossover transitions to the ground state. Again, the higher spin states would not be very likely to be populated in beta decay from the 7/2-

parent. As possible members of this multiplet one can take the 1006-keV level with spin 9/2, the 1138-keV level with spin 7/2, and the 1186-keV level with spin 5/2. The weighted average energy of these states is 1095 keV. This is in excellent agreement with the value of 1040 keV obtained for the 4+ excitation in ^{138}Xe.

The foregoing discussion of possible particle-core multiplets in ^{139}Cs is intended to indicate some of the nature expected in the structure of this nucleus. Without more knowledge of the spin and parity assignments for the states involved one can only speculate on the inclusion of a given level in one multiplet or another.

V. CONCLUSIONS

The studies of the beta decay of ^{139}Xe and the subsequent gamma-ray transitions in the daughter nucleus ^{139}Cs carried out in this study have resulted in the establishment of several new levels in ^{139}Cs. The absence of any supportive reaction data however, precludes the assignment of firm spin and parity values to these levels. Such information would be of considerable aid in understanding and interpreting the level structure of ^{139}Cs. It is doubtful whether further studies of the gamma-ray spectrum would provide any information beyond the determination of the energies and intensities of the weaker transitions to a somewhat greater degree of precision.

Further study of the beta and electron spectrum of the decay of ^{139}Xe would be in order, particularly in the determination of the values of the internal conversion coefficients and in measurement of the ground-state beta branching. Such studies should be feasible in the near future with the TRISTAN system following the installation of a new modular moving tape collector. The value for the ground-state beta branching determined in this study is based upon the measured value for the branching to the ground state and first excited state in the decay of ^{139}Ba and upon the gamma-ray intensities observed in the present work. A direct measurement would provide greater confidence in the spin assignment for

the ground state of ^{139}Xe. More precise values for the internal conversion coefficients would aid in establishing the multipolarities of many of the gamma-ray transitions and thereby aid in establishing the spins and parities of the levels.

Previous studies of the decay of ^{139}Cs only resulted in the placement of a few gamma-ray transitions in a partial level scheme for ^{139}Ba. As a result of this study the gamma-ray decay scheme is now essentially complete. Further gamma-ray studies would not likely produce any major changes in this level scheme.

The ^{139}Ba nucleus appears to have a structure much like the other N = 83 nuclides, with indications of single-particle excitations among the lower lying excited states. For this nucleus, just as for ^{139}Cs it would be helpful to have values for the internal conversion coefficients available for several of the transitions, in order to assign spins and parities of the excited states with greater precision for subsequent interpretation.

VI. LITERATURE CITED

1. Nagaoka, H. Kinetics of a system of particles illustrating the line and the band spectrum and the phenomena of radioactivity. Phil. Mag. Series 6. 7: 445. 1904.

2. Geiger, H. and Marsden, E. The laws of deflexion of alpha particles through large angles. Phil. Mag. Series 6. 25: 604. 1913.

3. Brink, D. M. Nuclear forces. p. 123. Oxford, Pergamon Press. 1965.

4. Jackson, D. F. Nuclear reactions. p. 17. London, Methuen and Company. 1970.

5. Bohr, N. and Wheeler, J. A. The mechanism of nuclear fission. Phys. Rev. 56: 426. 1939.

6. Ehrenberg, B. and Amiel, S. Independent yields of krypton and xenon isotopes in thermal-neutron fission of ^{235}U. Observation of an odd-even effect in the element yield distribution. Phys. Rev. C6: 618. 1972.

7. Hill, J. C. and Wiedenbeck, M. L. Levels in the N = 82 nucleus ^{139}La populated in ^{139}Ba decay. Nucl. Phys. A119: 53. 1968.

8. Berzins, G., Bunker, M. E. and Starner, J. W. The decay scheme of ^{139}Ba. Nucl. Phys. A128: 294. 1969.

9. Kelly, W. H., Beard, G. B., Chaffee, W. B. and Gonser, J. M. The 85-minute activity of ^{139}Ba. Nucl. Phys. 19: 79. 1960.

10. Wahlgren, M. A. and Meinke, W. W. Radiations from short-lived rare gas fission products. J. Inorg. Nucl. Chem. 24: 1527. 1962.

11. Ockenden, D. W. and Tomlinson, R. H. An apparatus for the study of short-lived fission product rare gases. Canad. J. Chem. 40: 1594. 1962.

12. Holm, G., Borg, S., Fagerquist, U. and Kropff, F. The decay of ^{139}Xe studied with isotope separator techniques. Arkiv Fysik 34: 447. 1967.

13. Alvager, T., Naumann, R. A., Petry, R. F., Sidenius, G. and Thomas, T. D. On-line studies of mass-separated xenon fission products. Phys. Rev. 167: 1105. 1968.

14. Cook, J. W. and Talbert, W. L., Jr. Private communication.

15. Achterberg, E., Iglesias, F.C., Jech, A. E., Moragues, J. A., Otero, D., Perez, M. L., Proto, A. N., Rossi, J. J., Scheuer, W. and Suarez, J. F. Conversion-coefficient measurements and spin-parity assignments for excited levels in ^{133} ^{135} ^{136}Xe, ^{135} ^{137} ^{139}Cs, and ^{138}Ba. Phys. Rev. C5: 1759. 1972.

16. Maleh, Isaac. Electronic angular momenta of some low-lying states of cerium; nuclear spin of cerium-143. Phys. Rev. 138: B766. 1965.

17. Fulmer, R. H., McCarthy, A. L. and Cohen, B. L. Nuclear structure studies in the 82-neutron region with stripping reactions. Phys. Rev. 128: 1302. 1962.

18. Bingham, F. W. and Sampson, M. B. Study of 83-neutron nuclei by deuteron stripping reactions. Phys. Rev. 128: 1796. 1962.

19. Rapaport, J. and Buechner, W. W. Stripping analysis of the ^{138}Ba(d,p)^{139}Ba reactions. Phys. Lett. 18: 299. 1965.

20. Weidner, C. A., Heusler, A., Solf, J. and Wurm, J. P. Optical-model parameters and the analysis of (d,p) stripping experiments of ^{138}Ba, ^{140}Ce, and ^{142} ^{144} ^{146}Nd. Nucl. Phys. A103: 433. 1967.

21. Rapaport, J. and Kerman, A. K. Study of the ^{138}Ba(d,p)^{139}Ba reaction for incident energies below the coulomb barrier. Nucl. Phys. A119: 641. 1968.

22. von Ehrenstein, D., Morrison, G. C., Nolen, J. A, Jr. and Williams, V. Study of the (d,p) reaction on the even-A barium isotopes 130-138. Phys. Rev. C1: 2066. 1970.

23. von Ehrenstein, D. and Tsangarides, M. C. Spins of ^{139}Ba levels from the ^{138}Ba(d,p) reaction with polarized deuterons. Bull. Am. Phys. Soc. 17: 511. 1972.

24. von Brentano, P., Marquardt, N., Wurm, J. P. and Zaidi, S. A. A. Isobaric analogue states in ^{139}La and ^{141}Pr. Phys. Lett. 17: 124. 1965.

25. Veeser, L. and Haeberli, W. Polarization measurements near isobaric analogue resonances in ^{139}La and ^{141}Pr. Nucl. Phys. A115: 172. 1968.

26. Moraques, J. A., Mariscotti, M. A. J., Gelletly, W. and Kane, W. R. ^{138}Ba(n,)^{139}Ba reaction and evidence for direct capture. Phys. Rev. 180: 1105. 1969.

27. Aksenov, V. A., Brodkin, E. B., Bushuev, A. V. and Polikarpov, V. I. Cs^{139} gamma radiation. Atomnaya Energiya 13: 271. 1962.

28. Zherebin, E. A., Krylov, A. I. and Polikarpov, V. I. Investigation of the decay of ^{139}Cs and ^{140}Cs. Soviet J. Nucl. Phys. 3: 717. 1966.

29. Rudstam, G., Lund, E., Westgaard, L. and Grapengiesser, B. Q-values of some nuclides on the neutron-rich side of stability. In Proc. Int. Conf. on the Properties of Nuclei Far From the Region of Beta Stability. Vol. 1, p. 341. Service d,Information Scientifique, CERN, 1970.

30. Talbert, W. L., Jr. and McConnell, J. R. Preparation for on-line studies of short-lived nuclei produced by a reactor. Arkiv Fysik 36: 99. 1967.

31. Talbert, W. L., Jr. and Thomas, D. Design considerations for a system to investigate short-lived nuclei produced at a reactor. Nucl. Instr. Methods 38: 306. 1965.

32. Larsen, J. T. Gamma-ray decay schemes for ^{142}Xe, ^{142}Cs, ^{142}Ba and ^{142}La. Unpublished Ph.D. thesis. Ames, Iowa, Library, Iowa State University of Science and Technology. 1970.

33. Talbert, W. L., Jr. Survey of existing on-line separators. In Proc. Int. Conf. on Electromagnetic Isotope Separators and the Techniques of Their Applications. p.14. Marburg. 1970.

34. Talbert, W. L., Jr., McConnell, J. R. and Skank, H. Experimental Techniques in use at the TRISTAN on-line isotope separator system. In Proc. Int. Conf. on Electromagnetic Isotope Separators and the Techniques of Their Applications. p.78. Marburg. 1970.

35. Schick, W. C., Jr., Talbert, W. L., Jr. and McConnell, J. R. Ge(Li)-Ge(Li) study of the decay of 14-sec ^{140}Xe. Phys. Rev. C4: 507. 1971.

36. Talbert, W. L., Jr. Experimental techniques using ISOL systems. In Proc. Int. Conf. on the Properties of Nuclei Far From the Region of Beta-Stability. Vol. 2, p.109. Leysin. 1970.

37. Olson, R. J. Gamma-ray decay schemes for ^{92}Kr, ^{92}Rb, and ^{92}Sr. Unpublished Ph.D. thesis. Ames, Iowa, Library, Iowa State University of Science and Technology. 1971.

38. Norman, J. H., Talbert, W. L., Jr., and Roberts, D. M. Optimizing activity separation in fission product decay chains. U. S. Atomic Energy Commission Report IS-1893. (Iowa State Univ., Ames) 1968.

39. Carlson, G. C., Schick, W. C., Jr., Talbert, W. L., Jr., and Wohn, F. K. Half-lives of some short-lived mass-separated gaseous fission products and their daughters. Nucl. Phys. A125: 267. 1969.

40. Wohn, F. K., Clifford, J. R., Carlson, G. H. and Talbert, W. L., Jr. A plastic scintillation detector for beta-ray spectrum measurements. Nucl. Instr. Methods. 101: 343. 1972.

41. Gunnink, R., Niday, J. B., Anderson, R. P. and Meyer, R. A. Gamma-ray energies and intensities. Lawrence Radiation Laboratory Report UCID-15439. University of California, Livermore. 1969.

42. Scranton, D. G and Manchester, E. G. The use of SIMPLOTTER, a high level plotting system. U. S. Atomic Energy Commission Report IS-2305 (Iowa State Univ., Ames) 1971.

43. Mariscotti, M. A. A method for automatic identification of peaks in the presence of background and its application to spectrum analysis. Nucl. Instr. Methods. 26: 309. 1967.

44. Grodstein, G. W. X-ray attenuation coefficients from 10 keV to 100 MeV. National Bureau of Standards Circular 583. 1957.

45. McGinnies, R. T. X-ray attenuation coefficients from 10 keV to 100 MeV. National Bureau of Standards Supplement to Circular 583. 1959.

46. Edwards, W. F., Boehm, F., Rogers, J. and Seppi, E. J. Relative intensities of gamma-rays following the decay of ^{182}Ta and ^{183}Ta. Nucl. Phys. 63: 97. 1965.

47. Sapyta, J. J., Funk, E. G. and Mihelich, J. W. The Decay of ^{182}Re (13h and 64h) and ^{182}Ta (115d) to ^{182}W. Nucl. Phys. A139: 161. 1969.

48. Rogers, P. C. and Gordon, G. E. Computer analysis of beta-ray and conversion electron spectra observed with low-resolution detectors. Nucl. Instr. 37: 259. 1965.

49. Clifford, J. R. Decay energies of gaseous fission products and their daughters for A=88 to 93. Unpublished Ph.D. thesis. Ames, Iowa, Library, Iowa State University of Science and Technology. 1972.

50. Raman, S. and Gove, N. B. Rules for spin and parity assignments based on log ft values. Phys. Rev. C7: 1995. 1973.

51. Lederer, C. M., Hollander, J. M., and Perlman, I. Tables of isotopes. 6th ed. New York, New York, Wiley and Sons. 1967.

52. Roy, R. R., and Nigam, B. P. Nuclear physics. p. 240. New York, New York, Wiley and Sons. 1967.

53. Bevington, P. R. Data reduction and error analysis for the physical sciences. p. 76. New York, New York, Mc Graw Hill. 1969.

54. Carlson, G. H., Talbert, W. L., Jr. and McConnell, J. R. The decays of mass-separated ^{138}Xe and ^{138}Cs. Phys. Rev. C: (To be published)

55. de-Shalit, A. Core excitations in nondeformed, odd-A nuclei. Phys. Rev. 122: 1530. 1961.

56. Kisslinger, L. S. A note on coupling schemes in odd-mass nuclei. Nucl. Phys. 78: 341. 1965.

57. Henry, E. A., Talbert, W. L., Jr. and McConnell, J.R. Gamma-ray decay schemes for ^{89}Kr and ^{89}Rb. Phys. Rev. C7: 222. 1973.

58. Moore, P. A., Riley, P. J., Jones, C. M., Mancusi, M. D. and Foster, J. L., Jr. Isobaric analog resonances in proton elastic scattering from ^{136}Xe. Phys. Rev. 180: 1213. 1969.

59. Cook, J. and Talbert, W. L., Jr. Private communication. 1973.

60. Christensen, P. R., Herskind, B., Borchers, R. R. and Westgaard, L. Neutron single-particle states in ^{143}Nd and ^{145}Sm. Nucl. Phys. A102: 481. 1967.

61. Newman, E., Toth, K. S. and Williams, I. R. Decay of 5.9-day ^{145}Eu to levels in ^{145}Sm. Phys. Rev. C7: 290. 1973.

62. Dave, V. R., Nelson, J. A. and Wilenzick. Energy levels of ^{133}Cs and ^{141}Pr from the (n,n'γ) reaction. Nucl. Phys. A142: 619. 1970.

63. Alexander, P. and Lau, J. P. Nuclear structure in ^{133} ^{135}Xe and ^{133} ^{135}Cs. Nucl. Phys. A121: 612. 1968.

64. Op de Beeck, J. P. and Walters, W. B. Decay of 9.2-h ^{135}Xe. J. Inorg. Nucl. Chem. 30: 2881. 1968.

65. Holm, G. Energy levels in the single closed-shell nucleus ^{137}Cs populated in the decay of 4-min ^{137}Xe. Arkiv Fysik 37: 1. 1968.

66. Schick, W. C., Jr., Talbert, W. L., Jr. and McConnell, J. R. Ge(Li)-Ge(Li) study of the decay of 14-sec ^{140}Xe. Phys. Rev. C7: 1995. 1973.

67. Larson, J. T., Talbert, W. L., Jr. and McConnell, J. R. Gamma-ray studies of the decays of ^{142}Xe, ^{142}Cs, ^{142}Ba, and ^{142}La. Phys. Rev. C3: 1372. 1971.

VII. ACKNOWLEDGMENTS

There are a number of people whose help and encouragement made the completion of this project possible, and the author wishes to express his deep appreciation for their contributions.

Dr. Willard L. Talbert, Jr. suggested the project and throughout its duration he has maintained a friendly spirit of encouragement and willingness to help in every way possible. Dr. Talbert was instrumental in leading the author to resume a graduate career after several years of teaching, and without his inspiring guidance and leadership it is doubtful that this project could have been completed.

John McConnell has spent many hours patiently teaching the author many of the intricacies of operating the isotope separator. His selfless devotion to the work of TRISTAN and his high standards of workmanship and in the performance of duties are in no small measure responsible for the success of the experimental work at TRISTAN.

Drs. Fred Wohn and William Schick, Jr. have freely given of their time and effort in many discussions and in assistance with the experimental system. They have provided the computer codes necessary for the analysis of the large amounts of data generated in a project such as this.

The author is grateful for the friendship and help of the other members of the TRISTAN group. Drs. G. H.

Carlson, J. R. Clifford, R. L. Bunting, J. K. Halbig, E. A. Henry, J. P. Adams, and R. J. Olson assisted in the collection of data. D. R. Lekwa has played an important role in the maintenance of the TRISTAN system.

Words cannot seem to express adequately the author's appreciation for his wife, Carol. She has displayed an exceptional amount of patience and courage during a very difficult time for the family. Her contribution to this effort cannot be emphasized enough.

Finally, the author, together with his wife and sons, would like to dedicate this thesis to the memory of Stephanie, during whose final illness much of this work was completed.